INTRINSIC AND SYNAPTIC MECHANISMS CONTROLLING THE EXCITABILITY OF LAYER 5 CORTICOCALLOSAL AND CORTICOCOLLICULAR NEURONS IN AUDITORY CORTEX

by

Ankur Joshi

B.S in Molecular Biology, Muskingum University, 2008

Submitted to the Graduate Faculty of

School of Medicine in partial fulfillment

of the requirements for the degree of

Doctor of Philosophy

University of Pittsburgh

2015

UNIVERSITY OF PITTSBURGH

SCHOOL OF MEDICINE

This dissertation was presented

by

Ankur Joshi

It was defended on

Dec 7, 2015

and approved by

Dr. Elias Aizenman, Professor, Neurobiology

Dr. Nathan Urban, Professor, Neurobiology

Dr. Anne-Marie Oswald-Doiron, Assistant Professor Neuroscience

Dr. Sandra J. Kuhlman, Assistant Professor, Department of Biological Sciences, Carnegie Mellon University

Dr. Daniel Polley, Associate Professor of Otology and Laryngology, Harvard University

Dissertation Advisor: Dr. Thanos Tzounopoulos, Associate Professor, Otolaryngology and Neurobiology

INTRINSIC AND SYNAPTIC MECHANISMS CONTROLLING THE EXCITABILITY OF LAYER 5 CORTICOCALLOSAL AND CORTICOCOLLICULAR NEURONS IN AUDITORY CORTEX

Ankur Joshi, PhD

University of Pittsburgh, 2015

Auditory cortex (AC) layer (L) 5B contains both corticocollicular neurons, a type of pyramidal-tract neuron projecting to the inferior colliculus, and corticocallosal neurons, a type of intratelencephalic neuron projecting to contralateral AC. It is known that these neuronal types display dichotomous *in vivo* responses to sound. While corticocollicular neurons display robust evoked responses to wide range of sound frequencies, corticocallosal neurons are responsive to a limited range of sound frequencies. However, the intrinsic and synaptic mechanisms shaping these dichotomous responses remain unexplored. It is also known that corticocollicular neurons are critical for learning-induced plasticity involved in relearning sound localization after monaural occlusion. This learning induced-plasticity also requires the release of acetylcholine (ACh) in the AC. However, the effect of ACh release on the excitability of corticocollicular neurons is unknown. Therefore, we recorded in brain slices of mouse AC from retrogradely labeled corticocollicular and neighboring corticocallosal neurons in L5B to identify the intrinsic and synaptic mechanisms that contribute to the *in vivo* responses of these neurons to sound, and to examine the effect of ACh release on corticocollicular and corticocallosal neurons to identify cell-specific mechanisms that enable corticocollicular neurons to participate in relearning sound localization. In comparison to corticocallosal neurons, corticocollicular neurons display a more depolarized resting membrane potential, faster action potentials and less spike frequency adaptation. In paired recordings between single L2/3 and labeled L5B neurons, trains of EPSCs showed no synaptic depression in L2/3→corticocollicular connections, but substantial depression in L2/3→corticocallosal connections. We propose that these differences in intrinsic and synaptic properties contribute to the dichotomous *in vivo*

responses of corticocallosal and corticocollicular neurons to sound. Additionally, ACh release generates nicotinic acetylcholine receptor (nAChR)-mediated depolarizing potentials in both corticocallosal and corticocollicular neurons, but muscarinic acetylcholine receptor (mAChR)-mediated hyperpolarizing potentials in corticocallosal neurons and mAChR-mediated prolonged depolarizing potentials in corticocollicular neurons. This prolonged mAChR-mediated depolarizing potential leads to persistent firing in corticocollicular neurons, whereas corticocallosal neurons lacking this prolonged mAChR-mediated depolarizing potential do not fire persistently. We propose that this mAChR-mediated persistent firing in corticocollicular neurons may be a mechanism required for relearning sound localization after monaural occlusion.

TABLE OF CONTENTS

LIST OF FIGURES

PREFACE

I would first like to thank my mentor Dr. Thanos Tzounopoulos for his rigorous training, endless support, unique leadership and invaluable friendship which helped me progress through graduate school. This work is a reflection of the significant time he spent on me, in order to make me a better scientist on a daily basis. I would also like to thank all my committee members- Dr. Elias Aizenman, Dr. Nathan Urban, Dr. Sandra Kuhlman and Dr. Anne-Marie Oswald- for their valuable discussions and directions on how to make my graduate work more meaningful. I would also like to thank Dr. Brent Doiron for his support and advice during the time he spent on my thesis committee. I also want to thank Dr. Daniel Polley for taking time to serve as the external examiner in my thesis defense.

I would also like to thank our collaborator, Dr. Gordon MG Shepherd at Northwestern University for all his support and help during my graduate school which resulted in a publication in the Journal of Neuroscience as well.

Next, I would like to thank all the members of Tzounopoulos lab for their help and friendship in these past two years, especially Dr. Charles Anderson and Dr. Bopanna Kalappa for their help inside the lab, and their kind friendship in general. I would also like to extend my gratitude to other members of the auditory group for valuable discussions that also helped in shaping my graduate work. Finally, I also want to thank my friends in Pittsburgh and my family for their support during graduate school.

1.0 INTRODUCTION

The auditory cortex (AC), located in the temporal lobe, is the final target of all afferent auditory information and is thought to be responsible for the conscious perception of sound (Purves et al., 2001; Hackett, 2015). It receives auditory information from subcortical structures via the auditory thalamus, also called the medial geniculate body (MGB). The auditory cortex is subdivided into a number of sections that varies based on species, but the general feature is that there is a primary region (A1) which is surrounded by a variable number of belt regions (Malmierca and Ryugo, 2011). A1 has a precise tonotopic organization, i.e. different areas of A1 respond to specific sound frequencies, whereas the belt areas are less precise in their tonotopy. The precise tonotopy in A1 arises due to its inputs from the ventral MGB, which itself is tonotopically organized; however, the AC belt areas are less precise in their tonotopy as they receive inputs from the belt areas of the MGB which are not very precise in their tonotopy (Purves et al). Additionally, like other areas of the sensory neocortex, the AC has a laminar organization, i.e. it is subdivided into layers (L) 1-6.

Based on their projection targets, there are three main classes of excitatory neurons in the neocortex, including the AC. The first class of excitatory neurons is the intratelencephalic (IT) neurons. IT neurons are located in L 2-6 and project solely within the telencephalon (cortex and striatum) (Shepherd, 2013); IT neurons are also the only excitatory neurons that project to the contralateral cortex via the corpus callosum and anterior commisure (Harris and Shepherd, 2015). The second class of excitatory neurons is the pyramidal tract (PT) neurons, which reside in L5B and project to subcerebral brain structures such as the midbrain, brainstem and the spinal cord (Shepherd, 2013). Corticothalamic neurons are the third and final class of excitatory neurons, which are located in L6 and project to the

ipsilateral thalamus (Shepherd, 2013). We will not discuss corticothalamic neurons, and interneurons (which are found in all cortical layers and comprise the remaining 20% of cortical neurons) here as the focus of this work is on the two classes of excitatory cell types in L5B of the AC, the IT and PT neurons, which will be discussed further in the document.

In the AC, L5B contains corticocollicular neurons, a type of PT neuron projecting to the inferior colliculus (IC), and corticocallosal neurons, a type of IT neuron projecting to contralateral AC (Games and Winer, 1988; Doucet et al., 2003). The initial motivation to study AC L5B corticocallosal and corticocollicular projection neurons arose from studies which show that putative AC L5 IT and PT neurons display dichotomous *in vivo* responses to sound (Turner et al., 2005; Sun et al., 2013). However, the role of intrinsic and synaptic properties in shaping the firing of AC L5 projection neurons has not been explored in the AC. Therefore, we investigated the intrinsic and synaptic properties of labeled L5B IT and PT neurons, namely corticocallosal and corticocollicular neurons respectively, to identify mechanisms that shape the distinct *in vivo* responses of AC L5 IT and PT neurons to sound.

In addition to displaying distinct responses to sound, AC L5B projections neurons also play crucial roles in auditory processing. Specifically, the corticocollicular projection is crucial for learning-induced plasticity in the AC as animals with corticocollicular projection lesions cannot relearn sound-localization after monaural occlusion (Bajo et al., 2010). This learning-induced plasticity is also dependent on cholinergic innervation of the AC as animals with lesions of Nucleus Basalis, the major source of cortical acetylcholine (ACh), cannot relearn sound localization after monaural occlusion (Leach et al., 2013). Despite the involvement of ACh and corticocollicular neurons in relearning sound localization, the effect of ACh on the excitability of corticocollicular neurons is unexplored. Therefore, we investigated the effects of ACh release on corticocollicular neurons to understand the mechanisms via which cholinergic modulation enables corticocollicular neurons to participate in relearning sound localization. It is also known that cholinergic modulation affects the activity of L5 IT and PT neurons differently in other neocortical areas (Dembrow et al., 2010). However, whether ACh has projection-specific effects on AC neurons is unknown. Therefore, we examined whether ACh release on AC L5B

corticocallosal and corticocollicular neurons leads to projection-specific neuromodulation in the AC or not.

Overall, the goal of this dissertation was to study the intrinsic and synaptic mechanisms that control the excitability of AC L5B projection neurons and allow them to play distinct roles in auditory processing.

1.1 PART 1

1.1.1 General classification of layer 5 projection neurons in the auditory cortex

Two types of projection neurons have been identified in L5 of the AC. They are called the intrinsic bursting (IB) and regular-spiking (RS) neurons. *In vitro* studies show that intracellular current injections cause an initial high frequency discharge of action potentials in IB neurons, and the spike train that follows maintains a sustained firing rate, i.e. lacks spike frequency adaptation (Hefti and Smith, 2000). On the other hand intracellular current injections lead to a train of action potentials in RS neurons, which is composed of single action potentials, and does not maintain a sustained firing rate, i.e. displays spike frequency adaptation (Hefti and Smith, 2000). IB neurons display significantly larger soma and apical dendrites compared to RS neurons; additionally, the apical dendrite of the IB neurons is characterized by the apical dendritic 'tuft' which extends into layer 1 while the apical dendrite of RS neurons lacks this tuft and terminates in L2/3 (Hefti and Smith, 2000; Sun et al., 2013). Based on anatomical evidence, it is believed that IB neurons project to the inferior colliculus (Games and Winer, 1988) and to the cochlear nucleus (Weedman and Ryugo, 1996b, a) whereas RS neurons project to the contralateral cortex (Games and Winer, 1988). Thus, IB neurons fall in the broader category of PT neurons, whereas RS neurons fall in the broader category of IT neurons. Since corticocollicular neurons projecting from AC L5B to the IC

constitute the majority of AC PT projection neurons (Doucet et al., 2003), it can be inferred that many IB neurons are corticocollicular neurons.

1.1.2 *In vivo* responses of layer 5 IT and PT neurons in the auditory cortex

In vivo studies have revealed that putative AC L5 IT and PT neurons display distinct responses to sound stimuli evidenced by their tonal receptive fields (TRFs). TRF represents the evoked responses of an AC neuron in response to tones of various frequencies over a range of sound intensities. PT neurons display broadly tuned TRFs, i.e. they exhibit sustained, reliable spiking in response to a wide range of sound frequencies (Sun et al., 2013). On the other hand, AC L5 IT neurons exhibit spiking over a limited range of sound frequencies and display narrowly tuned TRFs (Sun et al., 2013). Additionally, sound stimuli drive bursts of action potentials, containing up to 2-3 action potentials in PT neurons, whereas sound stimuli in IT neurons leads to generation of single action potentials (Turner et al., 2005; Sun et al., 2013). This *in vivo* bursting in PT neurons and the lack of it in IT neurons is reminiscent of the activity IB and RS neurons reported in the *in vitro* literature (Hefti and Smith, 2000). Another difference in the response of PT and IT neurons is the latency of spiking after sound stimulus, which is significantly shorter in PT neurons compared to IT neurons; on the other hand, the latency of response in PT neurons is comparable to latency of response in L4 neurons, suggesting that like L4 neurons, PT neurons are driven by direct thalamic input, whereas cortical input drives IT neurons (Sun et al., 2013).

1.1.3 Current understanding of the mechanisms shaping the *in vivo* responses of layer 5 IT and PT neurons in the auditory cortex

The broad tuning of PT neurons and the narrow tuning of L5 IT neurons in the AC has been attributed to the difference in the synaptic inputs received by them. The range of synaptic inputs received by neurons can be indirectly assayed by examining the subthreshold TRFs. In L5 PT neurons, broad suprathreshold

spike TRFs are matched by broad subthreshold TRFs, while the narrow suprathreshold spike TRFs in L5 IT neurons are matched with narrow subthreshold TRFs; this difference in the subthreshold TRFs indicates that L5 PT neurons receive a broader range of synaptic inputs compared to L5 IT neurons (Sun et al., 2013).

The difference in synaptic inputs received by AC PT and IT neurons is shaped by the excitatory and inhibitory inputs converging on these neurons. A direct examination of excitatory and inhibitory inputs in voltage clamp mode reveals that PT neurons display a broad excitatory TRF and a much narrower inhibitory TRF, indicating that excitatory inputs to PTs are broadly tuned while the inhibitory inputs to PTs show narrow tuning; on the other hand, IT neurons display a narrow excitatory TRF, which is matched to their inhibitory TRF (Sun et al., 2013). Overall, as the range of inhibitory inputs impinging on PT and IT neurons are not significantly different, the broad tuning of PT neurons to sound can be explained by the broad range of excitatory inputs received by PT neurons (Sun et al., 2013).

While the range of excitatory inputs received by PT and IT neurons can explain their *in vivo* responses to sound, we still do not have a clear understanding of the source and properties of these excitatory inputs. Additionally, synaptic inputs are not the only factor that shapes the firing of neurons, as intrinsic properties such as AP threshold, AP width, resting membrane potential, input resistance, etc. have a bearing on the excitability of neurons. Therefore, in order to fully understand how these neurons respond to sound, we have to explore cell-specific intrinsic and synaptic mechanisms of L5 IT and PT neurons.

1.1.4 Potential mechanisms shaping the *in vivo* responses of layer 5 IT and PT neurons in the auditory cortex

In vitro studies, using retrograde labeling, have revealed differences in intrinsic properties of L5 IT and PT neurons in various cortical areas (Morishima and Kawaguchi, 2006; Dembrow et al., 2010; Suter et al., 2013). Spike related properties in L5 motor, frontal and prefrontal cortices suggest that PT neurons are

intrinsically endowed to generate prolonged APs. In comparison to L5 IT neurons, PT neurons of the motor cortex display a more hyperpolarized AP threshold, narrow APs (half-width), and lack of spike frequency adaptation (Hattox and Nelson, 2007; Suter et al., 2013). Similar results have been reported in the prefrontal cortex where in comparison to L5 IT neurons, PT neurons display a more hyperpolarized AP threshold, faster APs and a lack of spike frequency adaptation (Dembrow et al., 2010). A difference in spike frequency adaptation between L5 IT and PT neurons has also been reported in the frontal cortex (Morishima and Kawaguchi, 2006). The lack of spike frequency adaptation in PT neurons suggests that they are intrinsically tuned to fire in a tonic or prolonged fashion, whereas adaptation in L5 IT neurons suggests that they are intrinsically tuned to display phasic or transient firing (Shepherd, 2013). Additionally, the linear relationship between stimulus intensity and the evoked firing rate in PT neurons (Suter et al., 2013) argues that PT neurons can fire reliably at high frequencies (Shepherd, 2013).

In L5 AC, intrinsic properties of labeled IT and PT neurons have not been examined systematically and hence their contribution to *in vivo* responses of L5 IT and PT neurons to sound is unknown. Therefore, an inquiry into the intrinsic properties of L5 IT and PT neurons using *in vitro* techniques can help us to understand the intrinsic mechanisms that shape their *in vivo* responses to sound.

In addition to intrinsic properties, the synaptic inputs impinging on neurons can also affect their excitability. We know that PT neurons receive a broader range of excitatory synaptic inputs in comparison to IT neurons (Sun et al., 2013), but the source or the nature of these excitatory inputs remains to be explored. One of the major sources of excitatory input to L5 pyramidal neurons is from L2/3 neurons (Adesnik and Scanziani, 2010; Anderson et al., 2010; Wallace and Jufang, 2011; Shepherd, 2013; Harris and Shepherd, 2015). L2/3 input to L5 pyramidal neurons can differ based on the location and the projection class of L5 pyramidal neurons. In the motor cortex L2/3 inputs to IT neurons in lower L5A are much stronger compared to inputs in upper L5A, while L2/3 inputs to IT neurons in L5B are weak regardless of the location; on the other hand, L2/3 inputs to PT neurons are stronger in upper L5B compared to lower L5B (Anderson et al., 2010). A comparison of L2/3 inputs to upper L5B IT and PT neurons reveal significantly stronger inputs to PT neurons (Anderson et al., 2010). The above discussion

highlights that the strength of excitatory inputs to L5 IT and PT neurons are region/cell-specific. Significant differences in the strength of L2/3 inputs to L5 IT and PT neurons can dramatically affect their ability to fire APs. Therefore, an *in vitro* examination of synaptic inputs in AC from L2/3 to L5 IT and PT neurons can help us understand the synaptic mechanisms shaping L5 IT and PT *in vivo* responses to sound.

Together, an *in vitro* understanding of intrinsic properties of AC L5 IT and PT neurons, and their synaptic inputs from L2/3 will be useful for understanding their dichotomous *in vivo* responses to sound. In order to do so, we have to selectively target L5 IT and PT neurons *in vivo*, which can help in the subsequent *in vitro* identification of these specific neurons for an in depth assessment of their properties.

1.1.5 Retrograde labeling as a tool to identify specific L5 IT and PT neurons- the corticocallosal and corticocollicular neurons in the auditory cortex

Retrograde labeling with fluorescent tracers has been used extensively to label and study distinct populations of projection neurons in the cortex (Anderson et al., 2010; Dembrow et al., 2010; Kiritani et al., 2012; Suter et al., 2013; Yamawaki et al., 2014). Corticocollicular neurons projecting from AC L5B to the IC constitute the majority of AC PT projection neurons (Doucet et al., 2003) while corticocallosal neurons projecting to the contralateral cortex constitute IT neurons (Games and Winer, 1988). Therefore, injections of retrograde tracers of different colors into the IC and the contralateral cortex can label distinct populations of corticocollicular and corticocallosal neurons. Corticocollicular neurons reside in L 5B of the AC (Doucet et al., 2003), whereas corticocallosal neurons are found in L2-6 (Harris and Shepherd, 2015). This anatomical segregation can allow us to target specific corticocallosal neurons within L5B of the AC. By studying the intrinsic and synaptic properties of labeled L5B corticocallosal and corticocollicular neurons, we can understand the mechanisms shaping the *in vivo* responses of L5 IT and PT neurons to sound.

1.1.6 The role of AC L5B corticocollicular projection neurons in behavioral auditory relearning

In addition to displaying distinct evoked responses to sound, L5 projection neurons also play an important role in auditory processing. Recent evidence shows that the corticocollicular projection from L5B AC to IC plays a critical role in behavioral auditory relearning (Bajo et al., 2010).

When we hear a sound, our two ears perceive the sound differently i.e. there is a difference in the intensity and timing of the sound reaching our ears. This difference along with the spectral cues generated by how the sound interacts with the external folds of our ears is used to locate the direction of the sound source (Leach et al., 2013). Perturbations in interaural timing and intensity, generated by monaural occlusion for example, can dramatically affect the ability of animals to localize sound (Bajo et al., 2010; Leach et al., 2013). However, under normal circumstances, animals learn to overcome this disruption by relying on the cues provided by the unoccluded ear and can relearn to localize sound (Bajo et al., 2010; Leach et al., 2013). The corticocollicular projection plays a crucial role in this learning-induced plasticity as animals with corticocollicular lesions cannot relearn sound localization after monaural occlusion (Bajo et al., 2010). It must be mentioned that under normal conditions, i.e. without monaural occlusion, animals with corticocollicular lesions can locate the sound source (Bajo et al., 2010), highlighting the fact that the corticocollicular projection plays a critical role during conditions that require an animal to adapt to altered cues.

Interestingly, the ability to relearn sound localization is not only dependent on corticocollicular projections, but also on the release of the neuromodulator ACh in the AC (Leach et al., 2013).

1.2 PART 2

1.2.1 Overview of acetylcholine and its role in modulating auditory processing

ACh is a neuromodulator that is important for learning (Kilgard, 2003; Ramanathan et al., 2009), memory (Winkler et al., 1995; Hasselmo and Stern, 2006) and tasks that require attention (Himmelheber et al., 2000; Herrero et al., 2008; Parikh and Sarter, 2008). The main source of cortical ACh is the Nucleus Basalis, a group of neurons in the basal forebrain (Lehmann et al., 1980; Dani and Bertrand, 2007). ACh shapes cortical functioning by modulating the activity of cortical neurons via the activation of two types of acetylcholine receptors, the nicotinic and muscarinic acetylcholine receptors (nAChRs and mAChRs) (Dani and Bertrand, 2007). nAChRs are ligand-gated pentameric ionotropic receptors, which belong to the cystine-family of receptors (Dani and Bertrand, 2007). The structure of these receptors is based on various combinations of twelve subunits (α2-α10 and β2-β4) (Gotti and Clementi, 2004). Two main types of nAChRs are found in the cerebral cortex: the homopentameric nAChRs composed of five α7 subunits and the heteropentameric nAChRs that contain two α4 subunits, two β2 subunits and a fifth subunit that can be α4, β2, or β5 (Albuquerque et al., 2009). Activation of nAChRs allows the flow of Na^+, K^+, and Ca^{2+}, which leads to the depolarization of the cell membrane. On the other hand, mAChRs belong to the family of G-protein coupled receptors (Ishii and Kurachi, 2006). There are five different types of mAChRs (M1-M5). The odd numbered mAChRs (M1, M3 and M5) are coupled to Gq proteins, while the even numbered mAChRs (M2 and M4) are coupled to Gi proteins (Brown, 2010). The cerebral cortex mainly contains M1, M2 and M4 types of mAChRs (Levey et al., 1991), and their activation leads to different intracellular signaling cascades which can cause both hyperpolarization and depolarization of the cell membrane by causing changes in potassium and calcium conductances (Brown, 2010; Thiele, 2013).

ACh plays an important role in auditory processing and plasticity. Electrical stimulation of the Nucleus Basalis, paired with an auditory stimulus results in tonotopic plasticity in A1; specifically, an over representation of the frequency of the auditory stimulus that was paired with Nucleus Basalis

stimulation is seen in A1 (Kilgard and Merzenich, 1998b). Similarly, pairing a sound stimulus with Nucleus Basalis stimulation modifies the excitation and inhibition generated in response to the paired stimuli; specifically, there in an increase in the amplitude of EPSCs and a decrease in the amplitude of IPSCs elicited in response to the paired stimuli (Froemke et al., 2007). These studies show that ACh causes tonotopic and synaptic modifications in the AC. ACh also participates in behavioral auditory plasticity. Stimulation of Nucleus Basalis with a preceding tone can induce stimulus-specific associative memory in the auditory cortex; when presented with a range of tones with different frequencies, animals can discriminate the specific tone that was paired with the Nucleus Basalis stimulation (Weinberger et al., 2006). Interestingly, this ability is dependent on the level of ACh released in the AC as weak stimulation of Nucleus Basalis does not induce stimulus-specific associative memory (Weinberger et al., 2006). In addition to shaping AC related plasticity, ACh is also important for normal auditory processing. Lesions of Nucleus Basalis can impair the ability of animals to locate short broadband sounds (40-500 ms stimulus durations) and the extent of impairment is positively correlated to the severity of lesions in the Nucleus Basalis (Leach et al., 2013). While animals retain their ability to locate sounds of longer durations after Nucleus Basalis lesions, they do so by sacrificing the speed of their responses as evidenced by longer latencies in their response times (Leach et al., 2013).

The studies cited above highlight the role of ACh in shaping auditory processing. However, the mechanisms by which ACh generates such changes are unknown as the specific neuronal types involved in different forms of auditory processing are not known.

1.2.2 Linking AC L5B corticocollicular neurons and acetylcholine in behavioral auditory processing

To bridge the gap in knowledge about the mechanisms by which ACh shapes auditory processing, we have to understand the effect of ACh release on specific neurons in the AC that are involved in auditory processing. This makes corticocollicular neurons an extremely interesting target, as they are involved in

learning-induced plasticity which is important for relearning sound localization after monaural occlusion (Bajo et al., 2010). This learning-induced plasticity requires ACh release in the AC, as animals with lesions of Nucleus Basalis are also unable to relearn sound localization after monaural occlusion (Leach et al., 2013). Therefore, the study of the effects of ACh release on corticocollicular neurons can help us to understand the mechanisms by which ACh enables relearning sound localization.

Studies also show that neuromodulators have distinct effects on the activity of L5 IT and PT neurons in the neocortex. In the medial prefrontal cortex, cholinergic activation can lead to distinct neuromodulation of L5 IT and PT neurons, which leads to increased excitability of PT neurons but not IT neurons (Dembrow et al., 2010). The presence of corticocallosal neurons (type of IT neurons) in L5B of the AC provides a target to understand whether ACh has projection specific effects in the AC neurons.

Together, an assessment of the effect of ACh on AC L5B corticocallosal and corticocollicular neurons will reveal the basic mechanisms by which ACh modulates neuronal activity and will contribute to the growing knowledge about the differences in the physiological properties of different projection neurons in the cortex. Specifically, the effect of ACh on AC L5B corticocallosal and corticocollicular neurons will lead to the understanding of the cell-specific mechanisms that enable corticocollicular neurons to play a critical role in relearning sound localization.

1.2.3 Summary of dissertation research

The first goal of this dissertation was to identify the intrinsic and synaptic mechanisms shaping the dichotomous *in vivo* responses of AC L5 IT and PT neurons. By the use of retrograde labeling, we identified distinct populations of AC L5B IT and PT neurons, namely the corticocallosal and corticocollicular neurons. Using *in vitro* electrophysiology, we showed that a combination of distinct intrinsic and synaptic properties promote sustained frequency-independent firing in corticocollicular neurons, while generating frequency dependent firing in corticocallosal neurons.

The second goal of this dissertation was to identify the mechanisms by which ACh affects the activity of corticocollicular neurons and enables them to participate in relearning sound localization after monaural occlusion, and to examine whether ACh has projection-specific neuromodulatory effects on AC L5B neurons. By the use of *in vivo* retrograde labeling, and *in vitro* electrophysiological methods combined with optogenetic activation of cholinergic fibers, we reveal that ACh has projection-specific effects on corticocollicular and corticocallosal neurons, which lead to mAChR-mediated persistent firing in corticocollicular neurons only. This persistent firing in corticocollicular neurons may represent a critical mechanism for ACh-mediated experience dependent plasticity involved in relearning sound localization after monaural occlusion.

2.0 CHAPTER 1: CELL-SPECIFIC ACTIVITY DEPENDENT FRACTIONATION OF LAYER 2/3 → 5B EXCITATORY SIGNALING IN MOUSE AUDITORY CORTEX

2.1 OVERVIEW

Auditory cortex (AC) layer (L) 5B contains both corticocollicular neurons, a type of pyramidal-tract neuron projecting to the inferior colliculus, and corticocallosal neurons, a type of intratelencephalic neuron projecting to contralateral AC. Although it is known that these neuronal types have distinct roles in auditory processing and different response properties to sound, the synaptic and intrinsic mechanisms shaping their input-output functions remain less understood. Here, we recorded in brain slices of mouse AC from retrogradely labeled corticocollicular and neighboring corticocallosal neurons in L5B. Corticocollicular neurons had, on average, lower input resistance, greater hyperpolarization-activated current (I_h), depolarized resting membrane potential, faster action potentials, initial spike doublets, and less spike frequency-adaptation. In paired recordings between single L2/3 and labeled L5B neurons, the probability of connection, amplitude, latency, rise time, and decay time constant of the unitary excitatory postsynaptic current (EPSC) were not different for L2/3→corticocollicular and L2/3→corticocallosal connections. However, short trains of unitary EPSCs showed no synaptic depression in L2/3→corticocollicular connections, but substantial depression in L2/3→corticocallosal connections. Synaptic potentials in L2/3→corticocollicular connections decayed faster and showed less temporal summation, consistent with increased I_h in corticocollicular neurons, whereas synaptic potentials in L2/3→corticocallosal connections showed more temporal summation. Extracellular L2/3 stimulation at two different rates resulted in spiking in L5B neurons; for corticocallosal neurons the spike rate was

frequency-dependent, but for corticocollicular neurons it was not. Together, these findings identify cell-specific intrinsic and synaptic mechanisms that divide intracortical synaptic excitation from L2/3 to L5B into two functionally distinct pathways with different input-output functions.

2.2 INTRODUCTION

The corticocollicular projection from auditory cortex (AC) to the inferior colliculus (IC) plays crucial modulatory roles in auditory processing (Winer, 2006; Suga, 2012; Stebbings et al., 2014). The functional properties of the corticocollicular projection have been studied by electrically stimulating AC while measuring IC responses (Yan and Ehret, 2002; Yan et al., 2005; Suga, 2012). For example, AC stimulation enhances the responses of IC neurons that are matched in best-frequency to the AC stimulated neuron, but suppresses IC responses that are unmatched (Suga, 2012). AC stimulation shifts the frequency tuning of IC neurons (Yan and Ehret, 2002), and modulates the gain of IC neurons' responses by elevating thresholds and reducing dynamic ranges (Yan and Ehret, 2002). Behavioral studies show that corticocollicular projections mediate learning-induced plasticity (Suga et al., 2002; Bajo et al., 2010). Whereas progress has been made towards characterizing AC→IC projections at the level of the IC (Doucet et al., 2003; Suga and Ma, 2003; Bajo et al., 2010), the intracortical circuits and cellular mechanisms shaping the activity of corticocollicular neurons remain incompletely understood.

Corticocollicular neurons in AC are located in L5B (Games and Winer, 1988; Doucet et al., 2003; Doucet and Ryugo, 2003; Slater et al., 2013). L5B also contains another major class of projection neurons, the corticocallosal neurons (Games and Winer, 1988). Corticocallosal neurons, which are found in other layers as well, project axons via the corpus callosum to the contralateral AC and thereby mediate interhemispheric connectivity between the right and left AC cortices (de la Mothe et al., 2006). Callosal projections are important in establishing a continuity of sensory representation across the two hemispheres (Hackett and Phillips, 2011).

Recent studies in a variety of cortical areas have revealed numerous differences in the physiological properties of pyramidal-tract (PT) neurons, of which corticocollicular are a sub-type, and intratelencephalic (IT) neurons, of which corticocallosal neurons are a sub-type (reviewed in Shepherd 2013). While anatomical differences and differential response properties to sound have been reported for L5 PT and IT neurons in AC (Turner et al., 2005; Atencio and Schreiner, 2010a, b; Sun et al., 2013), the differences in synaptic and intrinsic properties of L5B PT and IT neurons and their contribution to the firing of L5B projection neurons have not been systematically studied in AC.

Here, we investigated the intrinsic and synaptic properties of corticocollicular and corticocallosal neurons with the general aim of characterizing the dynamic synaptic properties of these two major classes of infragranular neurons in mouse AC. We used *in vivo* retrograde labeling combined with *in vitro* electrophysiology-based methods. Our results indicate L5B AC neurons, receive functionally distinct L2/3 input and exhibit different intrinsic properties. Together, these properties reveal an activity-dependent partition of L2/3→5B resulting in firing in corticocollicular neurons that is independent of the L2/3 stimulation rate, and in frequency-dependent, reduced firing in corticocallosal neurons at lower L2/3 stimulation rates.

2.3 RESULTS

2.3.1 Identification of corticocollicular and corticocallosal neurons in auditory cortex (AC)

To label corticocollicular and corticocallosal projection neurons in L5B of AC for subsequent targeted recordings in brain slices, we performed *in vivo* injections of fluorescent retrograde tracers. Small volumes of fluorescent microspheres were injected in the IC, while microspheres of different color were injected in the contralateral AC (Figure 2-1A). In brain slices prepared two to three days later, corticocollicular and corticocallosal neurons were selectively labeled (Figure 2-1B, C). Consistent with

previous studies of similar classes of projection neurons in A1 and in other cortical areas (Games and Winer, 1988; Akintunde and Buxton, 1992; Morishima and Kawaguchi, 2006), we found no double labeling (0 out of more than 660 neurons) of these two populations; that is, this labeling paradigm labels two types of L5B projection neurons that represent distinct, non-overlapping classes (Figure 2-1C).

While AC is stereotaxically localizable in the intact brain, AC localization is more challenging in brain slices because its areal borders are not sharply demarcated by cytoarchitectural features. In general, in this study we were guided by (1) anatomical landmarks such as the rhinal fissure and underlying hippocampal anatomy (Figure 2-1D1), and (2) the presence of retrogradely labeled neurons projecting to the inferior colliculus in localizing AC in slices (Figure 2-1D2) as well as retrogradely labeled neurons projecting to the contralateral auditory cortex (Figure 2-1D3). However, in the early phase of these studies we additionally localized the AC *ex-vivo* using a two-step procedure that was based on a functional assay *in vivo*. First, we localized AC *in vivo* by transcranially measuring flavoprotein autofluorescence (FA) signals elicited by acoustic stimulation (Figure 2-1E-G), and then we labeled AC identified by FA imaging with sulforhodamine (Figure 2-1D3) (Takahashi et al., 2006). FA signals are generated by mitochondrial flavoproteins due to changes in oxidation state caused by neuronal activity (Shibuki et al., 2003; Middleton et al., 2011). Mirror-reversed tonotopic gradients have been used to identify A1 and the anterior auditory field (AAF) in many mammalian species including mice (Kaas, 2011; Guo et al., 2012). In response to low frequency sound (5 KHz), we observed two distinct regions with increased FA activity, representing the caudal end of A1 and the rostral end of AAF (Figure 2-1E). The relative location of the FA signals (Figure 2-1F), the timing of the FA signals after the stimulus onset (Figure 2-1G), and the distance (Figure 2-1H) between the centers of two regions of the FA signals are consistent with localization of mouse A1 using either FA, electrophysiological recordings or optical Ca^{2+} imaging (Stiebler et al., 1997; Takahashi et al., 2006; Guo et al., 2012; Honma et al., 2013; Issa et al., 2014). After completion of FA-assisted localization of A1, we applied a fluorescent dye to mark the location of A1 (Lefort et al., 2009), enabling us to precisely localize the A1 region of auditory cortex in subsequently prepared brain slices (Figure 2-1D). These results suggest that FA- and sulforhodamine-

assisted A1 localization is an efficient approach for localizing A1 in brain slice recordings. The FA- and sulforhodamine-assisted A1 localization helped us to localize A1 in the initial phase of the project. Because these experiments revealed that the location of A1 was consistent in relation to the location of retrogradely labeled corticocollicular neurons, in subsequent experiments, we relied on retrograde labeling of corticocollicular neurons and on the rhinal fissure and underlying hippocampal anatomy for targeting our recordings to AC.

To characterize the dendritic morphology of corticocollicular and corticocallosal neurons we filled them with biocytin to reconstruct their dendritic arbors. Both cell types displayed the morphological hallmarks of cortical pyramidal neurons, with numerous branches in the basal perisomatic arbor and a prominent apical dendrite extending to the pia, branching into an apical tuft in L1 (Figure 2-2A). Neither the total dendritic length (Figure 2-2B, inset) nor the amount and horizontal spread of dendrites in the L5B perisomatic region (Figure 2-2B) differed between the two cell types ($n = 6$ corticocollicular, $n = 6$ corticocallosal; $p > 0.05$, rank-sum test). However, compared to corticocallosal neurons, corticocollicular neurons had more horizontally spreading apical tufts in layer 1 (Figure 2-2C). The vertical profiles of dendrites (dendritic length as a function of absolute or soma-normalized depth) did not differ significantly between corticocallosal and corticocollicular neurons (Figure 2-2D). These results indicate that the differences in dendritic structure between the two cell types are primarily in the distal dendritic arbors in the apical tufts but not in their basal arbors. These results appear broadly consistent with, but smaller in magnitude, than the reported morphological differences of putative PT and IT neurons in rat AC (Sun et al., 2013) and with prior reports for IT and PT neurons in other cortical areas and species (Gao and Zheng, 2004; Dembrow et al., 2010).

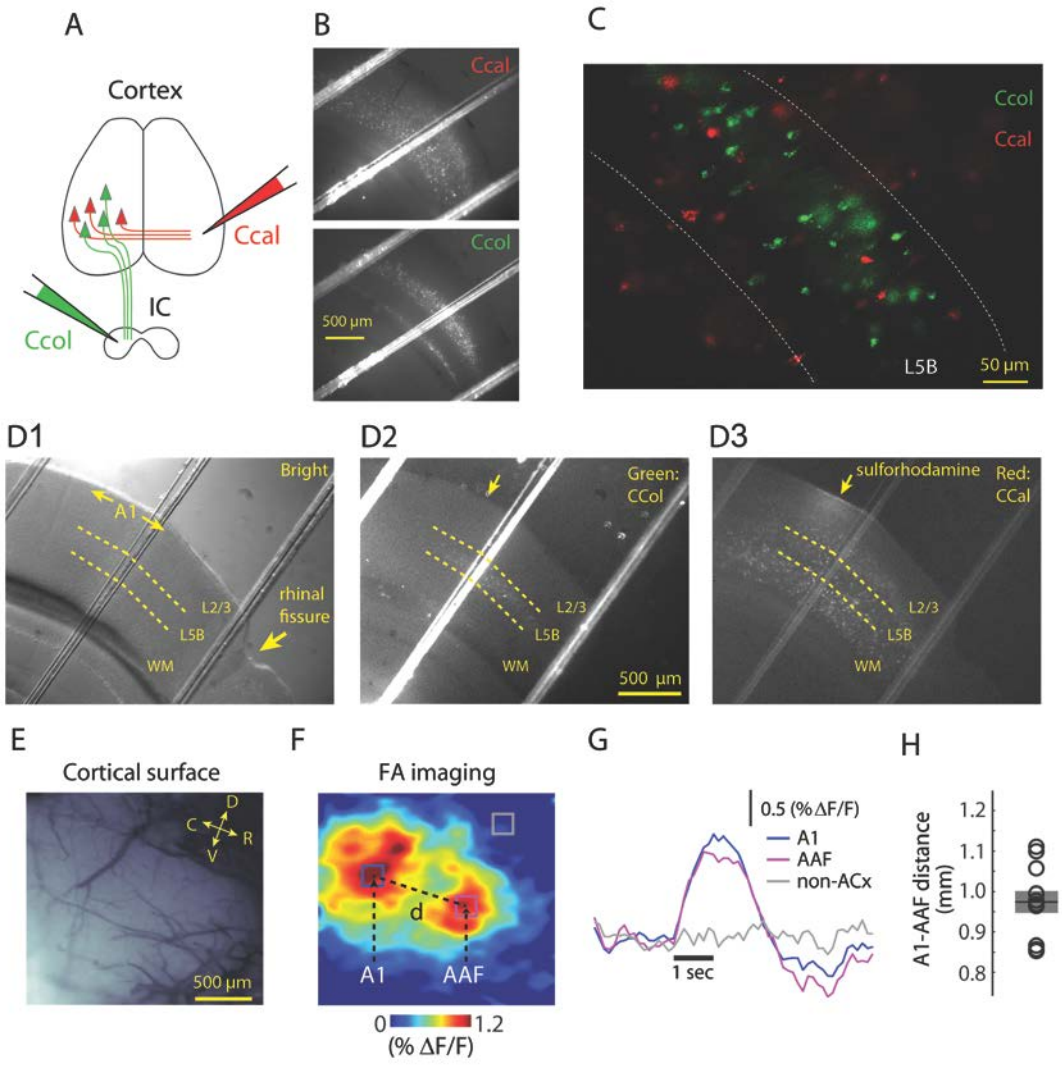

Figure 2-1: Localization and identification of AC corticocollicular (Ccol) and L5B corticocallosal (Ccal) neurons.

Legends for Figure 2-1

A, Labeling of corticocollicular and corticocallosal neurons with fluorescent tracers. Projection neurons in the AC were retrogradely labeled by injecting different colored fluorescent latex microspheres in the contralateral AC and the ipsilateral inferior colliculus.

B, Low magnification images (4X) show the full extent of the AC and labeled Ccal (top) and Ccol neurons (bottom).

C, Merged image showing intermingling but no double labeling of corticocollicular (green) and corticocallosal (red) neurons in L5B of AC.

D-H: *In vivo* localization of AC areas by FA imaging of sound-evoked activity was performed in 11 experiments.

D1-D3, Brightfield (D1), green (D2) and red (D3) fluorescent images, of a representative coronal slice that was labeled *in vivo* with sulforhodamine. The brightfield image (**D1**) indicates the rhinal fissure and the location of primary auditory cortex estimated from the stereotaxic coordinate mouse brain atlas (Franklin and Paxinos, 2001). The green fluorescent image (**D2**) shows retrogradely labeled corticocollicular neurons in L5B that are present in A1 and extend towards the rhinal fissure. The red fluorescent image (**D3**) shows the *in vivo* applied sulforhodamine spot. Sulforhodamine was applied to the pial surface *in vivo* and here identifies A1 in this coronal brain slice (FA-assisted A1 identification was performed as shown in E-F). **D3** also shows retrogradely labeled corticocallosal neurons that extend medially and laterally from A1. The upper and lower layer 5B boundaries are indicated by dashed lines (WM stands for white matter).

E, Image of cortical surface indicating caudal (C), rostral (R), dorsal (D) and ventral (V) direction.

F, In response to amplitude-modulated tones (carrier frequency of 5 kHz and modulation frequency of 20 Hz, 40-50 dB), FA image showing peaks of activity corresponding to A1 and non-A1 auditory cortical areas. The more caudal (left) of the two domains of activation is A1 and the more rostral (right) of the two

domains is the anterior auditory field (AAF). Image is an average of 10 trials and is from a frame taken 1 sec after stimulus onset. Images were smoothed using a spatial filter with a 100 µm space constant.

G, The average (10 trials) relative fluorescence from regions of interest at the peak of A1 (blue) and AAF (magenta) area. The horizontal bar indicates the duration of the auditory stimulus.

H, The distance between the centers of 5 kHz activation of A1 and AAF (974 ± 27 µm, n= 11).

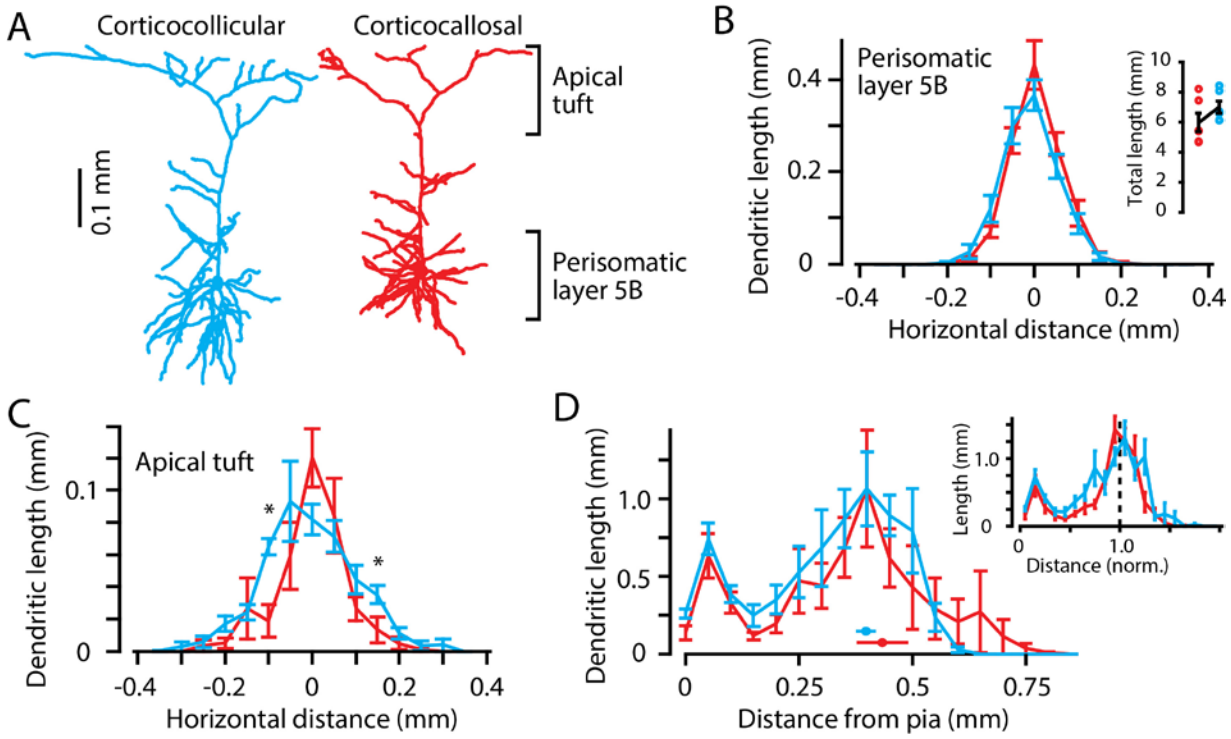

Figure 2-2: Dendritic morphology of corticocollicular and corticocallosal neurons in L5B of AC.

Legends for Figure 2-2

A, Example reconstructions.

B, Horizontal profile of the total dendritic length in the perisomatic/L5B region, showing the mean ± SEM for corticocollicular (blue, $n = 6$) and corticocallosal (red, $n = 6$) neurons. Each neuron's horizontal profile was calculated as the average in a 150-µm wide band extending horizontally across the perisomatic region, as indicated in **A**. No significant differences were found at any of the locations (rank-sum test). Inset: total dendritic length, plotted as the mean ± SEM for the two cell types (lines) along with the individual values (circles). The samples were not significantly different (rank-sum test).

C, Horizontal profile of the dendritic length in the apical tuft, showing the mean ± SEM for corticocollicular (blue, $n = 6$) and corticocallosal (red, $n = 6$) neurons. Each neuron's horizontal profile was calculated as the average in a 150-µm wide band extending horizontally across the apical tuft region, as indicated in **A**. Locations where values differed significantly are marked (*) ($p < 0.05$, rank-sum test).

D, Vertical profiles, calculated as the dendritic length in 50 µm bins and plotted as the mean ± SEM for the two cell types; no differences were found (rank-sum test). Inset: each profile was first normalized to the soma (distance = 1), rebinned, and plotted as the mean ± SEM; no differences were found (rank-sum test).

2.3.2 Intrinsic properties of L5B projection neurons

To characterize the intrinsic properties of the two classes of projection neurons, labeled corticocollicular and L5B corticocallosal neurons were targeted for whole-cell recordings in voltage- and current-clamp modes. Corticocollicular neurons, compared to corticocallosal neurons, had lower input resistance (Figure 2-3A, B), depolarized resting membrane potential (Figure 2-3C), and greater "sag potentials" in response to hyperpolarizing pulses (Figure 2-3D1, D2). Sag potentials were abolished by 10 µM ZD7288 (an I_h blocker, Figure 2-3D3) suggesting that I_h mediates these potentials. These results are consistent with

previous studies of corresponding classes of projection neurons in auditory, motor, and prefrontal cortex (Dembrow et al., 2010; Sheets et al., 2011; Shepherd, 2013; Slater et al., 2013; Suter et al., 2013).

Next, we evaluated the spike related properties of corticocollicular and corticocallosal neurons in L5B. Corticocollicular neurons displayed faster action potentials (Figure 2-4A, B). Moreover, the action potential threshold of corticocollicular neurons was more hyperpolarized (2-4C). In response to depolarizing current, repetitive firing patterns differed (Figure 2-4D). The initial linear slope of the current - firing frequency (f-I) function revealed that firing rate increased faster in corticocollicular neurons (Figure 2-4E, F); moreover the f-I function revealed that the threshold for eliciting firing was higher for corticocollicular neurons (Figure 2-4E, G). Corticocollicular neurons often fired faster initial doublets (Figure 2-4I, L, inset) at the onset of current injection while corticocallosal neurons do not (Figure 2-4I, L). Spike frequency decreased (adapted) over time in corticocallosal neurons while it remained nearly constant in corticocollicular neurons (Figure 2-4I, K). Initial instantaneous frequency for corticocollicular neurons was high (Figure 2-4J1), reflecting more fast-doublet firing. The relative constancy of the instantaneous firing frequency in corticocollicular neurons after the initial fast doublet (Figure 2-4J1 inset) indicates lack of spike frequency adaptation. Corticocallosal neurons exhibit low initial instantaneous firing frequency (Figure 2-4J2), because they do not show fast doublet firing. The relative decay of instantaneous firing frequency in corticocallosal neurons (Figure 2-4J2, inset) indicates spike frequency adaptation. Overall, corticocollicular neurons fire in a more tonic (nonadapting) pattern and corticocallosal neurons fire in a more phasic (adapting) pattern (Figure 2-4D-L). PT neurons in mouse somatosensory cortex (S1) show greater spike-frequency adaptation than their counterparts in mouse motor cortex (M1) (Miller et al., 2008); our results indicate that the AC corticocollicular neurons are more consistent with the M1 pattern, which has also been reported for PT neurons in secondary somatosensory cortex (Suter et al., 2013). Collectively, our results indicate that spiking properties of AC L5B projection neurons are cell-specific and are consistent with previous *in vitro* studies suggesting that PT neurons tend to fire in a tonic pattern, and IT fire in a more phasic pattern (Shepherd, 2013). Our results suggest that

these cell-specific intrinsic properties may contribute to the observed burst-like and more sustained firing in PT compared to IT L5 neurons in response to sound (Sun et al., 2013).

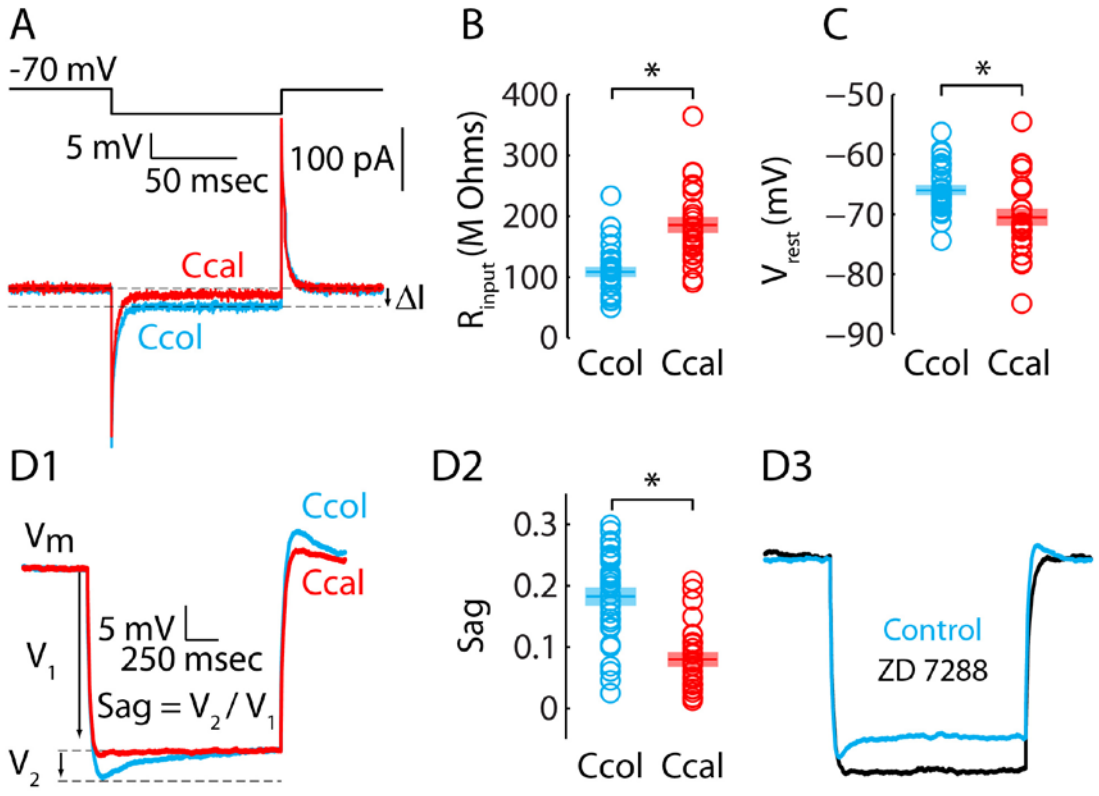

Figure 2-3: Intrinsic subthreshold properties of AC corticocollicular (Ccol) and L5B corticocallosal (Ccal) neurons are distinct.

Legends for Figure 2-3

A, Hyperpolarizing pulses (top) in voltage-clamp recording mode result in transient current responses (bottom). The difference between baseline and steady state hyperpolarized current (ΔI) is used to calculate the input resistance of Ccol and Ccal neurons.

B, The average input resistance is significantly lower for Ccol neurons (108.11 ± 7.06 MΩ, n = 32 vs. 185 ± 11.27 MΩ, n = 29, $p < 0.0001$).

C, The average resting membrane voltage, V_m, is significantly more depolarized for Ccol neurons (-65.98 ± 0.70 mV, n = 32 vs. -70.54 ± 1.22 mV, n = 29, $p = 0.0014$).

D1, Hyperpolarizing current injection reveals sag potentials in Ccol and Ccal neurons. Sag is measured by dividing the difference between the minimum voltage hyperpolarization and the steady state hyperpolarized voltage by the steady state hyperpolarized voltage.

D2, The average sag is significantly higher for Ccol neurons (0.18 ± 0.01, n = 32, vs. 0.08 ± 0.01, n = 20, $p < 0.0001$).

D3, Sag potentials are abolished by ZD7288 (black trace) indicating that they are mediated by hyperpolarization-activated cyclic nucleotide-gated (HCN) channels (average sag in control = 0.10 ± 0.01; post ZD7288 = 0.01 ± 0.01, n=3, $p < 0.01$).

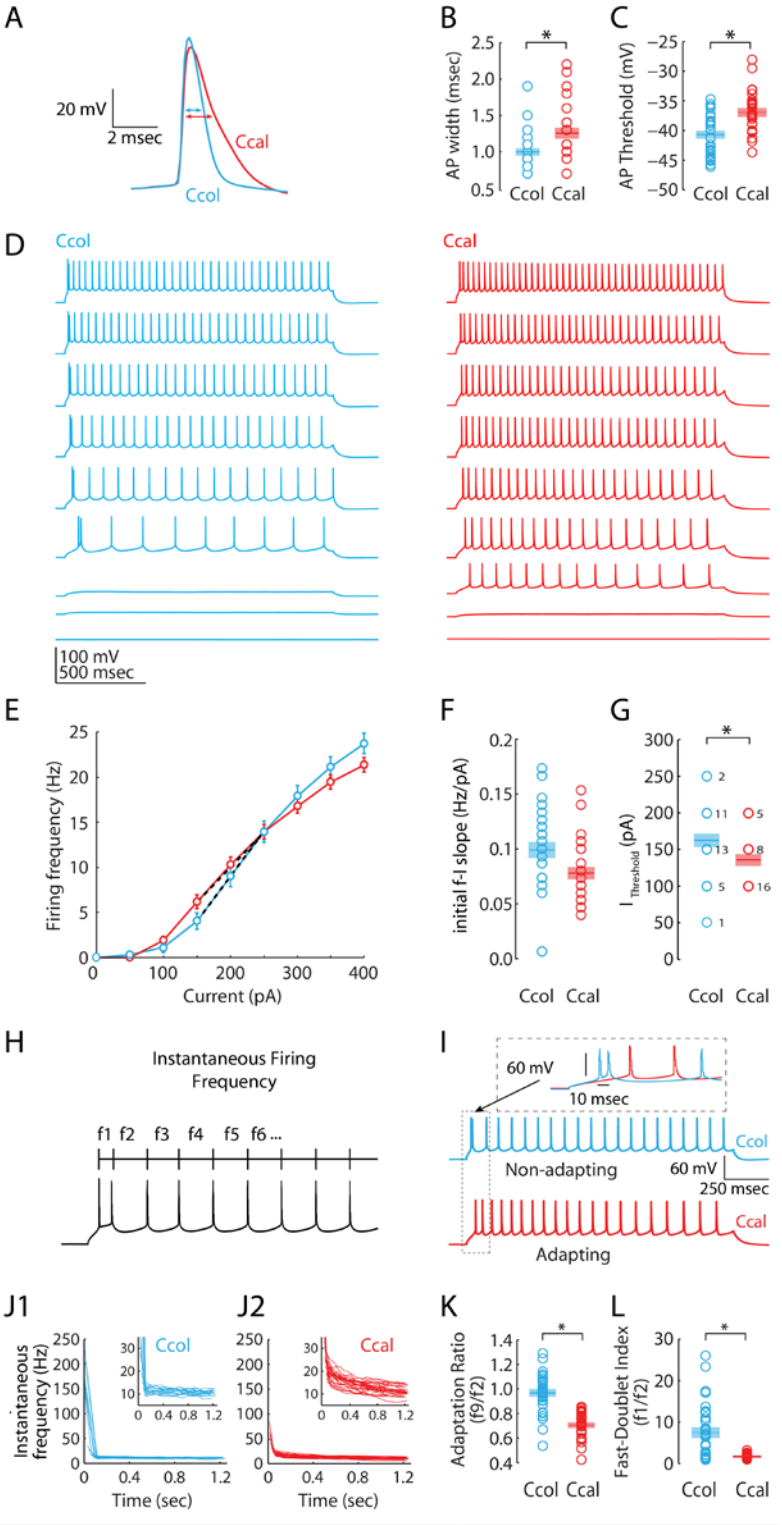

Figure 2-4: Action potential (AP) properties and spike frequency adaptation of AC corticocollicular (Ccol) and L5B corticocallosal (Ccal) neurons are distinct.

Legends for Figure 2-4

A, AP waveforms of representative Ccol and Ccal neurons. Arrows indicate AP width.

B, On average, Ccol neurons have narrower APs (1.00 ± 0.04 msec, n = 32, vs. 1.26 ± 0.07 msec, n = 29, p = 0.0016).

C, On average, Ccol neurons have a more hyperpolarized AP threshold (-40.70 ± 0.59 mV, n = 32, vs. -36.95 ± 0.65 mV, n = 29, p < 0.0001).

D, Representative firing of Ccol and Ccal neurons in response to increasing depolarizing current (0 - 400 pA, 50 pA increments).

E, Firing frequency as a function of injected current amplitude for Ccal and Ccol neurons (f-I relationship). The slope of the f-I curve between 150 and 250 pA is used to calculate the slope (gain) of the f-I curve.

F, The f-I slope is significantly steeper for Ccol neurons (0.11 ± 0.01 Hz/pA, n = 32 vs. 0.08 ± 0.004 Hz/pA, n = 29, p = 0.0007).

G, The smaller current that elicited firing is significantly higher for Ccol neurons (162.50 ± 8.09 pA, n = 32 vs. 131.03 ± 7.12 pA, n = 29, p = 0.005 Rank-sum test, numbers next to circles indicate the number of neurons that fire under this current injection).

H, Temporal patterning of action potential generation was analyzed by calculating instantaneous firing frequencies (i.e. inverse of the inter-spike interval).

I, Ccol often start to fire with a faster initial doublet (inset, marked by the arrow) at the onset of current injection compared to Ccal neurons. Spike frequency decreases (adapts) over time in Ccal neurons while it remains nearly constant in Ccol neurons.

J1 – J2, Instantaneous firing frequency as a function of time for Ccal and Ccol neurons. Initial instantaneous frequency for Ccol neurons is high, which indicates more fast-doublet firing. Insets illustrate instantaneous firing frequency in Ccol and Ccal neurons after the initial fast doublet.

K, The average adaptation ratio, AR = f_9/f_2, (see H and I for representative traces) is significantly lower for Ccal neurons and close to 1 for Ccol neurons (0.70 ± 0.02, n = 29, vs. 0.97 ± 0.03, n = 32, $p < 0.0001$).

L, The average fast-doublet index, FDI = f_1/f_2 (see H and I inset for representative traces), is significantly higher in Ccol neurons (7.50 ± 1.18, n = 32, vs. 1.73 ± 0.09, n = 29, $p < 0.0001$).

2.3.3 Unitary connections from L2/3 to L5B projection neurons

To assess synaptic properties within the AC intracortical circuits of L2/3 to L5B projection neurons, we recorded from synaptically coupled pairs of L2/3→corticocollicular and L2/3→corticocallosal neurons. Connections were assessed by eliciting presynaptic spikes in the L2/3 neuron while monitoring EPSCs in the corticocollicular or L5B corticocallosal neuron (Figure 2-5A, B). Connection rates were similar for L2/3→corticocollicular (14 connections found out of 235 tested) and L2/3→corticocallosal (11 connections found out of 223 tested) unitary connections. For all pairs we only tested the connectivity between from L2/3→corticocollicular or L2/3→cortococallosal neurons; we did not test for connectivity in the reverse direction. Unitary EPSC amplitude and other baseline unitary connection properties such as latency, rise time, and decay time constant were not different (Figure 2-5C-F).

Given the importance of short-term synaptic plasticity dynamics in sensory processing (Abbott and Regehr, 2004) and the more sustained synaptic response properties to sound in AC PT neurons (Sun et al., 2013), we hypothesized that short-term plasticity might differ between L2/3→corticocollicular and L2/3→corticocallosal synapses. Trains of action potentials at 20 Hz in the presynaptic L2/3 neuron evoked a depressing series of EPSCs in L5B corticocallosal neurons, but EPSC strength was maintained throughout the series of EPSCs in corticocollicular neurons (Figure 2-5G-I). Together, our results indicate that spatially intermingled AC L5B receive pathway-specific inputs that show distinct short-term synaptic plasticity. The cell/pathway-specific short-term plasticity of L5B corticocollicular and corticocallosal neurons favors a tonic (sustained) relay of information in the L2/3→corticocollicular pathway and a phasic (transient) relay of information in L2/3→corticocallosal pathway.

To explore the interaction of synaptic and intrinsic properties in shaping activity in corticocollicular and corticocallosal neurons, we next recorded unitary responses from the same connected pairs in current-clamp mode (Figure 2-6A, B). Consistent with our paired recordings in voltage-clamp mode, current-clamp experiments revealed that baseline unitary EPSP parameters did not differ between L2/3→corticocollicular and L2/3→corticocallosal connections (Figure 2-6C-E), with one exception: the decay time constant of the unitary EPSP for L2/3→corticocallosal connections was significantly longer (Figure 2-6F). This finding is consistent with lower amounts of I_h and higher input resistance in corticocallosal neurons (Figure 2-3B, D). Trains of action potentials in the presynaptic L2/3 neuron did not change significantly the peak of the unitary EPSPs in either L2/3→corticocollicular or L2/3→corticocallosal connections (Figure 2-6G, H). The peak amplitude of the series of EPSP reflects the combination of temporal summation and synaptic depression/facilitation; thus, to assess the contribution of temporal summation we measured the trough values in the EPSPs (Figure 2-6G). Trough values were higher for L2/3→corticocallosal connections, suggesting more temporal summation for L2/3→corticocallosal connections (Figure 2-6I). This result is consistent with the reduced levels of I_h in corticocallosal neurons (Figure 2-3D). Subtraction of trough from the peak values (peak minus trough) revealed greater values for L2/3→corticocollicular connections, suggesting that L2/3 inputs do not

depress for corticocollicular neurons, but depress for L5B corticocallosal neurons (Figure 2-6J). These results are consistent with our voltage-clamp mode experiments (Figure 2-5I) and unmask the interaction of cell-specific intrinsic and synaptic properties in shaping the differential kinetics and dynamics of L2/3 synaptic inputs to corticocollicular and L5B corticocallosal neurons.

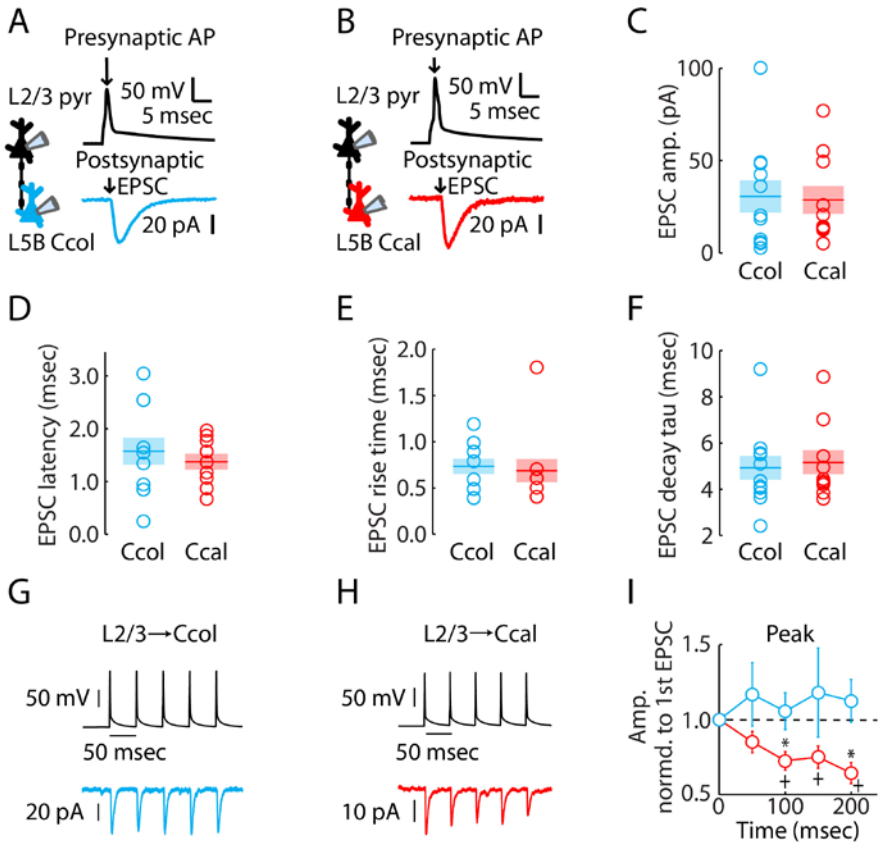

Figure 2-5: Paired recordings reveal similar basal synaptic properties but pathway-specific short-term plasticity of corticocollicular and L5B corticocallosal neurons; L2/3→corticocallosal connections depress, but L2/3→corticocollicular connections do not depress.

Legends for Figure 2-5

A, Example unitary L2/3→corticocollicular connection.

B, Example unitary L2/3→corticocallosal connection.

C, Average unitary EPSC amplitude (L2/3→Ccal = 28.90 ± 8.20 pA; L2/3→Ccol = 30.90 ± 8.80, $p > 0.05$).

D, Average unitary EPSC latency (L2/3→Ccol = 1.60 ± 0.30 msec, n=11; L2/3→Ccal = 1.40 ± 0.10 msec, n=10, $p > 0.05$).

E, Average unitary EPSC rise time (L2/3→Ccal= 0.70 ± 0.10 msec; L2/3→Ccol= 0.70 ± 0.10 msec, $p > 0.05$).

F, Average unitary EPSC decay tau (L2/3→Ccal = 5.10 ± 0.50 msec; L2/3→Ccol = 4.90 ± 0.50 msec, $p > 0.05$).

G, An example of action potential (AP) train in presynaptic L2/3 neuron eliciting a series of EPSCs in a Ccol neuron.

H, An example of AP train in presynaptic L2/3 neuron eliciting an EPSC train in a L5B Ccal neuron.

I, Average peak amplitudes of the EPSCs in the train, normalized to the peak amplitude of the first EPSC. Asterisks (*) indicate significant differences between L2/3→Ccol (n = 11) and L2/3→Ccal (n = 10) connections. (At time = 100 msec, L2/3→Ccal = 0.72 ± 0.06, L2/3→Ccol = 1.06 ± 0.12, $p = 0.037$; at time = 200 msec, L2/3→Ccal = 0.64 ± 0.07, L2/3→Ccol = 1.12 ± 0.14, $p = 0.01$). Pluses (+) indicate significant differences compared to 1st EPSC within L2/3→corticocallosal or L2/3→corticocollicular connections (compared to the first L2/3→Ccal EPSC, at time = 100 msec, L2/3→Ccal = 0.72 ± 0.06, p=

0.002; at time= 150 msec, L2/3→Ccal = 0.75 ± 0.07, p = 0.01; at time = 200 msec, L2/3→Ccal = 0.64 ± 0.07, p = 0.0009).

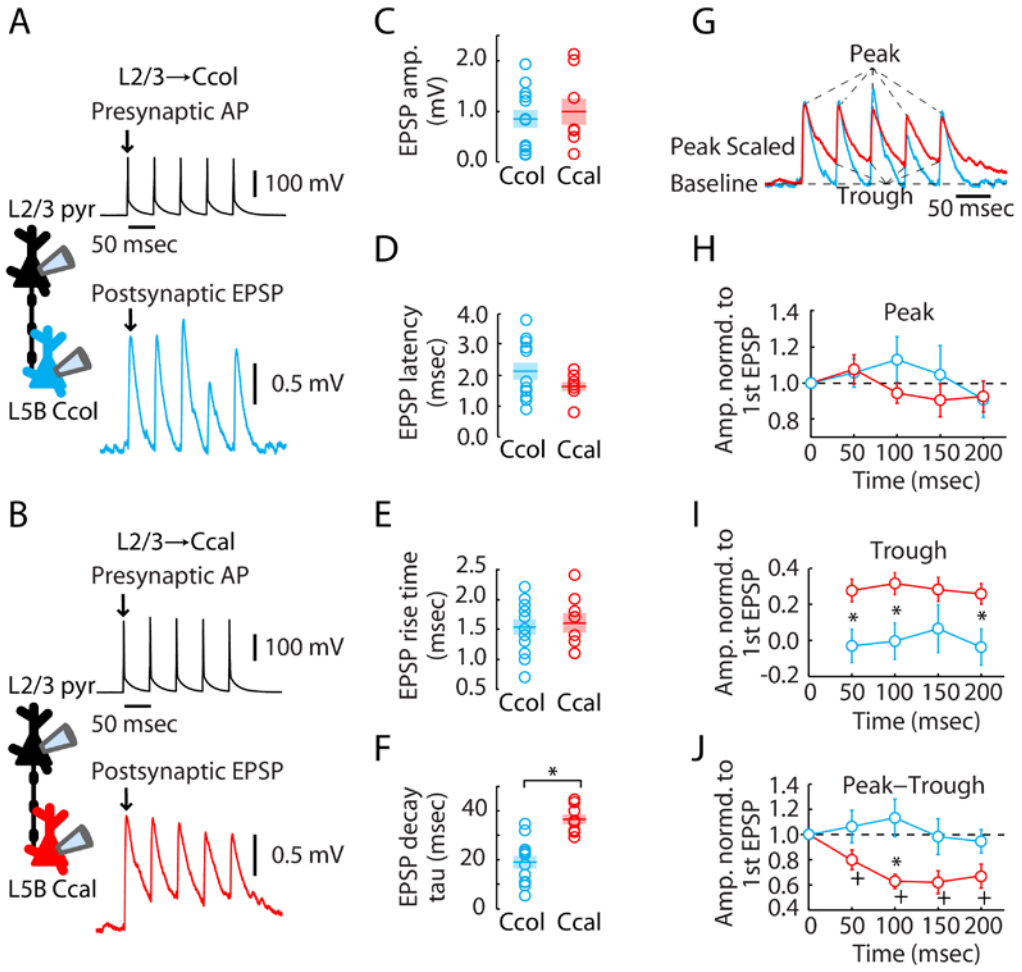

Figure 2-6: Synaptic dynamics of L2/3→corticocollicular and L2/3→corticocallosal connections in current clamp mode.

Legends for Figure 2-6

A, Example unitary L2/3→corticocollicular connection.

B, Example unitary L2/3→corticocallosal connection.

C, Average unitary EPSP amplitude (L2/3→Ccol = 0.80 ± 0.20; L2/3→Ccal = 1.00 ± 0.30 mV, $p > 0.05$).

D, Average unitary EPSP latency (L2/3→Ccol = 2.10 ± 0.30 msec, n = 11; L2/3→Ccal =1.60 ± 0.10 msec, n = 8, $p>0.05$).

E, Average unitary EPSP rise time (L2/3→Ccol = 1.5 ± 0.1 msec; L2/3→Ccal = 1.60 ± 0.20 msec, $p>0.05$).

F, Average unitary EPSP decay tau (L2/3→Ccol= 19.00 ± 2.60 msec; L2/3→Ccal = 36.50 ± 2.00 msec, $p = 0.0001$).

G, Overlay of traces from A and B**,** normalized to the first EPSP.

H, Average peak amplitudes of the EPSPs in the train, normalized to the amplitude of the first EPSP. No significant differences are observed between or within groups.

I, Trough amplitudes, normalized to the amplitude of the first EPSP. Asterisk (*) indicates significant differences between L2/3→Ccol and L2/3→Ccol connections (At time = 50 msec, L2/3→Ccal = 0.28 ± 0.06, L2/3→Ccol = -0.03 ± 0.09, $p = 0.024$; at time = 100 msec, L2/3→Ccal = 0.32 ± 0.06, L2/3→Ccol = 0.00 ± 0.10, $p = 0.028$; at time= 200 msec, L2/3→Ccal = 0.26 ± 0.06, L2/3→Ccol = -0.04 ± 0.1, $p = 0.039$).

J, Trough-subtracted peak EPSP amplitudes, normalized to the amplitude of the first EPSP. Peak-trough values were obtained by subtracting the peak amplitude of the EPSP from the trough amplitude of the

preceding EPSP; this resulted in four peak-trough values at 50, 100, 150 and 200 msec. The first value at time = 0 msec is not a peak-trough value: it is the normalized amplitude of the peak of the first EPSP. Asterisk (*) indicates significant differences between L2/3→Ccol and L2/3→Ccal connections (At time = 100 msec, L2/3→Ccol = 1.13 ± 0.15; L2/3→Ccal = 0.63 ± 0.06, p = 0.016. Pluses (+) indicate significant differences within L2/3→CCol or L2/3→CCal connections. Compared to the first L2/3→Ccal Peak-Trough, at time = 50 msec, L2/3→Ccal = 0.80 ± 0.08, p = 0.038; at time = 100 msec, L2/3 →Ccal = 0.63 ± 0.06, p = 0.0003; at time = 150 msec, L2/3→Ccal = 0.62 ± 0.09, p = 0.004; at time = 200 msec, L2/3→Ccal = 0.67 ± 0.10, p = 0.012).

2.3.4 In response to L2/3 stimulation, the combined effects of synaptic and intrinsic properties shape cell-specific L5B firing

The constancy of the peak voltage of unitary EPSPs, in either L2/3→corticocollicular or L2/3→corticocallosal connections during a 20 Hz train of presynaptic action potentials (Figure 2-6G), suggests that the spiking output of these two pathways in response to L2/3 repetitive stimulation would be similar. However, because EPSC and EPSP amplitudes (peak-trough) for L2/3→corticocallosal synapses depress (Figure 2-5I and 2-6J), the lack of depression of the peak voltages of L2/3→corticocallosal synapses is probably due to the increased summation (trough, Figure 2-6I) arising from longer synaptic decay time constants (Figure 2-6F). At lower stimulation frequencies, where summation is less or not occurring, we expect that the pathway-specific depression of L2/3→corticocallosal may reveal depression of EPSP peaks and postsynaptic firing in corticocallosal but not corticocollicular neurons.

To test this hypothesis, we investigated the effect of a lower frequency of presynaptic stimulation - 10 Hz, which generates less summation - on monosynaptic EPSPs and postsynaptic firing for L2/3→corticocollicular and L2/3→corticocallosal connections. Because the size of unitary EPSPs does not lead to firing in either corticocollicular or corticocallosal neurons, for this experiment we used extracellular electrical stimulation by positioning a stimulating electrode in L2/3 and recording EPSPs

from corticocollicular and corticocallosal neurons (in the same slice); these EPSPs were larger and capable to induce firing in both corticocollicular and corticocallosal neurons. This stimulation method presumably activated not only L2/3 pyramidal neurons but also other cell types (including interneurons mediating feedforward inhibition). However, we assume that a significant fraction of the postsynaptic responses represents inputs from L2/3 pyramidal neurons. A 20 Hz stimulation led to pathway-specific depression of L2/3→corticocallosal EPSCs similar to the one that we observed with paired-recordings (Figure 2-7A-C), suggesting that pathway-specific synaptic plasticity between L2/3→corticocollicular and L2/3→corticocallosal connections is a robust phenomenon maintained even at less stringent stimulation conditions. Importantly, 10 Hz stimulation led to similar pathway-specific depression in L2/3→corticocallosal EPSCs, while L2/3→corticocolicular EPSCs remain unaffected (Figure 2-7D-F). Because temporal summation of EPSPs is less in 10 Hz and synaptic depression is occurring at this frequency, in current-clamp mode, we observed a depression in the peak amplitude of L2/3→corticocallosal EPSPs during 10 Hz stimulation, which was absent in L2/3→corticocollicular EPSPs (Figure 2-7G-I). Therefore, we hypothesized that the synaptic dynamics we observe will have a differential frequency-dependent effect on the firing of the two projection neurons. Namely, 10 and 20 Hz stimulation of L2/3 is expected to lead to similar firing in corticocollicular neurons, but 10 Hz stimulation is expected to lead to decreased firing, compared to 20 Hz, in corticocallosal neurons. Consistent with our hypothesis, at threshold conditions (~50% firing in response to 10 pulses, 20 Hz stimulation protocol), transitions from 20 to 10 Hz stimulation left corticocollicular neurons unaffected (Figure 2-7J,K), but led to decreased firing in corticocallosal neurons (Figure 2-7L,M). This is an important finding, suggesting that in AC, synaptically driven corticocallosal output is modulated by frequency while corticocollicular output is frequency-independent.

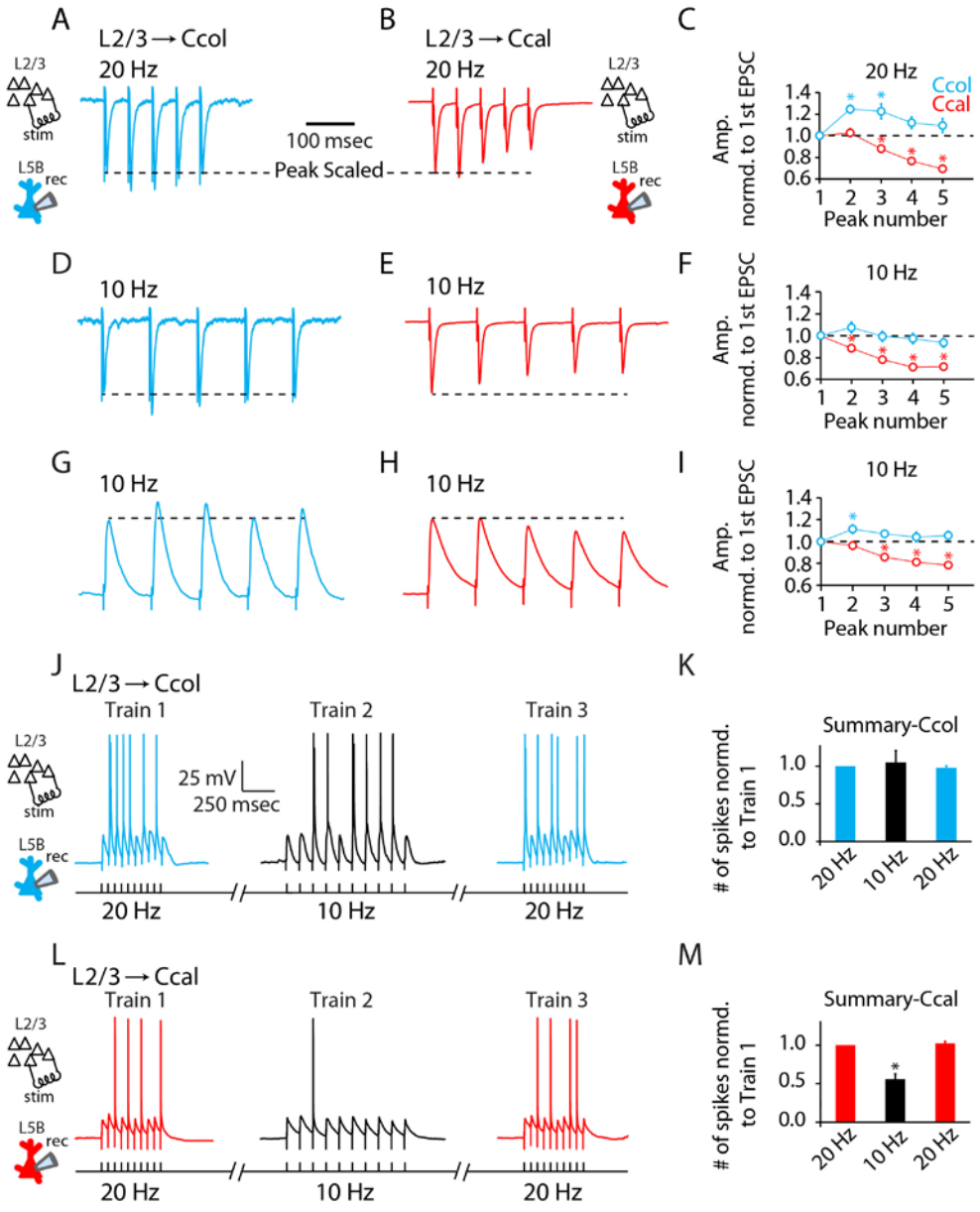

Figure 2-7: In response to L2/3 stimulation, the spiking of corticocallosal - but not corticocollicular - neurons is frequency-dependent.

Legends for Figure 2-7

A, An example of an EPSC train in a Ccol neuron elicited by a train of 20 Hz extracellular stimulation of L2/3.

B, An example of an EPSC train in a Ccal neuron elicited by a train of 20 Hz extracellular stimulation of L2/3. Dotted line in **A-I** indicates normalization to first EPSC/P.

C, Average peak amplitudes of the EPSCs from the trains as in **A** and **B**, normalized to the peak amplitude of the 1st EPSC. Red asterisks (*) indicate significant differences compared to 1st EPSC within L2/3→corticocallosal connection (compared to the 1st EPSC peak, at peak 3, L2/3→Ccal = 0.88 ± 0.03, p = 0.003; at peak 4, L2/3→Ccal = 0.77 ± 0.04, p < 0.0001; at peak 5, L2/3→Ccal = 0.70 ± 0.03, p < 0.0001; n = 14). Cyan asterisks (*) indicate significant differences compared to the 1st EPSC peak for the L2/3→corticocollicular connection (compared to the 1st EPSC peak, at peak 2, L2/3→Ccol = 1.25 ± 0.04, p = 0.0002; at peak 3, L2/3→Ccol = 1.23 ± 0.07, p = 0.01; n = 9).

D, An example of an EPSC train in a Ccol neuron elicited by a train of 10 Hz extracellular stimulation of L2/3.

E, An example of an EPSC train in a Ccal neuron elicited by a train of 10 Hz extracellular stimulation of L2/3.

F, Average peak amplitudes of the EPSCs from trains as in **D** and **E**, normalized to the peak amplitude of the 1st EPSC. Asterisks (*) indicate significant differences compared to 1st EPSC within L2/3→corticocallosal connection (compared to the 1st EPSC peak, at peak 2, L2/→Ccal = 0.88 ± 0.03, p = 0.0002, at peak 3, L2/3→Ccal = 0.78 ± 0.03, p < 0.0001; at peak 4, L2/3→Ccal = 0.72 ± 0.03, p < 0.0001; at peak 5, L2/3→Ccal = 0.72 ± 0.03, p < 0.0001; n = 14). There is no significant difference in the EPSC train for L2/3→Ccol connection (n = 9).

G, An example of an EPSP train in a Ccol neuron elicited by a train of 10 Hz extracellular stimulation of L2/3.

H, An example of an EPSP train in a Ccal neuron elicited by a train of 10 Hz extracellular stimulation of L2/3.

I, Average peak amplitudes of the EPSPs from the trains as in **G** and **H**, normalized to the peak amplitude of the 1st EPSP. Red asterisks (*) indicate significant differences compared to 1st EPSC within L2/3→corticocallosal connection (compared to the 1st EPSC peak, at peak 3, L2/3→Ccal = 0.86 ± 0.03, $p < 0.0001$; at peak 4, L2/3→Ccal = 0.81 ± 0.03, $p < 0.0001$; at peak 5, L2/3→Ccal = 0.78 ± 0.03, $p < 0.0001$; n = 14). Cyan asterisk (*) indicates a significant difference compared to 1st EPSC within L2/3→corticocollicular connection (compared to the first EPSC peak, at peak 2, L2/3→Ccol = 1.12 ± 0.04, $p = 0.01$; n = 9).

J, An example of spikes elicited in a Ccol neuron by three trains of extracellular stimulation of L2/3 (10 pulses in each train, delivered in succession at 20 Hz, 10 Hz and 20 Hz respectively). The breaks (/ /) indicate that at the end of each stimulation train, a 10 second pause was introduced before the starting the next train.

K, Average data for the example shown in **J**; number of spikes fired in each train have been normalized to the number of spikes fired in the 1st 20 Hz train. Ccol neurons fire similar number of spikes at 20 Hz and 10 Hz (compared with 20 Hz train 1, at 10 Hz train 2, Ccols fired an average of 1.04 ± 0.16 spikes, $p = 0.78$; 20 Hz train1 and 20 Hz train 3 are not significantly different, $p = 0.5$; n = 5).

L, Example traces, as the one in **J**, but for Ccal neurons.

M, Average data for the example shown in **L**; number of spikes fired in each train have been normalized to the number of spikes fired in the 1st 20 Hz train. Ccal neurons fire significantly fewer spikes at 10 Hz compared with those at 20 Hz (compared with 20 Hz train 1, at 10 Hz train 2, Ccals fired an average of

0.55 ± 0.07 spikes, p = 0.0002; 20 Hz train1 and 20 Hz train 3 are not significantly different, p = 0.5289; n = 6).

2.4 DISCUSSION

To characterize the synaptic and intrinsic properties of corticocollicular and corticocallosal neurons, we developed paradigms for *ex vivo* analysis of L5B projection neurons in mouse AC. Our approach was based on the combined use of retrograde fluorescent labeling to selectively label corticocollicular and L5B corticocallosal neurons, single-cell electrophysiology, and paired recordings to isolate unitary L2/3 connections to L5B projection neurons for quantitative assessment of synaptic properties. We show that sustained L2/3 activity unmasks a dynamic fractionation of the L2/3→5B pathway that generates frequency-independent firing in corticocollicular neurons and frequency-dependent firing in corticocallosal neurons. While we have not explored whether different subnetworks of L2/3 neurons project to corticocollicular and corticocallosal L5 neurons, our results are consistent with previous studies in somatosensory cortex showing that specific subnetworks in L5 receive input from different L2/3 subnetworks with distinct connection probabilities (Kampa et al., 2006). In this context, we propose that different subnetworks of L2/3→5B with similar connection probabilities but with distinct dynamic properties may underlie corticocallosal vs. corticocollicular auditory processing.

2.4.1 Linking the response properties of corticocollicular and corticocallosal neurons with synaptic and intrinsic properties

AC neurons display a variety of firing behaviors in response to acoustic stimuli. Firing can range from phasic to tonic, and can vary monotonically or non-monotonically with intensity (Volkov and Galazjuk, 1991; Schreiner et al., 1992; Calford and Semple, 1995; Barbour and Wang, 2003; Wang et al., 2005; de

la Rocha et al., 2008). L5B contains different types of projection neurons with different response properties (Turner et al., 2005; Atencio and Schreiner, 2010b, a; Sun et al., 2013). PT- and corticocallosal-type L5B neurons in AC display dichotomous sound-evoked responses, with PT-type neurons firing in a more sustained (tonic) pattern and corticocallosal-type neurons in a more transient (phasic) manner (Sun et al., 2013).

The lack of spike frequency adaptation (Figure 2-4I-K), the narrower action potentials (Figure 2-4A,B), and the increased gain in frequency-current relationships of corticocollicular neurons (Figure 2-4F) suggest that the spike properties of these neurons -- in accordance to their sound responses *in vivo* -- allow for more reliable, sustained firing. The observed burst-like (faster initial doublet) firing in corticocollicular neurons in the presence of blockers of excitatory and inhibitory synaptic transmission (Figure 2-4I,L) suggests that the intrinsic properties of corticocollicular neurons contribute to the bursting responses of PT neurons to sound (Sun et al., 2013).

The non-depressing excitatory L2/3 input to corticocollicular neurons is consistent with the *in vivo* long-lasting excitatory responses of PT neurons to acoustic stimuli (Sun et al., 2013). Given that the corticocollicular projection shapes the response properties of IC neurons, and mediates sound localization learning (Bajo et al., 2010), our results suggest that sustained activity in the corticocollicular pathway may play an important role in inducing these forms of L5-mediated, learning induced plasticity (Bajo et al., 2010).

The firing properties and the response properties of AC L5B projection neurons are determined not only by the intrinsic and L2/3 synaptic properties studied in our experiments, but also by excitatory and inhibitory synaptic inputs arising from other local intracortical sources. In addition to L2/3, a second source of input to L5B neurons is from other L5B neurons. Based on studies from other cortical areas, L5 PT and corticocallosal neurons form recurrent (within-class) connections, but across-class connectivity is asymmetric and in some cases even unidirectional from corticocallosal to PT neurons (Morishima and Kawaguchi, 2006; Brown and Hestrin, 2009b; Kiritani et al., 2012). If this hierarchical microcircuit organization occurs in AC L5B, which is currently unknown, it could further contribute to the

dichotomous tonic/phasic activity in L5B projection neurons, because activity in corticocollicular neurons would be further sustained through recurrent connectivity without propagating to the upstream corticocallosal neurons.

Other candidate mechanisms that could also contribute to differentially regulating L5B projection neuron activity are the thalamocortical input and the inhibitory microcircuit organization of L5B. Recently, an AC circuit model was proposed based on *in vivo* evidence (Sun et al., 2013) in which fast-spiking (FS) interneurons selectively connect to PT neurons, and non-FS interneurons selectively interact with corticocallosal neurons. Moreover, the same study suggested a direct influence of thalamocortical inputs on sound-evoked activity of PT- but not corticocallosal-type neurons (Sun et al., 2013). An additional mechanism that could further contribute to the dichotomous activity in L5B projection neurons involves interneurons and is suggested by findings in M1 and prefrontal cortex: in M1 disynaptic inhibition is stronger in corticocallosal neurons compared to PT neurons (Apicella et al., 2012), while in prefrontal cortex PT neurons receive stronger feedforward inhibition (Lee et al., 2014).

2.4.2 Types of excitatory inputs in AC

Our findings complement and extend previous studies of AC L5 neurons and their circuit organization (Winer and Prieto, 2001). Sherman and colleagues propose that glutamatergic inputs can be classified as Class 1 (“driver”) or Class 2 (“modulatory”) (Reichova and Sherman, 2004; Lee and Sherman, 2008, 2010; De Pasquale and Sherman, 2011; Viaene et al., 2011a, b, c). Class 1 inputs have larger initial EPSPs, exhibit paired-pulse depression, and activate only ionotropic glutamate receptors. Class 2 inputs exhibit paired-pulse facilitation and activate both ionotropic and metabotropic glutamate receptors, and depression can be converted to facilitation by activation of postsynaptic mGluR2 receptors (De Pasquale and Sherman, 2012). Our results suggest that L2/3 axons, an important source of Class 1 inputs, may be further sub-divided based on their projection target (corticocollicular vs. corticocallosal), with distinct short-term plasticity properties.

2.4.3 Short-term plasticity in the neocortex

Although in a few cases facilitating excitatory connections have been described (Wang et al., 2006; Thomson and Lamy, 2007; Covic and Sherman, 2011), excitatory synaptic connections between cortical pyramidal neurons are usually depressing (Atzori et al., 2001; Thomson and Lamy, 2007; Oswald and Reyes, 2008; Covic and Sherman, 2011; Reyes, 2011). Because L2/3 inputs to L5B corticocallosal neurons depress, corticocallosal output is reduced during sustained cortical activity in frequencies where temporal summation of EPSPs is reduced (Figure 2-7H, I). In contrast, the lack of depression in the L2/3 to corticocollicular pathway renders the corticocollicular pathway active during sustained cortical activity, irrelevant of the frequency of presynaptic stimulation (Figure 2-6 and Figure 2-7). Our results are consistent previous studies showing pathway-specific depression of callosal inputs to IT neurons but not in PT neurons in L5 neurons of prefrontal cortex (Lee et al., 2014). Moreover, our results are consistent with the observed depression of IT inputs to IT neurons but no depression of PT inputs to PT neurons in prefrontal cortex and motor cortex (Morishima and Kawaguchi, 2006; Kiritani et al., 2012). Together, these studies suggest that excitatory inputs to PT cells are non-depressing, while excitatory inputs to IT cells are depressing.

2.4.4 Conclusions

Our findings complement and extend previous cortical studies revealing pathway-specific, short-term plasticity of excitatory inputs in intracortical circuits. For example, short-term plasticity of excitatory inputs differs among L2/3→2/3, L2/3→5 and L5→5 connections (Williams and Atkinson, 2007). Our results reveal differential short-term plasticity even within the L2/3→5B pathway, which is determined by the projectional identity of the L5B neuron -- the anatomical targeting of its long-range axonal branches to downstream centers. In this context, our results also extend recent studies in many cortical areas that have established that the projectional identity of cortical pyramidal neurons can be a major determinant of

functional properties (Morishima and Kawaguchi, 2006; Brown and Hestrin, 2009b, a; Anderson et al., 2010; Dembrow et al., 2010; Little and Carter, 2013; Shepherd, 2013).

Together, our results identify an activity-dependent fractionation of L2/3 excitatory input into two dynamically distinct L2/3→5B pathways with specific input-output functions, which promote sustained firing in L2/3→corticocollicular connections during different L2/3 stimulation rates and reduced firing in L2/3→corticocallosal connections during lower L2/3 stimulation rates. We propose that this functional architecture may represent a general feature of neocortical circuit design enabling divergent output channels to carry distinct information, rather than simply copies of the same signals.

2.5 MATERIALS AND METHODS

2.5.1 Animals

ICR mice (Harlan) (P22–P24 for microsphere injection and P24-P32 for recordings) of either sex were used for all experiments. All experimental procedures were approved by the Institutional Animal Care and Use Committee of the University of Pittsburgh.

2.5.2 Stereotaxic injections

Mice were anaesthetized with isoflurane (induction: 3 % in O_2, 0.6 L/min; maintenance: 50% of induction dose) and positioned in a stereotaxic frame (Kopf). Projection neurons in the auditory cortex (AC) were retrogradely labeled by injecting different colored fluorescent latex microspheres (Lumafluor Inc.) in the contralateral AC (in a small craniotomy drilled 4 mm posterior to bregma and 4 mm lateral, injection depth 1mm) and the ipsilateral inferior colliculus (1 mm posterior to lambda and 1 mm lateral, injection depth 0.75 mm). A volume of ~ 0.1 μL microspheres was pressure injected (25 psi, 10-15 msec duration)

from capillary pipettes (Drummond Scientific Company) with a Picospritzer (Parker-Hannifin). The injection volume was distributed between several sites along the injection depth so as to label the entire extent of the injection site. After injection, the pipette was held in the brain for 1.5 minutes before slowly withdrawing. The animals were allowed to recover for at least 48 hours to allow time for retrograde transport of the tracers.

2.5.3 *In vivo* flavoprotein autofluorescence imaging

Mice (n=11) were anesthetized with urethane (induction: 1.5 mg/g; maintenance: 50% of induction dose). An incision (~1.5 cm) was made in the scalp and an intramuscular injection of lidocaine-epinephrine (2%) was delivered to the left temporal muscle. The temporal muscle was separated from the skull sufficiently to allow access to the underlying AC (~4.0 – 4.5 mm from the midline). The skull overlying the AC was thinned by careful drilling and left intact for transcranial flavoprotein autofluorescence (FA) imaging. Dental acrylic was used to secure a head post to the skull over the ipsilateral frontal cortex and to create a reservoir for artificial cerebrospinal fluid (aCSF), which was periodically applied over the recording site to keep the skull from drying out. Subsequently, mice were head-fixed and FA intrinsic signals were recorded while the animals were exposed to low intensity auditory stimuli (amplitude-modulated tone with a carrier frequency of 5 kHz and modulation frequency of 20 Hz, 40-50 dB from speakers placed ~ 10 cm from the ear). The skull was exposed to blue light (LED light: peak wavelength = 461.4 nm; FWHM = 19.3 nm; M470L3, ThorLabs) for 10 seconds; 1 second long acoustic stimuli were presented 3 seconds after initiation of exposure to blue light. During this time the endogenous FA signal (540 nm) was recorded by a CCD camera (Middleton et al., 2011). Two regions of sound evoked FA activity were consistently observed: The more caudal of the two regions corresponds to the primary auditory cortex (A1) and the more rostral one corresponds to the anterior auditory field (AAF) (see Figure 2-1). After FA imaging and AC identification a small piece of skull overlying the region identified as AC was exposed (by carefully scoring the perimeter of the thinned skull with a fine surgical blade and removing a small

bone flap with fine forceps) and sulforhodamine was applied to the pial surface to label AC for *in vitro* identification experiments immediately after FA-assisted AC localization.

2.5.4 Slice electrophysiology

Coronal slices (300 μm) containing AC were prepared from mice that had previously been injected with retrograde beads and, in some experiments (n=5, used for assessing intrinsic properties), had also undergone FA-assisted AC localization (see above and Results describing Figure 1). The cutting solution (pH 7.35) contained the following (in mM): 2.5 KCl, 1.25 NaH_2PO_4, 25 $NaHCO_3$, 0.5 $CaCl_2$, 7 $MgCl_2$, 7 dextrose, 205 sucrose, 1.3 ascorbic acid, and 3 sodium pyruvate (bubbled with 95% O_2/5% CO_2). The slices were transferred and incubated at 36°C in a holding chamber for 30 minutes. The holding chamber contained aCSF (pH 7.35) containing the following (in mM): 125 NaCl, 2.5 KCl, 1.25 NaH_2PO_4, 25 $NaHCO_3$, 2 $CaCl_2$, 1 $MgCl_2$, 10 glucose, 1.3 ascorbic acid, and 3 sodium pyruvate (bubbled with 95% O_2/5% CO_2). Post incubation, the slices were stored at room temperature until the time of recording. Whole-cell recordings in voltage- and current-clamp modes were performed on slices bathed in carbogenated aCSF, which was identical to the incubating solution. The flow rate of the aCSF was ~1.5 ml/min, and its temperature was maintained at 32-34°C using an in-line heating system (Warner). To examine intrinsic properties, the following drugs were added to the aCSF (in mM): 0.02 DNQX (AMPA receptor antagonist), 0.05 APV (NMDA receptor antagonist), and 0.02 gabazine (GABAA receptor antagonist). Layer 5B of the AC was identified as the layer containing corticocollicular neurons. Recordings were targeted to either green fluorescent corticocollicular neurons or red fluorescent corticocallosal neurons within L5B. Borosilicate pipettes (World Precision Instruments) were pulled into patch electrodes with 3-6 MΩ resistance (Sutter Instruments) and filled with a potassium based intracellular solution which was composed of the following (in mM): 128 K-gluconate, 10 HEPES, 4 $MgCl_2$, 4 Na_2ATP, 0.3 Tris-GTP, 10 Tris Phosphocreatine, 1 EGTA, and 3 sodium ascorbate. Data were sampled at 10 kHz and Bessel filtered at 4 kHz using an acquisition control software package Ephus

(www.ephus.org) (Suter et al., 2010). Pipette capacitance was compensated and series resistance for recordings was lower than 25 MΩ. Series resistance was determined in voltage clamp mode (command potential set at -70 mV) by giving a -5 mV voltage step. Series resistance was determined by dividing the -5 mV voltage step by the peak current value generated immediately after the step in the command potential. The data were not corrected for 10 mV liquid junction potential. R_{input} was calculated in voltage-clamp mode (command potential set to -70 mV) by giving a -5 mV step, which resulted in transient current responses. The difference between baseline and steady state hyperpolarized current (ΔI) was used to calculate R_{input} using the following formula: $R_{input} = -5\ mV/\Delta I - R_{series}$. The average resting membrane potential (V_m) was calculated by holding the neuron in voltage-follower mode (current-clamp, at I = 0) immediately after breaking in and averaging the membrane potential over the next 20 seconds. Sub- and suprathreshold membrane responses in current-clamp were elicited by injecting -200 to +500 pA in 50 pA increments (baseline V_m was maintained at -75 mV, by injecting the required current if necessary). Sag was measured during the -200 pA current injection, using the formula, $SAG = (V_{min}-V_{steady\text{-}state})/V_{steady\text{-}state}$. The first resulting action potential (AP) at rheobase was analyzed for AP width. AP width was calculated as the full width at the half-maximum amplitude of the AP. Adaptation ratio and fast-doublet index were measured at the current step that gave the closest AP firing rate to 10 Hz. Firing rate increases were quantified by calculating the initial (150-250 pA) slope of the frequency-current (f-I) relationship. We chose to calculate the slope between those three particular current points because they are above the non-linear region of the curves near the rheobase, and they are below the region of large current values where the f-I functions start to saturate. Adaptation ratio was calculated by dividing the instantaneous frequency between the 9^{th} and 10^{th} AP by the instantaneous frequency between the 2nd and 3rd AP (f9/f2) (Figure 2-4 H, K). Fast-doublet index was calculated by dividing the instantaneous frequency between the 1^{st} and 2^{nd} AP by the instantaneous frequency between the 2^{nd} and 3^{rd} AP (f1/f2) (Figure 2-4 H, I, L). In Figure 2-3 and Figure 2-4, which examine intrinsic properties, 24/32 corticocollicular and 24/29 corticocallosal neurons were recorded from the same slice.

2.5.5 Paired recordings

Whole-cell recordings were established from a L2/3 and a bead-labeled corticocollicular or L5B corticocallosal neuron. For these experiments, we used coronal slices without dye in the pipettes and therefore without direct assessment of intactness of dendritic arbors. Connectivity was assessed by evoking a train (five pulses, 20 Hz) of action potentials in the L2/3 neuron while monitoring the postsynaptic response in the L5B neuron; at least 20 trials of the presynaptic train were delivered (10 sec inter trial interval); multiple trials were averaged to detect the presence of a connection. Events that were >3 standard deviations of the baseline noise level (noise levels were measured during a 50 msec timing period prior to the first spike in the presynaptic neuron) detected as events and were further analyzed. EPSC or EPSP latency was calculated as the time from the peak of the presynaptic AP to the time where the postsynaptic signal was >3 standard deviations of the baseline noise level. EPSC or EPSP amplitudes were obtained by averaging a 1 msec window around the peak response. Rise time was defined as the time from 20-80% of the peak response. Decay time constants were measured by fitting an exponential function from peak of a single EPSP to its baseline response. EPSC or EPSP trains were normalized to the amplitude of the first EPSC or EPSP before analyzing them for short-term plasticity. In current-clamp mode recordings, neurons were held at -75 mV. For 12 out of 14 L2/3→corticocollicular connected pairs and for 9 out of 11 L2/3→corticocallosal pairs, both EPCSs and EPSPs were recorded from the same postsynaptic neuron. With the exception of two paired recordings, we were not able to obtain more than one pair per slice.

2.5.6 Extracellular L2/3 stimulation and postsysnaptic spiking experiments

Whole-cell recordings were established from bead-labeled corticocollicular or L5B corticocallosal neurons from the same slice; L2/3 was stimulated with a theta glass stimulating electrode filled with extracellular solution. The stimulation electrode was positioned in L2/3, ~200 μm from the pial surface,

and laterally to the recording electrode in L5B to avoid direct stimulation of L5B neurons. EPSCs were obtained while holding the neuron at -70 mV. EPSPs were obtained in current clamp mode (membrane potential maintained at -75 mV for both cell types). To examine the effect of stimulation frequency on the firing of corticocallosal or to corticocollicular neurons, we adjusted the stimulus intensity such that in response to a stimulus train of 10 pulses at 20 Hz, ~50% spikes were evoked in the postsynaptic corticocallosal or corticocollicular neuron. Two stimulus trains (10 pulses in each train) were delivered for each frequency in the following order: 20 Hz, 10 Hz and 20 Hz (inter train interval: 10 sec). The spikes evoked by the two trains were averaged; i.e., we averaged the number of spikes evoked by trains 1 and 2 (20 Hz), the number of spikes evoked by trains 3 and 4 (10 Hz), and the number of spikes evoked by trains 5 and 6 (20 Hz). A trial was considered complete if the average number of spikes evoked in trains 5 and 6 did not change by > 20% compared to the average spikes evoked in trains 1 and 2. For each neuron, the average number of spikes per frequency was normalized to the average number of spikes of the first two trains at 20 Hz. All recordings from the two different neuronal types were performed from the same slice.

2.5.7 Morphological reconstructions

As described in detail previously (Suter et al., 2013), neurons were filled with biocytin during whole-cell recordings, and the slices were fixed, processed for streptavidin-based fluorescent labeling, and imaged by 2-photon microscopy. For morphological reconstructions, the angle of cutting was slightly modified for optimal preservation of dendritic arbors. Dendrites were three-dimensionally traced in stitched image stacks (Neurolucida) and data sets were further analyzed to quantify dendritic length as previously described (Shepherd et al., 2005; Yamawaki et al., 2014).

2.5.8 Statistical analysis

Data that were normally distributed (based on Lilliefors test) were analyzed using unpaired t-tests. For non-normally distributed data, we used the Wilcoxon rank sum test (indicated in the manuscript wherever this was the case). Within group analysis for paired recordings was done using paired t-tests. Significance was reported if p value < 0.05.

3.0 CHAPTER 2: CHOLINERGIC MODULATION OF EXCITABILITY OF LAYER 5B PRINCIPAL NEURONS IN MOUSE AUDITORY CORTEX

3.1 OVERVIEW

The neuromodulator acetylcholine (ACh) is important for important cognitive functions, such as perception, attention and learning and memory. Whereas in most cases the cellular circuits or the specific neurons via which ACh exerts its cognitive effects remain unknown, it is known that auditory cortex (AC) corticocollicular neurons, projecting from layer (L) 5B to the inferior colliculus, are required for cholinergic-mediated relearning of sound localization after occlusion of one ear. Therefore, elucidation of the effects of ACh on the excitability of corticocollicular neurons will bridge cell-specific properties and cognitive properties of ACh. To identify cell-specific mechanisms that enable corticocollicular neurons to participate in sound localization relearning - because AC L5B contains another class of neurons called corticocallosal neurons, which project to the contralateral cortex - we investigated the effects of ACh release on both L5B corticocallosal and corticocollicular neurons. Using *in vitro* electrophysiology and optogenetics in mouse brain slices, we found that ACh generated nicotinic (n) AChR-mediated depolarizing potentials and muscarinic (m) AChR-mediated hyperpolarizing potentials in AC L5B corticocallosal neurons. In corticocollicular neurons, ACh release also generated nAChR-mediated depolarizing potentials. However, in contrast to the mAChR-mediated hyperpolarizing potentials in corticocallosal neurons, ACh generated prolonged mAChR-mediated depolarizing potentials in corticocollicular neurons. This prolonged depolarizing potentials generated persistent firing in corticocollicular neurons, whereas corticocallosal neurons lacking mAChR-mediated depolarizing

potentials did not show persistent firing. We propose that ACh-mediated persistent firing in corticocollicular neurons may represent a critical mechanism required for learning-induced plasticity in AC.

3.2 INTRODUCTION

Acetylcholine (ACh) release in the cortex is crucial for perception, attention, learning and memory (Bear and Singer, 1986; Edeline et al., 1994; Kilgard and Merzenich, 1998b; Weinberger, 2003; Froemke et al., 2007; Bajo et al., 2010; Hasselmo and Sarter, 2011; Leach et al., 2013). As a result, the Nucleus Basalis (NB), which is the main source of cortical ACh (Lehmann et al., 1980; Dani and Bertrand, 2007), has been implicated in all these cognitive aspects. Despite the importance of these cognitive functions, the specific cortical neuronal types mediating these functions, as well as the synaptic effects of ACh on these neurons remain poorly understood.

In the auditory cortex (AC), pairing electrical stimulation of NB with an auditory stimulus induces stimulus-specific representational cortical plasticity and auditory memory (Kilgard and Merzenich, 1998b, a; Weinberger et al., 2006; Froemke et al., 2007), and enhances discrimination learning (Reed et al., 2011). Moreover, cortical cholinergic input is required for normal perception of sound source location and experience-dependent plasticity involved in relearning sound localization after reversible occlusion of one ear (Leach et al., 2013). Although in most cases the specific neuronal population upon which ACh acts to exert its cognitive and perceptual effects is not known, recent studies revealed that the cholinergic and experience-dependent plasticity involved in relearning sound localization after reversible occlusion of one ear is lost after specific elimination of corticocollicular neurons (Bajo et al., 2010), an AC layer 5B (L5B) neuronal type projecting to the inferior colliculus (IC). The knowledge of the specific neuronal population mediating learning-induced auditory plasticity, as well

as the necessity of cortical ACh for this mechanism provide an ideal model for determining the cell-specific synaptic mechanisms via which ACh enables sound localization.

Here, we investigated the effects of exogenous and endogenous ACh on the synaptic excitability of L5B corticocollicular neurons. However, L5B contains different types of projection neurons including corticocollicular, and corticocallosal neurons - a second major class of L5 neurons with axons projecting to the contralateral A1. Because recent studies in a variety of cortical areas, including the AC, have revealed numerous differences in the physiological properties of pyramidal tract (PT) neurons, of which corticocollicular are a subtype, and intratelencephalic (IT) neurons, of which corticocallosal neurons are a subtype (for review, see Shepherd, 2013), we hypothesize that ACh may have cell-specific effects on the excitability of projection neurons. These cell-specific effects may be important for the cholinergic-mediated experience-dependent plasticity involved in relearning sound localization after plugging one ear (Bajo et al., 2010), as well as in the distinct role of PT and IT neurons in the delay period that occurs during movement planning (Li et al., 2015).

To study the effects of ACh on corticocollicular and L5B corticocallosal neurons, we used *in vivo* retrograde labeling, as well as *in vitro* electrophysiological methods combined with optogenetic activation of cholinergic fibers. We show that ACh has cell-specific effects on L5B projection neurons. Namely, ACh elicits nicotinic ACh receptor- (nAChR) mediated depolarizing potentials in both neuronal types, whereas ACh evokes muscarinic ACh receptor- (mAChR) mediated hyperpolarizing potentials in corticocallosal neurons, but long-lasting mAChR-mediated depolarizing potentials only in corticocollicular neurons. The long-lasting mAChR depolarizing potential generates persistent firing in corticocollicular neurons, which may be involved in top-down modulation of auditory learning.

3.3 RESULTS

3.3.1 Exogenous application of acetylcholine generates distinct responses in AC L5B corticocallosal and corticocollicular neurons

To study the effect of ACh on AC L5B corticocallosal and corticocollicular neurons, AC L5B projection neurons were targeted for whole-cell recordings in current-clamp mode. Briefly, fluorescent microspheres were injected in the IC *in vivo*, while microspheres of different color were injected in the contralateral AC. In brain slices prepared two to three days later, corticocollicular and corticocallosal neurons were selectively labeled (Joshi et al., 2015). Layer 5B of the AC was identified as the layer containing corticocollicular neurons as (Games and Winer, 1988; Doucet et al., 2003; Doucet and Ryugo, 2003; Slater et al., 2013; Joshi et al., 2015). In all our experiments, recordings were targeted to either red fluorescent corticocollicular neurons or green fluorescent corticocallosal neurons within L5B.

In 23 out of 42 corticocallosal neurons, puff application of 100 µM ACh onto their somata (20 p.s.i, ~ 50 µm from soma) generated a monophasic depolarizing potential (Figure 3-1 A1, A2 control black trace). This depolarizing potential was mediated by nAChRs, because it was blocked by the application of a cocktail of nAChR blockers (5 µM Mecamylamine hydrochloride + 50 µM Hexamethonium bromide) (Figure 3-1 A1, orange trace; Figure 3-1 A3 summary). Furthermore, this depolarizing potential was blocked by 500 nM Dihydro-β-erythroidine (DHβE), a selective antagonist of α-4 receptor subunit of nAChRs, indicating that it was mediated by α-4 subunit containing nAChRs (Figure 3-1 A2, magenta trace; Figure 3-1 A3 summary). In 3 out of 10 corticocallosal neurons, application of nAChR blockers eliminated the depolarizing potential and revealed a hyperpolarizing potential (Figure 3-1 B1, black trace- depolarizing potential , magenta trace-hyperpolarizing potential after application of DHBE). This hyperpolarizing potential was blocked by the application of 1 µM atropine (mAChR blocker) (Figure 3-1 B1, green trace; Figure 3-1 B2 summary) indicating that it was mediated by muscarinic acetylcholine receptors (mAChRs).

In the rest of the recorded corticocallosal neurons (19 out of 42), puffing ACh onto their somata generated biphasic responses - a depolarizing potential followed by a hyperpolarizing potential (Figure 3-1 C1, black trace). Sequential application of 1 μM atropine and nAChR blocker cocktail abolished the hyperpolarizing and depolarizing potentials respectively (Figure 3-1 C1, green trace-atropine, orange trace- nAChR blocker cocktail; Figure 3-1 C2 hyperpolarizing potential summary ; Figure 3-1 C3 depolarizing potential summary). Together, our results show that exogenous application of ACh results in excitatory and inhibitory potentials in corticocallosal neurons, which are mediated by nAChRs and mAChRs, respectively.

Next we studied the effect of exogenous ACh on corticocollicular neurons. In 18 out of 28 corticocollicular neurons, puffing ACh onto their somata (20 p.s.i, ~ 50 μm from soma) generated a depolarizing potential (Figure 3-2 A1, A2 control black trace), which was mediated by nAChRs, because it was blocked by the application of nAChR blockers (Figure 3-2 A1, orange trace; Figure 3-2 A3 summary). Furthermore, the depolarizing potential was also blocked by 500 nM DHβE, indicating that it was mediated by α-4 subunit containing nAChRs (Figure 3-2 A2, magenta trace; Figure 3-2 A3 summary). In 2/10 corticocollicular neurons, application of nAChR blockers eliminated the depolarizing potential and revealed a hyperpolarizing potential (Figure 3-2 B, black trace- depolarizing potential, magenta trace- hyperpolarizing potential after application of DHBE). These results suggest that application of ACh revealed similar monophasic potentials in corticocollicular and corticocallosal neurons.

However, in 10 of 28 corticocollicular neurons exogenous application of ACh revealed a distinct response. Namely, puffing of ACh generated a 2 peak (peak 1 and peak 2) depolarizing potential (Figure 3-2 C1, black trace). Sequential application of nAChR blockers and 1 μM atropine (mAChR blocker) abolished peak 1 and peak 2, respectively (Figure 3-2 C2, orange trace- nAChR blocker cocktail, green trace-atropine; Figure 3-2 C3 summary peak 1; Figure 3-2 C4, summary peak 2). We concluded that peak 1 was mediated by nAChRs and the slower peak 2 was mediated by mAChRs. Together our results show that the exogenous ACh caused nAChR-mediated depolarizing potentials, which were similar between

L5B corticocallosal and corticocollicular neurons. On the other hand exogenous ACh activated mAChRs, which, in turn, caused hyperpolarizing potential in corticocallosal neurons, but delayed, long-lasting depolarizing potentials in corticocollicular neurons.

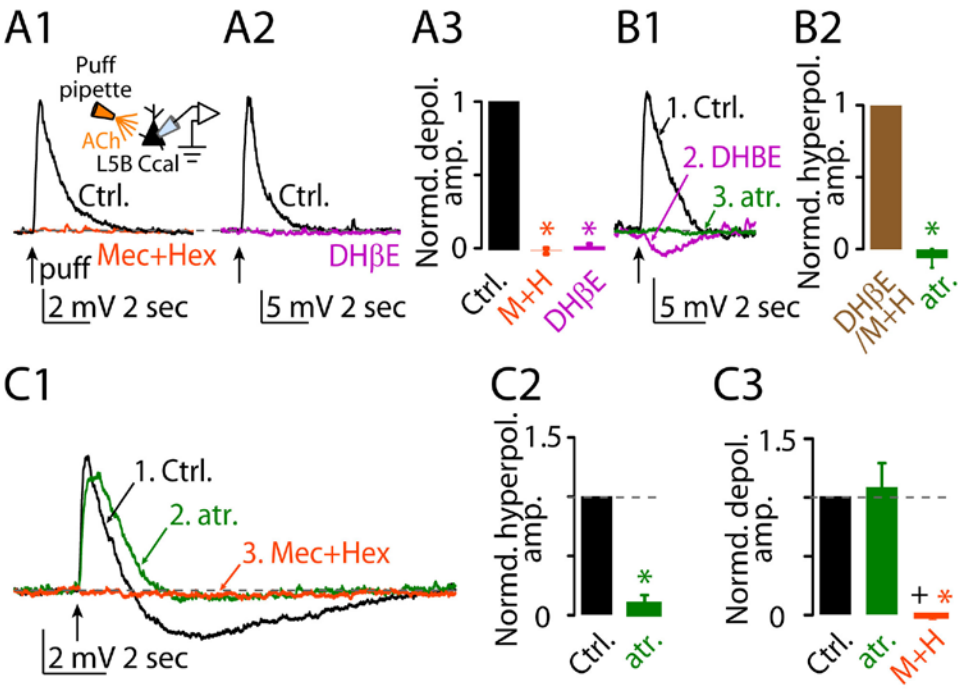

Figure 3-1: Puffing ACh generates nicotinic excitation and muscarinic inhibition in corticocallosal neurons.

Legends for Figure 3-1

A1, A single puff of 100 μM ACh (50 ms, 20 psi) denoted by the black arrow, generates a monophasic depolarizing potential (Ctrl. black trace) in a subset of corticocallosal neurons. The depolarizing potential is abolished by the addition of a cocktail of nAChR blockers (5 μM Mecamylamine hydrochloride + 50 μM Hexamethonium bromide, orange trace).

A2, The monophasic depolarizing potential (Ctrl. black trace) is also abolished by the addition of 500 nM DHβE (magenta trace).

A3, Group data summarizing the effects of the application of nAChR blocker cocktail and DHβE on the monophasic depolarizing potential (depolarizing potential amplitude in aCSF: 1.0 ± 0.0; depolarizing potential amplitude is significantly reduced after the addition of nAChR blockers as indicated by the orange asterix: -0.003 ± 0.02, n = 4, p-value = 0.0007); depolarizing potential amplitude is significantly reduced after the addition of DHβE as indicated by the magenta asterix: 0.03 ± 0.02; n = 3, p-value = 0.02).

B1, In 3/10 neurons, application of nAChR blocker cocktail (1 neuron) or DHβE (2 neurons) abolished the monophasic depolarizing potential but revealed a hyperpolarizing potential (Ctrl. black trace - depolarizing potential; DHβE magenta trace - hyperpolarizing potential). This hyperpolarizing potential was abolished by the addition of 1 μM atropine (green trace), a blocker of all mAChRs.

B2, Group data summarizing the effect of the application of atropine on the hyperpolarizing potential revealed in the presence of nAChR blockers (hyperpolarizing amplitude in aCSF: 1.0 ± 0.0; hyperpolarizing amplitude is significantly reduced after the addition of atropine as indicated by the green asterix: -0.06 ± 0.07, n = 3, p-value = 0.004).

C1, A single puff of 100 μM ACh (50 ms, 20 psi, 50 μm away from the soma) denoted by the black arrow, generates biphasic (depolarizing/hyperpolarizing) potentials - (Ctrl. black trace) in another subset of corticocallosal neurons. Sequential application of 1 μM atropine (green trace), a blocker of all mAChRs and a cocktail of nAChR blockers (5 μM Mecamylamine hydrochloride + 50 μM

Hexamethonium bromide) (orange trace) abolished the hyperpolarizing and depolarizing potential respectively.

C2, Group data summarizing the effect of the application of atropine on the hyperpolarizing potential in the biphasic response. The amplitudes of the responses have been normalized to amplitude of the hyperpolarizing potential in aCSF (hyperpolarizing potential amplitude in aCSF: 1.0 ± 0.0; hyperpolarizing potential amplitude is significantly reduced after the addition of atropine as indicated by the green asterix: 0.10 ± 0.08, n = 6, p-value < 0.0001).

C3, Group data summarizing the effects of the application of atropine and nAChR blocker cocktail on the depolarizing potential in the biphasic response. The amplitudes of the responses have been normalized to amplitude of the depolarizing potential in aCSF (depolarizing potential amplitude in aCSF: 1.0 ± 0.0, n = 6; depolarizing potential amplitude after the addition of atropine is not significantly different compared to the depolarizing potential amplitude in aCSF: 1.09 ± 0.21, n = 6, p > 0.05; depolarizing potential amplitude after the addition of nAChR blocker cocktail is significantly reduced compared to the depolarizing potential amplitude in aCSF (indicated by the orange asterix) and atropine (indicated by the plus sign): -0.01 ± 0.02, n = 6, n = 6, p < 0.01 compared to compared to aCSF, p < 0.01 compared to atropine)**.**

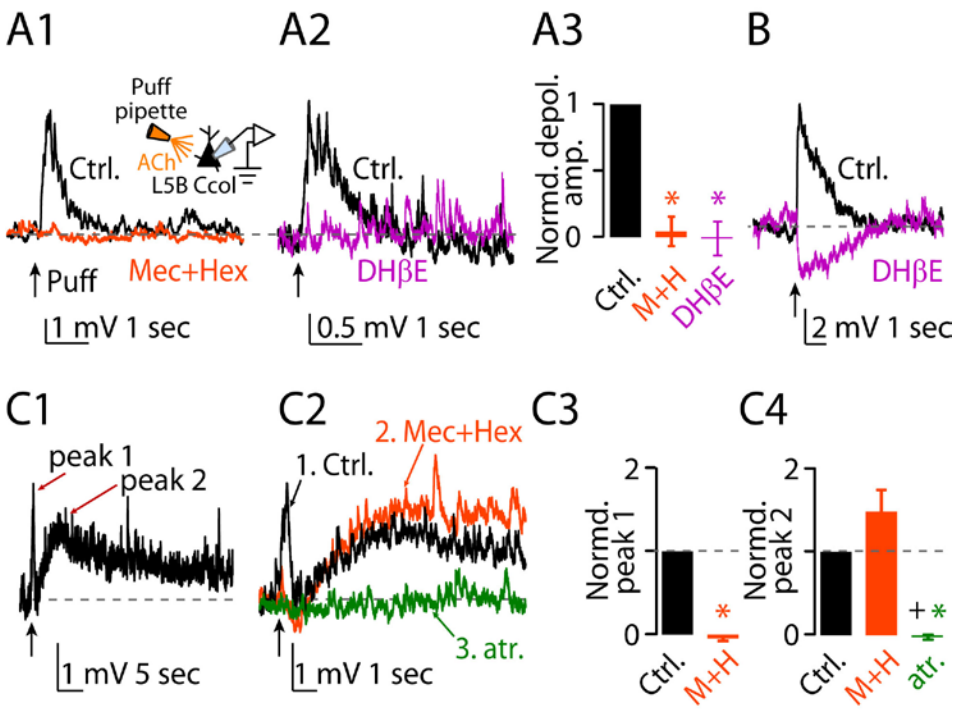

Figure 3-2: Puffing ACh generates nicotinic and muscarinic excitation in corticocollicular neurons.

Legends for Figure 3-2

A1, A single puff of 100 μM ACh (50 ms, 20 psi) denoted by the black arrow, generates monophasic depolarizing potential (Ctrl. black trace) in a subset of corticocollicular neurons. The depolarizing potential is abolished by the addition of a cocktail of nAChR blockers (5 μM Mecamylamine hydrochloride + 50 μM Hexamethonium bromide, orange trace).

A2, The monophasic depolarizing potential (Ctrl. black trace) is also abolished by the addition of 500 nM DHβE (magenta trace).

A3, Group data summarizing the effects of the application of nAChR blocker cocktail and DHβE on the monophasic depolarizing potential (depolarizing potential amplitude in aCSF: 1.0 ± 0.0; depolarizing potential amplitude is significantly reduced after the addition of nAChR blockers as indicated by the red

asterix: 0.05 ± 0.11, n = 4, p-value = 0.003); depolarizing potential amplitude is significantly reduced after the addition of DHβE as indicated by the magenta asterix: -0.01 ± 0.13; n = 4, p-value = 0.004).

B, In 2/10 neurons, application of nAChR blocker cocktail (1 neuron) or DHβE (1 neuron) abolished the monophasic depolarizing potential but revealed a hyperpolarizing potential (Ctrl. black trace - depolarizing potential; DHβE magenta trace –hyperpolarizing potential).

C1, A single puff of 100 μM ACh (50 ms, 20 psi, 50 μm away from the soma) denoted by the black arrow, generates 2 peak depolarizing potential (black trace, peak 1 and peak 2) in another subset of corticocollicular neurons.

C2, Sequential application of a cocktail of nAChR blockers (5 μM Mecamylamine hydrochloride + 50 μM Hexamethonium bromide) (orange trace) and 1 μM atropine (green trace), a blocker of all mAChRs abolished peak 1 and peak 2 respectively.

C3, Group data summarizing the effects of the application of nAChR blocker cocktail on peak 1 of 2 peak depolarizing potentials. The amplitudes of the responses have been normalized to amplitude of peak 1 in aCSF (peak 1 amplitude in aCSF: 1.0 ± 0.0; peak 1 amplitude is significantly reduced after the addition of nAChR blocker cocktail as indicated by the orange asterix: -0.07 ± 0.02, n = 3, p = 0.0003).

C4, Group data summarizing the effects of the application of nAChR blocker cocktail and atropine on peak 2 in 2 peak depolarizing potential. The amplitudes of the responses have been normalized to amplitude of peak 2 in aCSF (peak 2 amplitude in aCSF: 1.0 ± 0.0; peak 2 amplitude after the addition of nAChR blocker cocktail is not significantly different compared to the depolarizing potential amplitude in aCSF: 1.47 ± 0.27, n = 3, p-value > 0.05; peak 2 amplitude after the addition of atropine is significantly

reduced compared to the depolarizing potential amplitude in aCSF (indicated by the green asterix) and nAChR blocker cocktail (indicated by the plus sign) : -0.02 ± 0.03, n = 3, $p < 0.01$ compared to aCSF, $p < 0.02$ compared to nAChR blocker cocktail).

3.3.2 Endogenous release of acetylcholine evokes distinct responses in corticocollicular and corticocallosal neurons

Next, we determined whether endogenous release of ACh on AC L5B corticocallosal and corticocollicular neurons has actions similar to those of exogenous ACh. To investigate the effect of endogenous ACh, we used the *ChAT-ChR2-EYFP* mouse line, which expresses the light activated cation channel channelrhodopsin (ChR2) selectively in cholinergic axons (Zhao et al., 2011). To confirm the presence of *ChR2-EYFP* fibers amongst AC L5B corticocallosal and corticocollicular neurons, we performed *in vivo* injections of fluorescent retrograde tracers in *ChAT-ChR2-EYFP* mice. Small volumes of red fluorescent microspheres (red emission) were injected in the IC, while choleratoxin (far red emission) was injected in the contralateral AC (Figure 3-3 A). Mice were perfused a week later and then their brains were cryoprotected and subsequently sectioned on a microtome into 50 μm thick AC-containing sections. Epifluorescence imaging revealed labeled corticocollicular neurons in L5B of the AC (Figure 3-3 B), whereas choleratoxin labeled corticocallosal neurons were present in L5 B and other layers of the auditory cortex (Figure 3-3 C). EYFP containing green cholinergic axons were also present in L5B AC (Figure 3-3D). An overlay of the three separate images (Figure 3-3 B, C and D) revealed an intermingled population of auditory cortex L5B corticocollicular and corticocallosal neurons (red and blue) amongst green cholinergic axons (Figure 3-3 E), thus confirming the presence of cholinergic axons in L5B of the auditory cortex.

To assess the effects of endogenous release of ACh on AC L5B corticocallosal neurons, we used widefield illumination of the slice with a blue LED ($\lambda = 470$ nm) to activate ChR2-containing cholinergic terminals and evoke ACh release. In 12 out of 21 corticocallosal neurons, endogenous release of ACh by

stimulation with a single pulse of blue light (pulse width = 5 ms) generated a monophasic depolarizing potential, which was similar to the monophasic depolarizing potential we observed with exogenous ACh (Figure 3-4 A1 - control black trace). To assess the pharmacology of these responses, we stimulated with 10 pulses of blue light (at 50 Hz), as the responses were more robust. This monophasic depolarizing potential was mediated by nAChRs because it was blocked by the application of nAChR blockers (Figure 3-4 A2, orange trace; Figure 3-4 A4 summary). Furthermore, the depolarizing potential was also blocked by 500 nM DHβE, indicating that it was mediated by α-4 subunit containing nAChRs (Figure 3-4 A3, magenta trace; Figure 3-4 A4 summary).

In 4 out of 21 corticocallosal neurons, endogenous release of ACh with a single pulse of blue light generated biphasic responses – a depolarizing potential followed by a hyperpolarizing potential (Figure 3-4 B1 - control black trace). Sequential application of 1 μM atropine and nAChR blockers abolished the hyperpolarizing and depolarizing potential respectively, showing that biphasic response was mediated by n- and mAChRs (Figure 3-4 B2 - Control black trace depolarization/hyperpolarization, green trace after atropine, orange trace after nAChR blockers; Figure 3-4 B3 the summary of the effect of atropine on the hyperpolarizing potential; Figure 3-4 B4 summary of the effect of atropine and nAChR blockers on the depolarizing potential). Finally, in 5 out 21 corticocallosal neurons, endogenous release of ACh by optogenetic stimulation with a single pulse of blue light generated a hyperpolarizing potential (Figure 3-4 C1 - control black trace). This hyperpolarizing potential was mediated by mAChRs, because it was abolished by the application of 1 μM atropine (Figure 3-4 C2 Control black trace hyperpolarizing potential, green trace atropine, Figure 3-4 C3 summary). Although we did not observe monophasic hyperpolarizing potentials with extracellular ACh application, taken together, our results indicate that exogenous and endogenous ACh had similar effects on the excitability of L5B corticocallosal neurons.

Next we studied the effect of endogenous ACh on the excitability of corticocollicular neurons. In 5 out of 13 corticocollicular neurons, 1 or 10 pulses of blue light elicited monophasic responses (Figure 3-5 A1). Because corticocollicular neurons consistently gave responses to 60 pulses delivered at 50 Hz, we employed this stimulation protocol for assessing the response of corticocollicular neurons to endogenous

ACh. Under these conditions, in 7 out of 13 corticocollicular neurons, endogenous release of ACh generated a monophasic depolarizing potential, which was similar to the monophasic depolarizing potential we observed with exogenous ACh (Figure 3-5 A2 - control black trace). This depolarizing potential was mediated by α-4 subunit containing nAChRs, because it was blocked by DHβE (Figure 3-5 A2, magenta trace; Figure 3-5 A3 summary). Moreover, in 2 out of 5 corticocollicular neurons which showed a depolarizing potential, application of nAChR blockers eliminated the depolarizing potential and revealed a hyperpolarizing potential, which was blocked by the application of atropine (Figure 3-5 B) indicating that it was mediated by mAChRs. These results show that the responses due to endogenous ACh resemble the responses obtained with exogenous application of ACh.

In 6 out of 13 corticocollicular neurons, photostimulation of cholinergic fibers elicited a broader depolarizing potential that exceeded the train of photostimulation (Figure 3-5 C1, black trace). This broad depolarizing potential was reminiscent of the peak 2 of the '2 peak depolarizing potential' obtained in response to exogenous ACh. Because peak 2 of the '2 peak depolarizing potential' was mediated by mAChRs (Figure 3-2 C1, C2), we tested whether the broad depolarizing potential was also mediated by mAChRs. Application of 1 μM atropine revealed a narrower depolarizing potential (Figure 3-5 C1, green trace) which was subsequently eliminated by application of nAChR blockers (Figure 3-5 C1, C3 orange trace). Together these results suggest that endogenous ACh, like exogenous ACh, generates n- and mAChR-mediated depolarizing potentials in corticocollicular neurons; the mAChR-mediated depolarizing potentials are long-lasting.

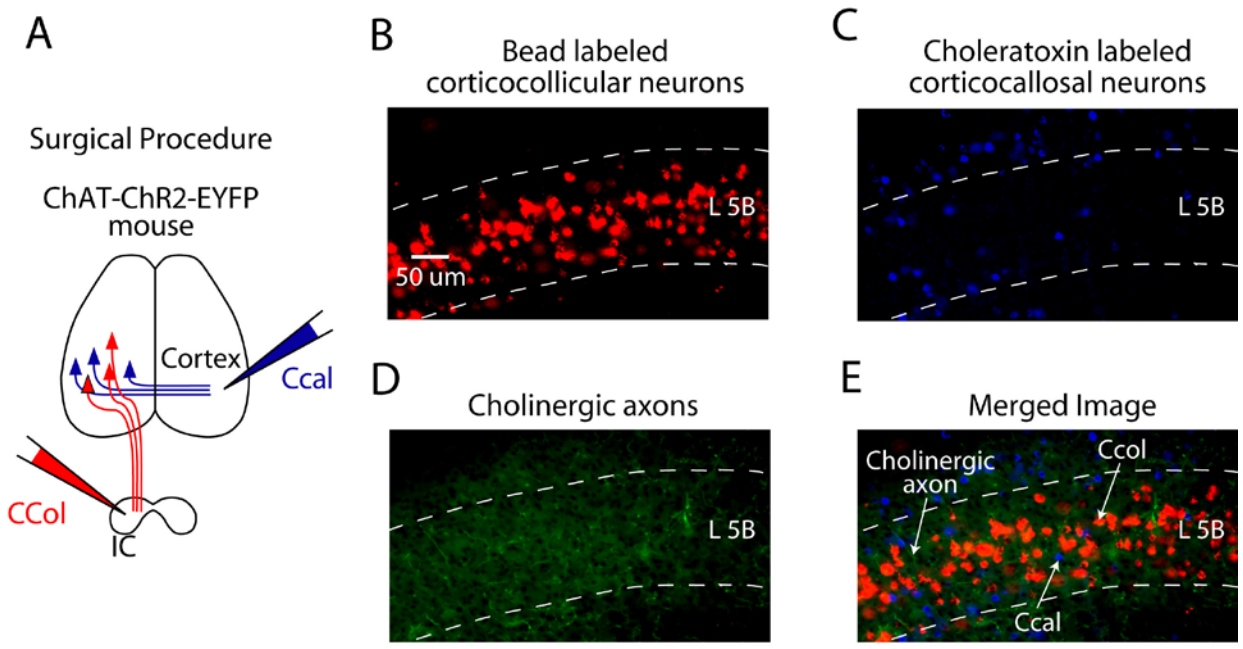

Figure 3-3: Cholinergic axons are present in the auditory cortex and are intermingled amongst corticocollicular and corticocallosal neurons.

Legends for Figure 3-3

A. Labeling of corticocollicular and corticocallosal neurons with fluorescent tracers. Projection neurons in the AC were labeled by injecting different colored retrograde tracers in the contralateral AC (choleratoxin to label corticocallosal neurons) and the ipsilateral inferior colliculus (red fluorescent microspheres to label corticocollicular neurons).

B. 20 X epifluorescence image showing labeled corticocollicular neurons in L5B of the AC.

C. 20 X epifluorescence image showing labeled corticocallosal neurons in L5B and other layers of the AC.

D. 20 X epifluorescence image showing green cholinergic axons in L5B of AC. E. Merged image showing intermingled population of corticocallosal and corticocollicular neurons amongst green cholinergic axons in L5B of AC.

E. Merged image **(B, C,** and **D** combined**)** showing intermingled population of corticocallosal and corticocollicular neurons amongst green cholinergic axons in L5B of AC.

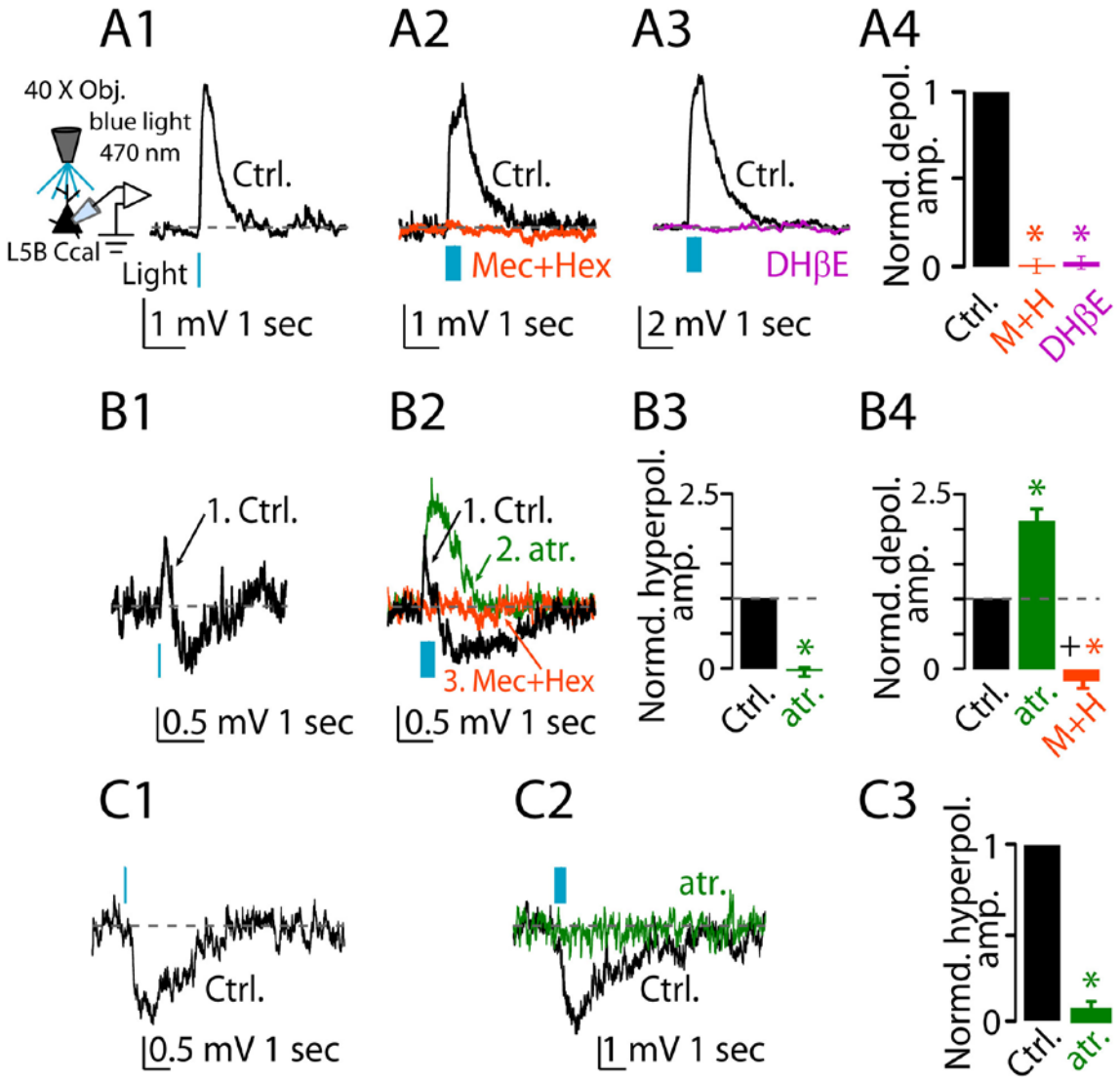

Figure 3-4: Release of endogenous ACh by optogenetic stimulation generates nicotinic excitation and muscarinic inhibition in corticocallosal neurons.

Legends for Figure 3-4

A1, Optogenetic stimulation with a single pulse (λ = 470 nm, pulse width 5 ms) denoted by the blue vertical bar, generates a monophasic depolarizing potential (Ctrl. black trace) in a subset of corticocallosal neurons. *Note: pharmacology was established using optogenetic stimulation with 10 pulses (λ = 470 nm, pulse width 5 ms) denoted the blue rectangle.*

A2, The monophasic depolarizing potential is abolished by the addition of a cocktail of nAChR blockers (5 μM Mecamylamine hydrochloride + 50 μM Hexamethonium bromide, orange trace).

A3, The monophasic depolarizing potential (Ctrl. black trace) is also abolished by the addition of 500 nM DHβE (magenta trace).

A4, Group data summarizing the effects of the application of nAChR blocker cocktail and DHβE on the monophasic depolarizing potential (depolarizing potential amplitude in aCSF: 1.0 ± 0.0; depolarizing potential amplitude is significantly reduced after the addition of nAChR blockers as indicated by the red asterix: 0.01 ± 0.04, n = 3, p = 0.001); depolarizing potential amplitude is significantly reduced after the addition of DHβE as indicated by the magenta asterix: 0.03 ± 0.04; n = 5, p < 0.0001).

B1, Optogenetic stimulation with a single pulse (λ = 470 nm, pulse width 5 ms) denoted by the blue vertical bar, generates a biphasic (depolarizing/hyperpolarizing) potentials (Ctrl. black trace) in another subset of corticocallosal neurons**.**

B2, Sequential application of 1 μM atropine (green trace), a blocker of all mAChRs and a cocktail of nAChR blockers (5 μM Mecamylamine hydrochloride + 50 μM Hexamethonium bromide) (orange trace) abolished the hyperpolarizing and depolarizing potential respectively.

B3, Group data summarizing the effect of the application of atropine on the hyperpolarizing potential in the biphasic response. The amplitudes of the responses have been normalized to amplitude of the hyperpolarizing potential in aCSF (hyperpolarizing potential amplitude in aCSF: 1.0 ± 0.0; hyperpolarizing potential amplitude is significantly reduced after the addition of atropine as indicated by the green asterix: -0.05 ± 0.07, n = 3, p = 0.008).

B4, Group data summarizing the effects of the application of atropine and nAChR blocker cocktail on the depolarizing potential in the biphasic response. The amplitudes of the responses have been normalized to amplitude of the depolarizing potential in aCSF (depolarizing potential amplitude in aCSF: 1.0 ± 0.0, $n = 6$; depolarizing potential amplitude after the addition of atropine is significantly increased compared to the depolarizing potential amplitude in aCSF: 2.07 ± 0.15, $n = 3$, $p < 0.01$; depolarizing potential amplitude after the addition of nAChR blocker cocktail is significantly reduced compared to the depolarizing potential amplitude in aCSF (indicated by the plus sign) and atropine (indicated by the green asterix): -0.17 ± 0.08, $n = 3$, $p < 0.02$ compared to compared to aCSF, $p < 0.03$ compared to atropine**)**.

C1, Optogenetic stimulation with a single pulse ($\lambda = 470$ nm, pulse width 5 ms) denoted by the blue vertical bar, generates a monophasic hyperpolarizing potential (Ctrl. black trace) in another subset of corticocallosal neurons.

C2, The hyperpolarizing potential is abolished by the addition of a 1 μM atropine (green trace), a blocker of all mAChRs.

C3, Group data summarizing the effects of the application of atropine on inhibitory responses (hyperpolarizing potential amplitude in aCSF: 1.0 ± 0.0; hyperpolarizing potential amplitude is significantly reduced after the addition of atropine 0.12 ± 0.08; $n = 3$, $p = 0.008$).

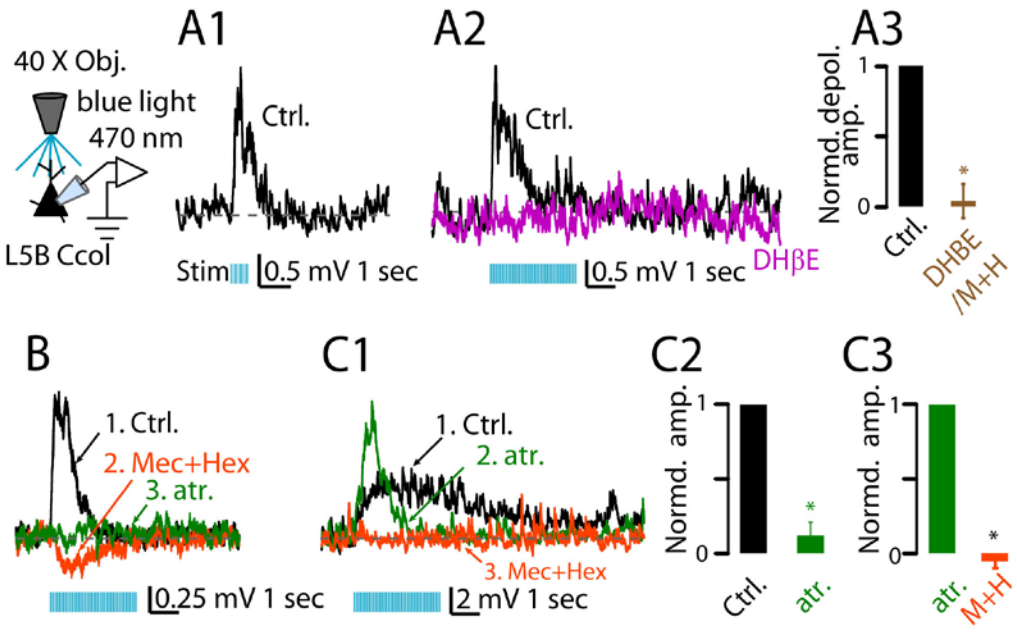

Figure 3-5: Release of endogenous ACh by optogenetic stimulation generates nicotinic and muscarinic excitation in corticocollicular neurons.

Legends for Figure 3-5

A1, Optogenetic stimulation with 1 or 10 pulses (λ = 470 nm, pulse width 5 ms @ 50 Hz) denoted by the blue rectangle, generates a monophasic depolarizing potential (Ctrl. black trace) in small number (5/13) of corticocollicular neurons.

A2, Optogenetic stimulation with 60 pulses (λ = 470 nm, pulse width 5 ms @ 50 Hz) denoted by the blue rectangle, generates a monophasic depolarizing potential (Ctrl. black trace) in a subset of corticocollicular neurons. The depolarizing potential is abolished by the addition 500 nM DHβE (magenta trace) in 2 neurons and a cocktail of nAChR blockers (5 μM Mecamylamine hydrochloride + 50 μM Hexamethonium bromide, data not shown) in 1 neuron.

A3, Group data summarizing the effects of the application of nAChR blocker cocktail and DHβE on the monophasic depolarizing potential (depolarizing potential amplitude in aCSF: 1.0 ± 0.0; depolarizing potential amplitude is significantly reduced after the addition of nAChR blockers/ DHβE as indicated by the brown asterix: 0.05 ± 0.12, n = 3, p-value = 0.003).

B, In 2/5 neurons, the application of nAChR blocker cocktail abolished the monophasic depolarizing potential but revealed an hyperpolarizing potential (Ctrl. black trace.- depolarizing potential; orange trace, Mecamylamine hydrochloride + Hexamethonium bromide - hyperpolarizing potential). This hyperpolarizing potential was abolished by the addition of 1 μM atropine (green trace), a blocker of all mAChRs in 2/2 neurons.

C1, Optogenetic stimulation with 60 pulses (λ = 470 nm, pulse width 5 ms @ 50 Hz) denoted by the blue rectangle, generates a broad depolarizing potential (Ctrl. Black trace) in another subset of corticocollicular neurons. Application of 1 μM atropine, a blocker of all mAChRs changed the shape of the broad depolarizing potential to resemble that of a monophasic depolarizing potential (green trace). Post atropine treatment, application of a cocktail of nAChR blockers (5 μM Mecamylamine hydrochloride + 50 μM Hexamethonium bromide- orange trace) abolished the remaining response.

C2, Group data summarizing the effects of the application atropine on broad depolarizing potentials. To quantify the mAChR-mediated component in the broad depolarizing potential, we plotted the response after the application of atropine (green trace, **C1**) onto the original broad depolarizing potential (black trace, **C1**). The muscarinic component was quantified as the membrane depolarization of the black trace, by averaging 500 ms of membrane depolarization from the time point 50 msec after the green trace reached baseline value. (depolarizing potential amplitude in aCSF: 1.0 ± 0.0; depolarizing potential amplitude is significantly reduced after the addition of atropine: 0.12 ± 0.09; n = 4, p = 0.002).

C3, Group data summarizing the effect of the application of nAChR blocker cocktail on the remaining monophasic depolarizing potential (green trace) in **C1**. The nicotinic component was the membrane potential (average of 20 ms around the peak of the green trace in **C1** (depolarizing potential amplitude in aCSF: 1.0 ± 0.0; depolarizing potential amplitude is significantly reduced after the addition of atropine: -0.05 ± 0.04; n = 4, p = 0.0001).

3.3.3 Muscarinic AChRs mediate persistent firing in corticocollicular neurons

Our results show that release of ACh onto AC L5B pyramidal neurons resulted in distinct responses in corticocollicular and corticocallosal neurons. The most prominent difference is seen in a subset of corticocollicular neurons, which exhibit a fast nicotinic depolarizing potential and a prolonged muscarinic depolarizing potential upon the release of ACh. Such a prolonged depolarizing potential has the potential to cause neurons to fire persistently in response to transient suprathreshold stimulus. Because, cholinergic activation leads to persistent firing in cortical neurons, which is associated with mnemonic and learning tasks (Haj-Dahmane and Andrade, 1996, 1998; Wang, 2001; Egorov et al., 2002; Egorov et al., 2006; Fransen et al., 2006; Gulledge et al., 2009; Dembrow et al., 2010; Hedrick and Waters, 2015), we hypothesized that corticocollicular neurons displaying prolonged mAChR-mediated depolarizing potentials will display persistent firing in response to endogenous ACh release or exogenous ACh application.

Consistent with our hypothesis, puffing or endogenous release of ACh onto corticocallosal neurons with monophasic depolarizing potentials or biphasic (depolarizing /hyperpolarizing potentials) responses (Figure 3-6 A1, B1, C1), when held near their action potential (AP) threshold, elicited transient firing but failed to elicit any persistent firing (Figure 3-6 A2, B2, C2). Plots of the firing frequency as a function of time indicated that corticocallosal neurons fired APs only during the stimulus or immediately after stimulus termination (Figure 3-6 A3, B3, C3). Note that even 60 pulses stimulation did not induce persistent firing in corticocallosal neurons (Figure 3-6 C4, C5, C6). Similar results were obtained from

exogenous puffing or endogenous release of ACh onto corticocollicular neurons exhibiting monophasic depolarizing potentials (Figure 3-6, D1-D3, E1-E3). However the subset of corticocollicular neurons which exhibit 2 peak depolarizing potentials or broad depolarizing potentials (Figure 3-7 A1, B1), showed persistent firing in response to either exogenous or endogenous ACh (Figure 3-7 A2, B2). Plots of the firing frequency as a function of time indicated that corticocollicular neurons which exhibit broad depolarizing potentials fired APs for > 10 seconds after stimulus termination (Figure 3-7 A3, B3). Persistent firing was abolished upon application of atropine, suggesting that mAChRs are crucial for the persistent firing of corticocollicular neurons (Figure 3-7 A4, A5, B4, B5). Finally, the intrinsic properties, such as AP threshold and AP width, did not change from the onset of firing and during the spike train (Figure 3-7 C, D), suggesting that mAChRs promote persistent firing without affecting the intrinsic AP properties. This finding suggests that ACh is capable of converting AC neurons projecting to the IC into a "persistent" mode, whereas intracortically projection neurons do not enter this mode. The persistent firing maybe essential for the ACh-dependent, learning-induced plasticity mediated by corticocollicular neurons (Bajo et al., 2010; Leach et al., 2013).

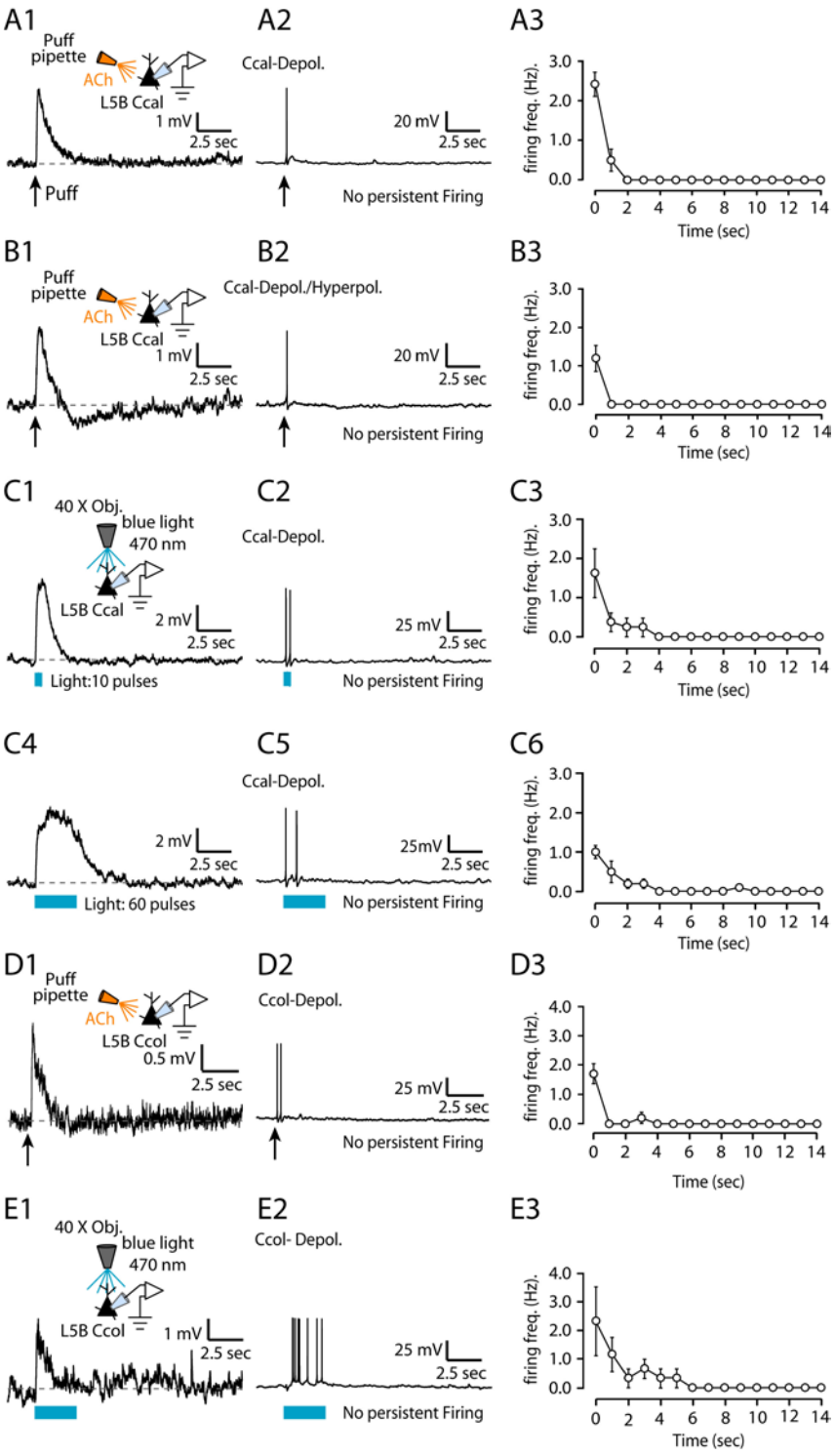

Figure 3-6: ACh release generates transient spiking in corticocallosal and corticocollicular neurons lacking prolonged mAChR-mediated depolarizing potentials.

Legends for Figure 3-6

A1, An example of a corticocallosal neuron, which responds with a monophasic depolarizing potential to a puff of 100 μM ACh (50 ms, 20 psi), denoted by the black arrow.

A2, The same neuron as in **A1**, when held close to its action potential threshold, fires transiently in response to a puff of ACh. This transient spiking was observed in 7/7 corticocallosal neurons with monophasic depolarizing potentials.

A3, Average firing frequency quantified for 15 seconds starting at the time of stimulus onset (t = 0) for APs as in **A2** (n = 7).

B1, An example of a corticocallosal neuron, which responds with a biphasic potential to a puff of 100 μM ACh (50 ms, 20 psi, 50 μm away from the soma).

B2, The same neuron as in **B1**, when held close to its action potential threshold, fires transiently in response to a puff of ACh. This transient spiking was observed in 5/5 corticocallosal neurons with biphasic responses.

B3, Average firing frequency quantified for 15 seconds starting at the time of stimulus onset (t = 0) for APs as in **B2** (n = 5).

C1, An example of a corticocallosal neuron, which responds with a monophasic depolarizing potential to release of endogenous ACh by optogenetic stimulation with 10 pulses of blue light (λ = 470 nm, pulse width = 5 ms @ 50 Hz).

C2, The same neuron as in **C1**, when held close to its action potential threshold, fires transiently in response to the same optogenetic stimulation used in **C1**. This transient spiking was observed in 4/4 corticocallosal neurons with monophasic depolarizing potentials.

C3, Average firing frequency quantified for 15 seconds starting at the time of stimulus onset (t = 0) for APs as in **C2** (n = 4).

C4, The corticocallosal neuron as in **C1**, responds with a broader monophasic depolarizing potential to release of endogenous ACh by optogenetic stimulation with 60 pulses of blue light (λ = 470 nm, pulse width = 5 ms @ 50 Hz).

C5, The same neuron as in **C4**, when held close to its action potential threshold, fires transiently in response to the same optogenetic stimulation used in **C4**.

C6, Average firing frequency quantified for 15 seconds starting at the time of stimulus onset (t = 0) for APs as in **C5** (n = 5).

D1, An example of a corticocollicular neuron, which responds with a monophasic depolarizing potential to a puff of 100 μM ACh (50 ms, 20 psi, 50 μm away from the soma).

D2, The same neuron as in **D1**, when held close to its action potential threshold, fires transiently in response to a puff of ACh. This transient spiking was observed in 5/5 corticocollicular neurons with monophasic depolarizing potentials.

D3, Average firing frequency quantified for 15 seconds starting at the time of stimulus onset (t = 0) for APs as in **D2** (n = 5).

E1, An example of a corticocollicular neuron, which responds with a monophasic depolarizing potential to the release of endogenous ACh by optogenetic stimulation with 60 pulses of blue light (λ = 470 nm, pulse width = 5ms @ 50 Hz).

E2, The same neuron as in **E1**, when held close to its action potential threshold, fires transiently in response to the same optogenetic stimulation used in **E1**. This transient spiking was observed in 3/3 corticocollicular neuron with a monophasic depolarizing potentials.

E3, Average firing frequency quantified for 15 seconds starting at the time of stimulus onset (t = 0) for APs as in **E2** (n = 3).

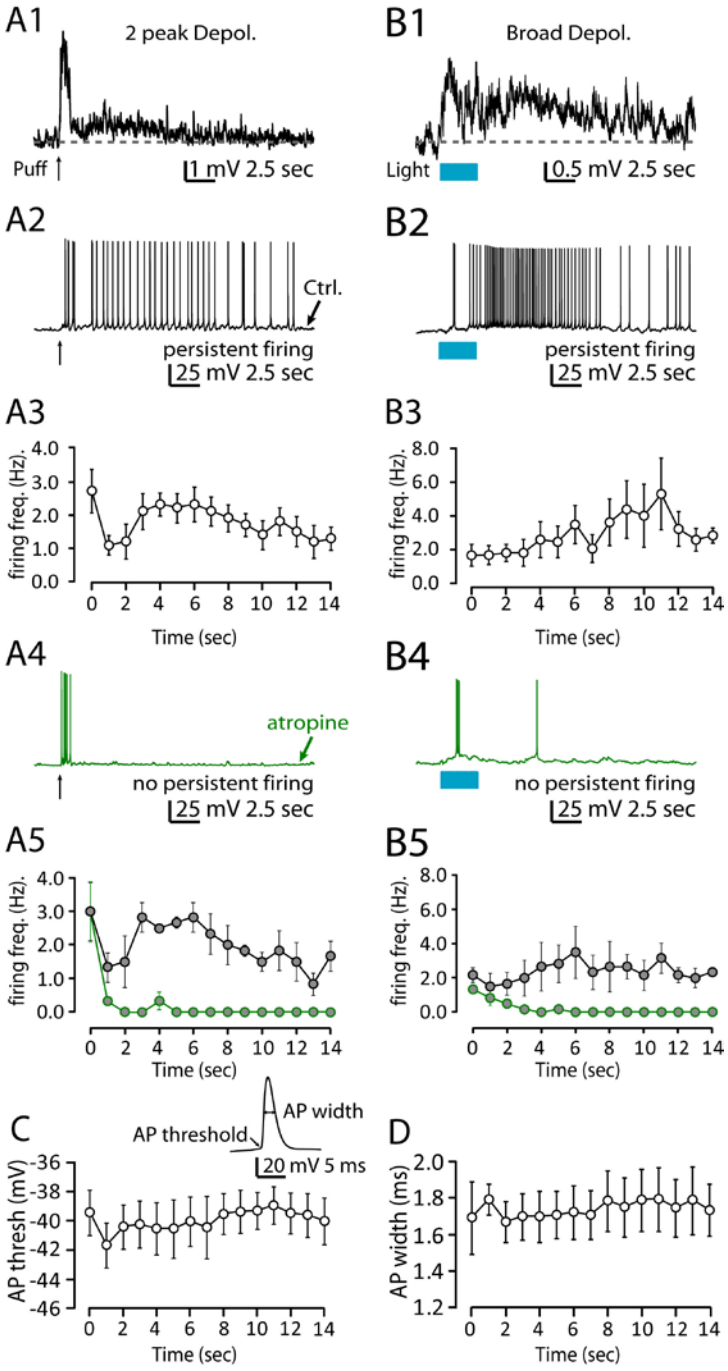

Figure 3-7: ACh release generates persistent firing in corticocollicular neurons that show prolonged mAChR-mediated depolarizing potentials, and this persistent firing is abolished by atropine.

Legends for Figure 3-7

A1, An example of a corticocollicular neuron, which responds with a 2 peak depolarizing potential to a puff of ACh.

A2, The same neuron as in **A1**, when held close to its action potential threshold, fires persistently in response to a puff of ACh. This persistent firing was observed in 5/5 corticocollicular neurons with 2 peak depolarizing potentials.

A3, Average firing frequency quantified for 15 seconds starting at the time of stimulus onset (t = 0) for trains of APs as generated in **A2** (n = 5).

A4, After the application of 1 μM atropine, the same neuron as in **A1 and A2**, fails to fire persistently in response to a puff of ACh. This effect of atropine was seen in 3/3 persistently firing corticocollicular neurons with 2 peak depolarizing potentials.

A5, Average firing frequency quantified for 15 seconds starting at the time of stimulus onset, before and after the application of atropine. Atropine causes a significant reduction in the firing of the neuron indicated by the black asterix. (Average firing frequency for the last five seconds (t = 10-14) in control: 1.52 ± 0.34; Average firing frequency for the last five seconds (t = 10-14) in atropine: 0.00 ± 0.00, n = 3, $p < 0.05$).

B1, An example of a corticocollicular neuron, which responds with a broad depolarizing potential to the release of endogenous ACh by optogenetic stimulation with 60 pulses of blue light (λ = 470 nm, pulse width = 5ms @ 50 Hz).

B2, The same neuron as in **B1**, when held close to its action potential threshold, fires persistently in response to the same optogenetic stimulation used in **B1**. This persistent firing was observed in 4/4 corticocollicular neurons with broad depolarizing potentials.

B3, Average firing frequency quantified for 15 seconds starting at the time of stimulus onset for trains of APs as generated in **B2** (n = 4).

B4, After the application of 1 μM atropine, the same neuron as in **B1 and B2**, fails to fire persistently in response to the same optogenetic stimulation used in **B1 and B2**. This effect of atropine was seen in 3/3 persistently firing corticocollicular neurons with broad depolarizing potentials.

B5, Average firing frequency quantified for 15 seconds starting at the time of stimulus onset, before and after the application of atropine. Atropine causes a significant reduction in the firing of the neuron indicated by the black asterix. (Average firing frequency for the last five seconds in control: 2.36 ± 0.54; Average firing frequency for the last five seconds in atropine: 0.00 ± 0.00, $n = 3$, $p < 0.05$).

C-D, AP threshold and AP width were quantified as a function of time for the persistent firing generated in response to optogenetic stimulation as in **B2**. The inset shows the first AP from the spike train in **B2** along with its AP threshold and AP width.

C, Group average showing the AP threshold plotted as a function of time. The AP threshold did not change significantly during persistent firing (average AP threshold during stimulus (t = 0-2): -40.63 ± 1.55, average AP threshold during the last five seconds of the train (t = 10-14): -39.62 ± 1.36, $n = 4$, $p = 0.16$).

D, Group average showing the AP width plotted as a function of time. The AP width did not change significantly during persistent firing (average AP width during stimulus (t = 0-2): 1.70 ± 0.12, average AP width during the last five seconds (t = 10-14): 1.77 ± 0.16, n = 4, p = 0.22).

3.4 DISCUSSION

To assess the effects of ACh on the excitability of L5B projection neurons, we used *in vivo* retrogradely fluorescent labeling to selectively label corticocollicular and L5B corticocallosal neurons, single-cell electrophysiology, exogenous application of ACh as well as selective stimulation of cholinergic fibers. Whereas exogenous and endogenous ACh generated fast nAChR-mediated depolarizing potentials in corticocollicular and corticocallosal neurons, ACh release generated mAChR-mediated hyperpolarizing potentials in corticocallosal neurons but long-lasting mAChR-mediated depolarizing potentials in corticocollicular neurons. The long-lasting mAChR depolarizing potentials were crucial for the persistent firing observed selectively in corticocollicular neurons, which may be involved in auditory learning.

3.4.1 Acetylcholine-mediated persistent firing in corticocollicular neurons: roles and mechanisms

ACh-mediated neuronal modulation causes persistent firing in several neocortical areas as well as in the substantia nigra pars compacta and subthalamic nucleus (Andrade, 1991; Haj-Dahmane and Andrade, 1996; Egorov et al., 2002; Yamashita and Isa, 2003a, b; Egorov et al., 2006; Fransen et al., 2006; Gulledge et al., 2009; Dembrow et al., 2010; Hedrick and Waters, 2015). In these brain areas, persistent firing of selective neuronal populations is a proposed cellular mechanism underlying learning and mnemonic functions, such as working memory (Wang, 2001; Hasselmo and Stern, 2006; Barak and Tsodyks, 2014). Our results show that cholinergic activation generates persistent firing in a subset of corticocollicular neurons, which display prolonged mAChR-mediated depolarizing potentials. Because

these neurons are crucial for cholinergic-mediated auditory learning of sound localization (Bajo et al., 2010; Leach et al., 2013), we propose that persistent firing in corticocollicular neurons is a critical mechanism for auditory learning. Moreover, we predict that mAChR blockers will block this form of auditory learning.

ACh-mediated persistent firing in other brain areas relies either on mAChR-mediated enhancement of postsynaptic calcium and enhancement of afterdepolarizing potentials (ADP) generated by a calcium-activated nonselective cation current, or activation of nAChRs and elevations in postsynaptic calcium (Haj-Dahmane and Andrade, 1999; Egorov et al., 2002; Yamashita and Isa, 2003a, b; Egorov et al., 2006; Zhang and Seguela, 2010; Rahman and Berger, 2011; Hedrick and Waters, 2015). Our results show that the persistent firing activity of corticocollicular neurons in response to ACh release is mediated by mAChRs. Whereas our studies did not evaluate the role of postsynaptic calcium, because mAChR activation does not affect the spiking properties of corticocollicular neurons and because the time course of persistent firing matches the time course of the mAChR-mediated prolonged depolarization, we propose that it is this depolarization that generates persistent firing lasting for about 10-20 sec after stimulus termination. Therefore, our studies support an additional mechanism for generating persistent firing in cortical neurons.

3.4.2 Cell-specific cholinergic neuromodulation of AC L5B corticocallosal and corticocollicular neurons

AC L5B corticocallosal and corticocollicular neurons fall in the broader category of IT and PT neurons respectively. PT tract neurons project to subcortical targets whereas IT neurons project to the contralateral cortex. Studies in different cortical areas showed that PT and IT type neurons differ not only in their projection targets, but also display differences in their anatomical (Gao and Zheng, 2004; Dembrow et al., 2010; Sun et al., 2013), intrinsic (Dembrow et al., 2010; Sheets et al., 2011; Slater et al., 2013; Suter et al., 2013; Joshi et al., 2015) and synaptic/circuit properties (Morishima and Kawaguchi, 2006; Anderson

et al., 2010; Dembrow et al., 2010; Kiritani et al., 2012; Lee et al., 2014; Joshi et al., 2015). These multiple projection-specific cellular and synaptic mechanisms collectively promote dichotomous activity in L5 neurons, leading to sustained (tonic) responses in corticocollicular neurons, and transient (phasic) responses in corticocallosal neurons. This hypothesis is further validated by the dichotomous response PT and IT neurons to sound *in vivo* (Sun et al., 2013). Our results, which are consistent with differential effects of neuromodulatory systems on PT and IT neurons (Dembrow et al., 2010; Avesar and Gulledge, 2012; Gee et al., 2012; Sun et al., 2013), further contribute to the dichotomous phasic/tonic activity in L5 projection neurons, because ACh promotes persistent firing in PT, but not in IT neurons.

The distinct responses of PT and IT neurons to cholinergic modulation suggest that they subserve distinct functions. This is consistent with recent findings showing that during motor planning and movement behavior activity with a contralateral population bias arises specifically in PT, but not in IT, neurons (Li et al., 2015). The ability of PT neurons to undergo persistent firing beyond their stimulus input makes them good candidates to contribute to persistent activity that occurs during the delay period that occurs during movement planning. Indeed, recent findings show that population activity in PT neurons appears and persists for hundreds of milliseconds prior to movement onset (Li et al., 2015).

3.4.3 nAChR- and mAChR-mediated responses in Layer 5 cortical pyramidal neurons

Several studies have used exogenous ACh and one study (Hedrick and Waters, 2015) has used endogenous ACh (Hedrick and Waters, 2015) to study cholinergic neuromodulation in L5 cortical neurons. Exogenous and endogenous ACh causes mAChR-mediated hyperpolarizing and depolarizing responses as well as facilitation and inhibition in L5 principal neurons of different cortices (Metherate et al., 1992; Gulledge and Stuart, 2005; Gulledge et al., 2007). Overall, these responses are consistent with mAChRs mediating slow depolarizing potentials observed in corticocollicular neurons and hyperpolarizing potentials in corticocallosal neurons in L5B AC. However, the biphasic response seen in AC L5 corticocallosal neurons is unique to the AC. In AC L5 corticocallosal neurons, biphasic responses

consisted of a depolarization followed by a hyperpolarization, which were mediated by nAChRs and mAChRs respectively, whereas in the somatosensory cortex biphasic responses consisted of a hyperpolarization followed by a depolarization, which were both mediated by mAChRs (Gulledge and Stuart, 2005).

Exogenous application or endogenous release of ACh also generates nAChR-mediated responses in L5 pyramidal neurons somatosensory, prefrontal and motor cortices (Zolles et al., 2009; Poorthuis et al., 2013; Hedrick and Waters, 2015). Nicotinic AChR-mediated depolarizing responses in L5 prefrontal cortex are mediated by α-7 subunit containing nAChRs (Poorthuis et al., 2013), whereas depolarizing responses in L5 somatosensory cortex are mediated by α-7 subunit containing and α-4 subunit containing nAChRs (Zolles et al., 2009). In L5B of the AC, exogenous and endogenous ACh generates nAChR-mediated depolarizing potentials in both corticocallosal and corticococollicular neurons, which are mediated by α-4 containing nAChRs, presumably α4β2 nAChRs. Our results are similar to results obtained from motor cortex, which showed that the α-4 subunit containing nAChR-mediated depolarizing potentials in L5 pyramidal neurons (Hedrick and Waters, 2015).

The hypothesized combined effect of mAChs and nAChRs on AC receptive fields is to reduce receptive field width and to enhance responsiveness within the sharpened receptive field (reviewed by Metherate, 2011). Several *in vivo* studies have shown that stimulation of NB enhances, via mAChRs, afferent responses in AC evoked by thalamic (Metherate et al., 1992; Metherate and Ashe, 1993) or acoustic stimulation (Edeline et al., 1994; Chen and Yan, 2007). This result is consistent with the mAChR-mediated prolonged depolarizing potentials that we observed in corticocollicular neurons. Moreover, sharpening of receptive fields by mAChRs is consistent with the biphasic and inhibitory potentials we observed in L5B corticocallosal neurons. Moreover, although previous studies have shown that nAChRs enhance responsiveness via presynaptic regulation of thalamocortical transmission (reviewed by Metherate, 2004), our results add an additional mechanism that can enhance responsiveness. Namely, the nAChR-mediated depolarizing potentials observed in corticocollicular L5B corticocallosal also contribute ACh-mediated enhanced responsiveness of AC receptive fields. Together, our results are

consistent with *in vivo* studies revealing sharpening and enhancement of AC receptive fields by ACh. Importantly, our results provide cellular and synaptic mechanisms via which ACh mediates its effects on AC receptive fields.

3.5 MATERIALS AND METHODS

3.5.1 Animals

ICR mice (Harlan) (P22–P30 for microsphere injection and P24-P40 for recordings) of either sex were used for experiments that examined the effect of exogenous application of ACh on corticocollicular and corticocallosal neurons. *ChAT-ChR2-EYFP* mice (C57BL/6J strain) (B6.Cg-Tg(Chat-COP4*H134R/EYFP)6Gfng/J; The Jackson Laboratory) (P30–P40) for microsphere injection and P32-P45 for recordings) of either sex were used for experiments that examined the effect of endogenous release of ACh on corticocollicular and corticocallosal neurons. All experimental procedures were approved by the Institutional Animal Care and Use Committee of the University of Pittsburgh.

3.5.2 Stereotaxic injections

Mice were anaesthetized with isofluorane (induction: 3% in O_2, 0.6 L/min; maintenance: 50% of induction dose) and positioned in a stereotaxic frame (Kopf). Projection neurons in the (AC were retrogradely labeled by injecting different colored fluorescent latex microspheres (Lumafluor Inc.) in the contralateral AC (in a small craniotomy drilled 4 mm posterior to bregma and 4 mm lateral, injection depth 1mm) and the ipsilateral inferior colliculus (1 mm posterior to lambda and 1 mm lateral, injection depth 0.75 mm). A volume of ~ 0.1 μL microspheres was pressure injected (25 psi, 10-15 msec duration) from capillary pipettes (Drummond Scientific Company) with a Picospritzer (Parker-Hannifin). The

injection volume was distributed between several sites along the injection depth so as to label the entire extent of the injection site. After injection, the pipette was held in the brain for 1.5 minutes before slowly withdrawing. The animals were allowed to recover for at least 48 hours to allow time for retrograde transport of the tracers.

3.5.3 Slice electrophysiology

Coronal slices (300 μm) containing AC were prepared from mice that had previously been injected with retrograde beads. The cutting solution (pH 7.35) contained the following (in mM): 2.5 KCl, 1.25 NaH_2PO_4, 25 $NaHCO_3$, 0.5 $CaCl_2$, 7 $MgCl_2$, 7 dextrose, 205 sucrose, 1.3 ascorbic acid, and 3 sodium pyruvate (bubbled with 95% O_2/5% CO_2). The slices were transferred and incubated at 36°C in a holding chamber for 30 minutes. The holding chamber contained aCSF (pH 7.35) containing the following (in mM): 125 NaCl, 2.5 KCl, 1.25 NaH_2PO_4, 25 $NaHCO_3$, 2 $CaCl_2$, 1 $MgCl_2$, 10 glucose, 1.3 ascorbic acid, and 3 sodium pyruvate (bubbled with 95% O_2/5% CO_2). Post incubation, the slices were stored at room temperature until the time of recording. Whole-cell recordings in voltage- and current-clamp modes were performed on slices bathed in carbogenated aCSF, which was identical to the incubating solution. The flow rate of the aCSF was ~1.5 ml/min, and its temperature was maintained at 32-34°C using an in-line heating system (Warner). Layer 5B of the AC was identified as the layer containing corticocollicular neurons. Recordings were targeted to either green fluorescent corticocollicular neurons or red fluorescent corticocallosal neurons within L5B. Borosilicate pipettes (World Precision Instruments) were pulled into patch electrodes with 3-6 MΩ resistance (Sutter Instruments) and filled with a potassium based intracellular solution which was composed of the following (in mM): 128 K-gluconate, 10 HEPES, 4 $MgCl_2$, 4 Na_2ATP, 0.3 Tris-GTP, 10 Tris Phosphocreatine, 1 EGTA, and 3 sodium ascorbate. Data were sampled at 10 kHz and Bessel filtered at 4 kHz using an acquisition control software package Ephus (www.ephus.org) (Suter et al., 2010). Pipette capacitance was compensated and series resistance for recordings was lower than 25 MΩ.

3.5.4 Puffing experiments

After establishing whole-cell recording from corticocallosal or corticocollicular neurons, 100 μM ACh was puffed for 20 ms at 20 p.s.i from a patch pipette placed 50 μm from the neuronal soma. Responses were identified if they were >2.5 standard deviations of the baseline noise level (noise levels were measured during a 100 msec timing period prior to the ACh puff) and were further analyzed.

3.5.5 Optogenetic experiments

After establishing whole-cell recordings from corticocallosal or corticocollicular neurons, we used wide-field illumination (using the 40 X objective) with a blue LED (470 nm at maximum intensity, Thor Labs) to activate ChR2 containing cholinergic axons. Stimulations ranged from a single 5 ms pulse of blue light to 10 or 60 pulses (5 ms each, 50 Hz). Responses were identified if they were > 2.5 standard deviations of the baseline noise level (noise levels were measured during a 100 msec timing period prior to illumination) and were further analyzed.

To test for persistent firing, neurons were depolarized by a current injection to a membrane potential that was close to firing threshold. Firing frequency of the APs elicited in response to ACh release was plotted as a function of time starting from the stimulus onset (time, t=0) to 15 seconds after the termination of the stimulus. Persistent firing was defined as the ability of the neuron to fire APs at least 5 seconds after the stimulus (t=0) termination. AP threshold was measured as the membrane potential corresponding to the time where the first derivative of the AP crossed 10 mV/second. AP width was calculated as the full-width at the half-maximum amplitude of the AP.

3.5.6 Pharmacology

The identity of the receptors mediating the responses elicited by the release of ACh on corticocollicular or L 5B corticocallosal neurons was established by applying blockers of nAChRs and mAChRs (nAChR mediated responses identified by the application of a cocktail of nAChR blockers Mecamylamine hydrochloride (5 μM) + Hexamethonium bromide (50 μM), or Dihydro-β-erythroidine (DHβE) (500 nM); mAChR mediated responses identified by the application of atropine (1 μM). The blockers were applied for at least 10 minutes before assessing their effects on the evoked responses. All drugs were obtained from Sigma.

3.5.7 Anatomy

For anatomical visualization of EYFP-containing cholinergic axons amongst corticocollicular and L 5B corticocallosal neurons, ChAT-ChR2-EYFP mice were injected with red colored fluorescent latex microspheres in the IC to label corticocollicular neurons, and choleratoxin (far red emission) in the contralateral auditory cortex to label corticocallosal neurons. Mice were allowed to recover for 7 days and were subsequently perfused with 4% paraformaldehyde (PFA). The brains were extracted and post-fixed in 4 % PFA for 4 hours, after which they were cryoprotected overnight in 25% sucrose solution maintained at 4 degrees Celsius. The brains were washed with phosphate buffer solution the next day and were sectioned on a microtome into 50 μm thick sections, containing the auditory cortex. The sections were mounted and imaged on an Olympus microscope with a 20 X objective using standard filters for green, red and far-red emissions. The acquired images were subsequently processed in ImageJ for brightness and contrast.

3.5.8 Statistical analysis

Paired t-test was used for all statistical analysis to compare the effect of drug applications on responses generated by exogenous or endogenous release of ACh. In cases where 2 drugs were added sequentially, a one-way ANOVA was used to examine the effect of each drug application on the response. Significance was reported if p-value was found to be < 0.05.

4.0 GENERAL DISCUSSION

The novelty of this dissertation arises from the use of retrograde labeling of AC L5B projection neurons, which allowed us to identify distinct cell-specific intrinsic and synaptic properties of AC L5B corticocallosal and corticocollicular neurons. This is significant as such a comparison has not been conducted in AC L5 previously. These cell-specific intrinsic and synaptic properties reveal potential mechanisms that contribute to the dichotomous *in vivo* responses of AC L5 projection neurons to sound and enable them to participate in relearning sound localization after monaural occlusion. Furthermore our findings corroborate and extend the knowledge, about differences in the general properties of IT and PT neurons in the neocortex.

4.1 PART 1

4.1.1 Corticocollicular labeling marks the location of AC

We used *in vivo* flavoprotein autofluorescence imaging and retrograde labeling of corticocollicular neurons to locate the auditory cortex in mice. Our results show that AC can be located by playing low frequency sounds (5 kHz) which reveal two distinct non-overlapping regions in the AC, where the caudal region represents the primary auditory cortex (A1) and the rostral region represents the anterior auditory fields (AAF). This result is consistent with many previous studies that have employed mirror-reversed tonotopic gradients to identify A1 and AAF in at least twenty species (Kaas, 2011) including mice

(Stiebler et al., 1997; Takahashi et al., 2006; Guo et al., 2012; Honma et al., 2013). Furthermore, we consistently found retrogradely labeled corticocollicular neurons in brain slices (prepared from mice that had undergone AC localization) in the regions of the mouse cortex that corresponded to the *in vivo* location of A1. Therefore in general, retrograde corticocollicular labeling can be used as an effective way to locate and target AC in future *in vitro* studies.

4.1.2 Morphology of AC L5B corticocallosal and corticocollicular neurons

In general, the morphology of AC L5B corticocallosal and corticocollicular neurons is similar to the morphology of L5 pyramidal neurons in the neocortex and is characterized by anatomical features found in pyramidal neurons such as a basal perisomatic arbor and a prominent apical dendrite which extends into layer 1. Previous studies have reported that the morphology of putative L5 IT and PT neurons in the AC (the RS and IB neurons respectively) is extremely varied, in that PT neurons are characterized by a tufted dendrite which extends into layer 1, while L5 IT neurons lack this apical tuft and their dendrites do not reach layer 1 and are limited to L2/3 (Hefti and Smith, 2000; Sun et al., 2013). Our morphological reconstructions show that AC L5B corticocallosal and corticocollicular neurons are mostly similar in their morphology. Unlike putative L5 IT, neurons, the apical dendrites of both L5B corticocallosal and corticocollicular neurons extend into layer 1 of the AC. The only difference we find is that corticocollicular neurons display more horizontally spreading apical tufts compared to corticocallosal neurons, similar to AC L5 putative IT and PT neurons (Hefti and Smith, 2000). Our results are also congruous to labeled L5 IT and PT neurons in medial prefrontal cortex, where more horizontal spread is reported in the apical dendrites of PT neurons in comparison to IT neurons (Dembrow et al., 2010).

4.1.3 Intrinsic properties of AC L5B corticocallosal and corticocollicular neurons and their contribution to *in vivo* responses of AC L5 IT and PT neurons to sound

Differences in intrinsic properties of IT and PT neurons are well established in various cortical areas, but how these differences translate into behavioral functions remains poorly understood (Shepherd, 2013). Our findings discussed below provide a plausible explanation of how differences in the intrinsic properties of AC L5B projection neurons can help shape their distinct *in vivo* behavior to sound.

The output of a neuron in response to a stimulus is not just a function of its synaptic connectivity, but also a function of how it responds to the stimulus itself (Shepherd, 2013). Therefore, we examined intrinsic properties of AC L5B corticocallosal and corticocollicular neurons in the presence of blockers of synaptic excitation and inhibition. Our results show that AC L5B corticocallosal and corticocollicular neurons have distinct intrinsic properties which affect their spiking behavior.

An analysis of sub-threshold intrinsic properties reveal that corticocollicular neurons display significantly more hyperpolarization-activated current- I_h, compared to corticocallosal neurons. Consistent with the role of I_h in the setting a depolarizing the resting membrane potential (Robinson and Siegelbaum, 2003), corticocollicular neurons also have a more depolarized resting membrane potential compared to corticocallosal neurons. However, consistent with the presence of I_h, corticocollicular neurons also have decreased input resistance compared to corticocallosal neurons. Increased I_h in corticocollicular neurons compared to corticocallosal neurons is consistent with studies showing greater I_h in PT than IT neurons in the medial prefrontal cortex (Dembrow et al., 2010; Gee et al., 2012) and motor cortex (Sheets et al., 2011; Suter et al., 2013). Greater I_h in corticocollicular neurons in comparison to corticocallosal neurons also supports the finding that HCN 1 mRNA levels are higher in PT neurons in comparison to IT neurons (Sheets et al., 2011). It can be argued that the greater presence of I_h in corticocollicular neurons also makes them more susceptible to neuromodulatory influences that affect I_h. For example, noradrenaline reduces I_h in PT neurons in the medial prefrontal cortex and increases the

temporal summation of EPSPs which drives the generation of APs, whereas IT neurons are unaffected by noradrenaline (Dembrow et al., 2010).

Our results also reveal that corticocollicular and corticocallosal neurons display distinct suprathreshold spike related properties. Corticocollicular neurons in comparison to corticocallosal neurons display a more hyperpolarized AP threshold, narrower APs and a lack of spike frequency adaptation. Furthermore, we found that at the onset of the current injection, corticocollicular neurons tend to fire two APs in quick succession (a doublet) while corticocallosal neurons do not. This doublet is similar to the *in vitro* burst like behavior reported in putative AC IB neurons (Hefti and Smith, 2000). Additionally, the ability of corticocollicular neurons to fire doublets in the presence of blockers of synaptic transmission suggest that intrinsic properties of corticocollicular neurons contribute to the observed *in vivo* burst like behavior of putative AC PT neurons in response to sound (Sun et al., 2013). While we have not explored the underlying mechanisms generating this bursting behavior, increase in intracellular Ca^{2+} is important for bursting behavior (Slater et al., 2013). Furthermore, the difference in suprathreshold intrinsic properties such as the narrow AP width and lack of spike frequency adaptation suggests that corticocollicular neurons are capable of generating sustained APs in comparison to corticocallosal neurons. This result can also explain the *in vivo* responses of putative AC L5 PT neurons to a wide range of sound frequencies in comparison to IT neurons (Sun et al., 2013). In general, spike frequency adaptation in corticocallosal neurons and the lack of it in corticocollicular neurons is consistent with the existing literature, which shows similar differences in firing patterns in L 5 IT and PT neurons in the, frontal cortex (Morishima and Kawaguchi, 2006; Dembrow et al., 2010) and the motor cortex (Suter et al., 2013).

4.1.4 Synaptic connections from L2/3 to AC L5B corticocallosal and corticocollicular neurons and their contribution to *in vivo* responses of AC L5 IT and PT neurons to sound

We examined unitary connections from L2/3→L5B corticocallosal and corticocollicular neurons as L2/3 is a major source of excitatory input to L5 pyramidal neurons (Adesnik and Scanziani, 2010; Anderson et al., 2010; Wallace and Jufang, 2011; Shepherd, 2013; Harris and Shepherd, 2015). Our results - the similar connection probability and similar strength of the unitary EPSC amplitude between L2/3→L5B corticocallosal neurons and corticocollicular neurons suggests that in L5B AC, the strength of inputs from L2/3 to 5B to projection neurons is similar. A previous study in the motor cortex found that in upper L5B, L2/3 inputs to PT neurons are stronger than inputs to IT neurons (Anderson et al., 2010). Since we did not evaluate the probability of connections or the strength of unitary EPSC amplitude based on the location of the postsynaptic neurons in L5B, we cannot be certain if the similarity in the strength of input from L2/3→L5B corticocallosal and corticocollicular neurons is a specific feature of the AC. However, given that AC is a sensory neocortical area involved in different tasks than the motor cortex, it may very well be that the similarity in the strength of L2/3 input to different classes of AC L5B projection neurons is a feature unique to the sensory neocortex or to the AC itself.

The major finding of our study is that unitary excitatory inputs from L2/→L 5B corticocallosal neurons and corticocollicular neurons display distinct short term plasticity; specifically, L2/3→ L5B corticocallosal inputs are depressing, while L2/→L5B corticocollicular inputs are non-depressing. A study in the AC using extracellular presynaptic stimulation showed that excitatory inputs from L2/3 to layer 5B are subdivided into depressing and facilitating inputs (Covic and Sherman, 2011). Our results support this finding, but more importantly, reveal that differences in short term plasticity of L2/3 inputs to L5B neurons in AC is dependent on the projectional identity of the L5B neuron. Our result also supports the recent finding in the medial prefrontal cortex, where inputs from the contralateral cortex (i.e. callosal inputs) to L5 IT neurons are depressing whereas inputs to L5 PT neurons are non-depressing. Additionally, our data is consistent with the short-term plasticity observed in the inputs to L5 IT and PT

neurons of the neocortex. In L5 of the motor cortex, IT→IT excitatory connections are depressing, while P→PT excitatory connections are non-depressing (Kiritani et al., 2012). In L5 of the frontal cortex, IT→IT connections are depressing while IT→PT connections are non-depressing (Morishima and Kawaguchi, 2006). These studies and ours results show that excitatory connections to PT neurons are non-depressing while excitatory connections to IT neurons are depressing.

While most excitatory connections between pyramidal neurons are depressing (Atzori et al., 2001; Thomson and Lamy, 2007; Oswald and Reyes, 2008; Covic and Sherman, 2011; Kiritani et al., 2012), our data supports the limited but emerging evidence which suggests that pathway specific short-term plasticity may be a general feature of the neocortex enabling different projection neurons to subserve divergent roles in cortical processing. Indeed, the non-depressing L2/3 inputs to corticocollicular neurons, indicating a sustained relay of information, could contribute to the sustained *in vivo* activity of putative AC PT neurons to sound (Sun et al., 2013). This view is further supported by our result which shows that depressing inputs to AC L5B corticocallosal neurons result in reduced AP generation during sustained cortical activity in frequencies where temporal summation of EPSPs is reduced. On the other hand, the lack of depressing inputs to corticocollicular neurons promotes consistent AP generation during sustained cortical activity regardless of the frequency of the presynaptic activity.

4.1.5 Putative mechanisms shaping the activity of AC L5B corticocallosal and corticocollicular neurons and their potential to contribute to *in vivo* responses of AC L5 IT and PT neurons to sound

It is known that IT and PT neurons make recurrent connections (within-class) in the neocortex (Morishima and Kawaguchi, 2006; Wang et al., 2006; Kiritani et al., 2012). But another defining feature - hierarchical connectivity-exists in the neocortex. In simple terms, this implies that presynaptic IT neurons excite postsynaptic IT and PT neurons but presynaptic PT neurons only excite postsynaptic PT neurons but not IT neurons (Shepherd, 2013). This has been shown in the frontal cortex where IT neurons show unidirectional connectivity toward PT neurons (Morishima and Kawaguchi, 2006). Similar results have

been found in the L5B motor cortex - unidirectional connectivity is seen between IT and PT neurons (Anderson et al., 2010; Kiritani et al., 2012). Unidirectional connectivity is also seen from L2/3-IT and L5A-IT to PT neurons in the motor cortex (Anderson et al., 2010; Kiritani et al., 2012). In is unknown whether the concept of hierarchical connectivity applies to AC L5B corticocallosal and corticocollicular neurons. However, such a potential mechanism can further contribute to the distinct *in vivo* sound responses of AC L5B IT and PT neurons as L5B corticocallosal neurons would provide another source of excitation to corticocollicular neurons which would be amplified due to recurrent activity amongst corticocollicular neurons and the lack of upstream propagation to corticocallosal neurons.

While we did not explore the role of interneurons in shaping the *in vitro* spiking output of AC L5B corticocallosal and corticocollicular neurons, evidence from the motor cortex suggests that fast-spiking (FS) interneurons (INs) in L5B can affect the activity of L5B IT and PT neurons differently. In the motor cortex, both L5B IT and PT neurons excite FS INs powerfully, which subsequently inhibit L5B IT and PT neurons; however, the net inhibition on L5B IT neurons is significantly stronger compared to PT neurons (Apicella et al., 2012). Such cell-specific inhibition could be another potential mechanism which could lead to lead to differential spiking output in AC L5B corticocallosal and corticocollicular neurons and could also explain the distinct *in vivo* responses of AC L5B IT and PT neurons to sound. However, whether this is applies to AC L5B IT and PT neurons is uncertain, as FS-mediated inhibition onto L5B PT neurons is stronger compared to the inhibition onto L5B IT neurons in other areas of the cortex such as the medial prefrontal cortex (Lee et al., 2014).

An additional mechanism contributing to the *in vivo* response of L5 IT and PT neurons could arise from thalamocortical inputs to the AC. Sun et al., (2013) suggested that AC PT neurons are driven by direct thalamic input, whereas intracortical input drives AC L5 IT neurons. This is supported by the observation that cortical silencing abolishes sound evoked responses in L5 IT neurons, whereas PT neurons still retain their broad TRFs (Sun et al., 2013). A recent study shows that thalamic inputs in the motor cortex preferentially excite L6 IT neurons in comparison to L5B IT neurons, the latter being mostly excited by within-class neurons (Yamawaki and Shepherd, 2015). This is consistent with the report that *in*

vivo responses of L5 IT neurons to sound are not driven directly by thalamic input (Sun et al., 2013). Given the findings of Sun et al., and a recent study which showed that optogenetic activation of thalamocortical axons generates robust responses in AC L5 pyramidal neurons (unlabeled neurons) (Ji et al., 2015), optogenetic approaches combined with retrograde labeling of AC L5B corticocallosal and corticocollicular can provide a clearer understanding of the thalamocortical mechanisms shaping the *in vivo* responses of AC L5B IT and PT neurons to sound.

4.2 PART 2

4.2.1 Effect of acetylcholine release on AC L5B corticocallosal and corticocollicular neurons in comparison to other neocortical areas

We find that endogenous and exogenous ACh release onto AC L5B projection neurons generates nAChR-mediated depolarizing potentials in both corticocallosal and corticocollicular neurons. However, ACh release generates mAChR-mediated hyperpolarizing potentials in corticocallosal neurons but mAChR-mediated long lasting depolarizing potentials in corticocollicular neurons. Overall, our results are consistent with the presence of nAChRs and mAChRs on cortical pyramidal neurons (Vanderzee et al., 1992).

The nAChR-mediated responses observed by us are consistent with the nAChR-mediated responses seen in L5 pyramidal neurons of the somatosensory and prefrontal cortices upon exogenous application of ACh (Zolles et al., 2009; Poorthuis et al., 2013). Additionally, these responses are also consistent with the nAChR-mediated responses seen in L5 pyramidal neurons of the motor cortex upon endogenous release of ACh (Hedrick and Waters, 2015). However, the pharmacology of these responses shows that different nAChR-subunits participate in nAChR-mediated responses in different cortical areas. nAChR-mediated responses seen in L5 pyramidal neurons of the prefrontal cortex are mediated by α-7

subunit containing nAChRs (Poorthuis et al., 2013), while both α-7 subunit containing nAChRs and α-4 subunit containing nAChRs (the response has 2 nicotinic components) mediate the responses in L5 pyramidal neurons of the somatosensory cortex (Zolles et al., 2008). On the other hand, the nAChR-mediated responses observed by us are mediated by α-4 containing nAChRs (likely α4β2 nAChRs) and are consistent with the α-4 containing nAChR-mediated responses seen in L5 pyramidal neurons of the motor cortex (Hedrick and Waters, 2015). The pharmacology of different nAChR-mediated responses suggests that the expression of specific nAChRs may be region specific. In fact, in the prefrontal cortex itself, nAChR mediated responses in L5 pyramidal neurons are mediated by α -7 subunit containing nAChRs (Poorthuis et al., 2013), while nAChR mediated responses in L6 pyramidal neurons are mediated by α-4 subunit containing nAChRs (Kassam et al., 2008; Poorthuis et al., 2013).

The mAChR-mediated depolarizing and hyperpolarizing responses seen by us are consistent with exogenous ACh generating mAChR-mediated depolarizing and hyperpolarizing responses in L5 pyramidal neurons of the prefrontal, somatosensory and visual cortices (Gulledge and Stuart, 2005; Gulledge et al., 2007); additionally, they are also consistent with endogenous ACh generating mAChR-mediated depolarizing and hyperpolarizing responses in L5 pyramidal neurons of the motor cortex (Hedrick and Waters, 2015). In L5 pyramidal neurons of the somatosensory cortex, exogenous ACh release also generates mAChR-mediated biphasic responses, which consist of a hyperpolarization followed by a depolarization (Gulledge and Stuart, 2005). Endogenous ACh also generates mAChR-mediated biphasic responses in parvalbumin-expressing interneurons in the hippocampus (Bell et al., 2015). However, the biphasic response observed by us upon exogenous and endogenous release of ACh onto AC L5B corticocallosal neurons is distinct in two ways- firstly, it consists of a depolarization followed by a hyperpolarization, and secondly, nAChRs mediate the depolarization and mAChRs mediate the hyperpolarization.

It should be added that in the motor cortex, ACh release generates mAChR-mediated hyperpolarizing and depolarizing responses in both L5 IT and PT neurons, indicating that mAChRs do not have projection specific effects in the L5 pyramidal neurons of the motor cortex (Hedrick and Waters,

2015). However, our results show that in the AC, ACh release leads to mAChR-mediated hyperpolarizing responses only in L5B corticocallosal (IT) neurons, and mAChR-mediated depolarizing responses only in corticocollicular (PT) neurons. This indicates that unlike motor cortex, mAChRs in the AC have projection specific effects on L5B pyramidal neurons. This phenomenon could be specific to the AC, or may represent differences in sensory neocortex v/s. other neocortical areas.

We did not establish the pharmacology of the mAChRs mediating the hyperpolarizing potentials in corticocallosal neurons and the slow depolarizing potentials in corticocallosal neurons. However, based on previous studies in various cortices, M1 mAChR most likely mediates the hyperpolarizing potentials and depolarizing potentials observed in corticocallosal and corticocollicular neurons respectively. The activation of M1-type mAChR has been linked to the depolarizing responses in cortical pyramidal neurons by the inhibition of sub-threshold voltage-gated K^+ channels or M-channels (McCormick and Prince, 1986; Brown, 2010). As M1-type mAChRs are coupled to Gq proteins, their activation results in the hydrolysis of phosphatidylinositol-4,5-bisphosphate (PIP_2), which leads to the closure of M-channels, and generates a depolarizing current (Brown, 2010). M1 channel activation can also cause depolarizing responses by the opening of Ca^{2+} activated nonspecific cation channels (Haj-Dahmane and Andrade, 1998; Zhang and Seguela, 2010; Rahman and Berger, 2011). On the other hand, M1 activation can cause hyperpolarizing responses in cortical pyramidal neurons by opening of small conductance potassium (SK) channels (Gulledge and Stuart, 2005). M1 activation causes the cleavage of PIP_2 into inositol 1,4,5-trisphosphate (IP3) and diacylglycerol (DAG). IP3 binds to receptors on endoplasmic reticulum releasing intracellular Ca^{2+} which bind and opens SK channels, causing an efflux of K^+ leading to hyperpolarizing responses. Indeed, in L5 pyramidal neurons of the somatosensory cortex, depolarizing responses are blocked by the application of pirenzepine, a M1 mAChR-selective antagonist (Gulledge and Stuart, 2005), which also blocks the hyperpolarizing responses in the L5 pyramidal neurons of the somatosensory and prefrontal cortices (Gulledge and Stuart, 2005; Gulledge et al., 2007). It should be mentioned that activation of the M2-type mAChR can also cause inhibitory effects via the activation of Gi proteins and subsequent opening of inward rectifying potassium channels (Brown, 2010). However, studies suggest

that inhibitory responses in cortical neurons are mediated by M1-type mAChRs (Gulledge and Stuart, 2005; Gulledge et al., 2007).

We also observed some differences in the effects of exogenous and endogenous release of ACh onto corticocallosal neurons. Both exogenous and endogenous release of ACh generates nAChR-mediated monophasic depolarizing potentials and nAChR/mAChR mediated biphasic responses in corticocallosal neurons. However, exogenous release of ACh never generates monophasic hyperpolarizing potentials in corticocallosal neurons, whereas endogenous release of ACh results in mAChR-mediated monophasic hyperpolarizing potentials in some corticocallosal neurons. This difference indicates that while exogenous application of ACh can activate both nAChRs and mAChRs, endogenous release sometimes fails to activate nAChRs. This phenomenon cannot be explained by the lack of nAChRs on the subset of corticocallosal neurons that display monophasic hyperpolarizing potentials in response to endogenous ACh release; the presence of nAChRs on all corticocallosal neurons is supported by nAChR mediated depolarizing potentials or biphasic responses (which also contain nAChR-mediated depolarizing potentials) in response to exogenous release of ACh. The possibility, that mAChR-mediated inhibition is concealing the nAChR-mediated depolarizing potentials is also not plausible as the blockade of the hyperpolarizing potentials by atropine fails to reveal any nAChR-mediated response. Additionally, the possibility that there is insufficient release of endogenous ACh to activate nAChRs seems implausible as the ACh release is sufficient to activate nAChRs on other corticocallosal neurons. Therefore, the monophasic mAChR-mediated hyperpolarizing potentials in corticocallosal neurons could arise from the fact that nAChRs are located away from the release sites of ACh, and ACh fails to reach these receptors before its reuptake. This possibility can be tested by inhibiting ACh esterase, the enzyme responsible for breaking down ACh, and observing whether blocking ACh reuptake generates a nAChR-mediated response.

We also observed that during exogenous application of ACh onto corticocallosal neurons, the depolarizing potential in the biphasic response was unchanged after the blockade of the hyperpolarizing potential. However, during endogenous release of ACh onto corticocallosal neurons, the depolarizing

potential in the biphasic response was significantly increased after the blockade of the hyperpolarizing potential. This phenomenon could be due to the difference in the onset of the hyperpolarizing potential (latency of the hyperpolarizing potential) by exogenous v/s. endogenous release of ACh. Faster onset of the hyperpolarizing potential in response to endogenous release of ACh probably limits the size of the preceding nAChR-mediated depolarizing potential, whereas the slower onset of the hyperpolarizing potential in response to exogenous ACh does not affect the size of the preceding depolarizing potential. This proposition can be tested by blocking the nAChR-mediated depolarizing potential in the biphasic responses generated by both exogenous and endogenous release of ACh, and measuring the latency of the remaining hyperpolarizing potential. We predict that the latency of the hyperpolarizing potential generated by exogenous ACh will be significantly greater than the latency of the hyperpolarizing potential generated by endogenous ACh.

4.2.2 Upregulation of cholinergic tone due to extra copies of *VAChT* gene and VAChT protein in *ChAT-ChR2-EYFP* mice

The occurrence of monophasic hyperpolarizing potentials mediated by mAChRs in corticocallosal neurons upon endogenous release of ACh could also arise due to another issue. We used the *ChAT-ChR2-EYFP* mice (C57BL/6J strain) (B6.Cg-Tg(Chat-COP4*H134R/EYFP)6Gfng/J; The Jackson Laboratory) for our experiments to test the effect of endogenous release of ACh. *ChAT-ChR2-EYFP* mice are bacterial artificial chromosome (BAC) transgenic mice which express ChR2 protein under the control of the choline acetyltransferase (*ChAT*) promoter (Zhao et al., 2011). The *ChAT* gene produces choline acetyltransferase, the enzyme which is responsible for the synthesis ACh. The *ChAT* locus also contains the vesicular acetylcholine transporter (*VAChT*) gene, as the entire open reading frame for the *VAChT* lies within the intron between the first and second exons of *ChAT* gene (Bejanin et al., 1994; Erickson et al., 1994; Roghani et al., 1994; Cervini et al., 1995).Therefore, the BAC, which is designed to create *ChAT-ChR2-EYFP* mice, also contains the *VAChT* gene (Kolisnyk et al., 2013). *In vitro* studies have shown that

an increased expression of VAChT protein results in an increased cholinergic tone, evidenced by increased amplitude of miniature EPSCs and greater number of synaptic vesicles containing ACh (Song et al., 1997). A recent study revealed that *ChAT-ChR2-EYFP* mice contain 56 copies of *VAChT* gene, which causes a 550% increase in VAChT protein in the hippocampus and a 350% increase in VAChT protein in the brainstem (Kolisnyk et al., 2013). Given that over expression of VAChT protein results in an increased cholinergic tone (Song et al., 1997), the increased expression of VAChT protein in *ChAT-ChR2-EYFP* mice will also lead to an increase in the cholinergic tone of these mice. This is supported by the finding that *ChAT-ChR2-EYFP* mice show enhanced motor endurance, which is consistent with an increase in the cholinergic tone in these mice (Kolisnyk et al., 2013). Such an increased cholinergic tone can desensitize nAChRs, and potentially lead to the monophasic hyperpolarizing potentials seen in corticocallosal neurons that are mediated by mAChRs, upon endogenous release of ACh. This can also explain why we always see nAChR-mediated responses in corticocallosal neurons in brain slices prepared from ICR mice (non-transgenic), upon puffing exogenous ACh.

4.2.3 Significance of persistent firing in corticocollicular neurons and its relation to relearning sound localization

Persistent firing is the ability of a single neuron to generate sustained APs in response to transient supra-threshold stimulus and can last from hundreds of milliseconds to seconds (Wang, 2001; Major and Tank, 2004). Single cell persistent activity is thought to be the cellular substrate for learning and memory in the brain (Wang, 2001; Hasselmo and Stern, 2006). *In vitro* studies show that pyramidal neurons in cortical areas responsible for learning and memory show persistent firing in response to cholinergic activation, which is mediated by mAChRs (Haj-Dahmane and Andrade, 1998; Egorov et al., 2002). Studies also show that entorhinal cortex neurons display persistent firing during behavioral tasks that assess working memory (Suzuki et al., 1997; Young et al., 1997); importantly, drugs that block mAChRs can cause deficits in working memory (Penetar and McDonough, 1983; Schon et al., 2005). The studies cited above

propose that learning and memory are influenced by the cholinergic activation of persistent firing in cortical neurons.

It is known that Nucleus Basalis, the main source of cortical ACh, is crucial for learning-induced plasticity involved in the relearning of sound localization after plugging one ear (Leach et al., 2013). This cholinergic-mediated experience-dependent plasticity involved in relearning sound localization after reversible occlusion of one ear is also lost after eliminating corticocollicular neurons (Bajo et al., 2010). This indicates that cholinergic modulation of the activity of corticocollicular neurons may be crucial for auditory learning. Our results show that ACh release generates persistent firing in a subset of corticocollicular neurons which display prolonged mAChR-mediated depolarizing potentials. Thus, mAChR-mediated persistent firing in corticocollicular neurons may be a critical mechanism for relearning sound localization after monaural occlusion by earplugging one ear.

4.2.4 General mechanisms mediating persistent firing in cortical neurons

Studies in other cortical areas have also shown that cholinergic activation can lead to persistent firing in L5 pyramidal neurons (Haj-Dahmane and Andrade, 1998; Egorov et al., 2002; Gulledge et al., 2009; Dembrow et al., 2010; Hedrick and Waters, 2015). In L5 neurons of M1, persistent firing is mediated by nAChRs as the persistent firing is blocked by nAChR antagonists (Hedrick and Waters, 2015). Additionally, it is mediated by an increase in postsynaptic intracellular Ca^{2+}, which is dependent on the activation of nAChRs as persistent firing is not abolished in the presence of blockers of mAChRs. In other regions of the cortex such as the prefrontal, entorhinal and anterior cingulate cortices, persistent firing in pyramidal neurons is mediated by mAChRs as it is blocked by the application of mAChR antagonist atropine (Haj-Dahmane and Andrade, 1998; Egorov et al., 2002; Zhang and Seguela, 2010); mAChR-mediated increase in postsynaptic Ca^{2+} activates a non-specific cation current which results in afterdepolarizing potentials causing persistent activity (Haj-Dahmane and Andrade, 1998; Egorov et al., 2002; Zhang and Seguela, 2010). The role of Ca^{2+} activated non-specific cation current in the generation

of mAChR-mediated persistent firing is validated by studies which show that flufenamic acid- a blocker of Ca^{2+} activated non-specific cation currents, abolishes mAChR-mediated persistent firing (Egorov et al., 2002; Zhang and Seguela, 2010). The persistent firing observed by us is also mediated by mAChRs. We did not evaluate whether the persistent firing is generated by Ca^{2+} activated non-specific cation currents. However, the persistent firing seen by us may not driven by Ca^{2+} activated non-specific cation currents as we did not observe any changes in the spiking properties (AP width and AP threshold) of corticocollicular neurons during persistent firing, while Ca^{2+} activated non-specific cation current driven persistent spiking has been shown to be accompanied by changes in spike properties such as AP threshold and AP width (Dembrow et al., 2010).

4.2.5 Cell autonomous/circuit mediated persistent firing

Cell-autonomous persistent firing is the ability of a neuron to fire APs persistently in the absence of local circuit involvement, i.e. the neuron fires persistently in the presence of blockers of synaptic transmission. Cell autonomous persistent firing after cholinergic activation has been reported in L5 pyramidal neurons of the entorhinal cortex, medial prefrontal cortex as well as in the motor cortex (Egorov et al., 2002; Dembrow et al., 2010; Hedrick and Waters, 2015). In our experiments, the persistent firing in corticocollicular neurons upon ACh release is abolished by the application of atropine, which shows that it is mediated by the activation of mAChRs. However, we did not test whether persistent firing in corticocollicular neurons seen after ACh release, can be sustained in the presence of blockers of synaptic transmission. Therefore we cannot state for certain if the observed persistent firing in corticocollicular neurons is cell-autonomous or whether it requires the involvement of the local circuits.

4.2.6 Significance of the effects of acetylcholine release on AC L5B corticocallosal and corticocollicular neurons in relation to cholinergic modulation of evoked responses in the auditory cortex

Studies show AC responses generated by thalamic stimulation are enhanced when paired with the stimulation of Nucleus Basalis (Metherate and Ashe, 1993). Responses in AC generated by sensory stimuli are also enhanced after pairing the auditory stimuli with Nucleus Basalis stimulation (Edeline et al., 1994; Chen and Yan, 2007; Froemke et al., 2007). Similar enhancements in tone evoked responses in the AC are also seen when the tone is paired with continuous administration of external ACh (McKenna et al., 1988). These studies suggest that afferent responses in AC are heavily modulated by ACh. Furthermore, these enhancements in AC responses are mediated by mAChRs as they are abolished in the presence of mAChR blocker atropine (McKenna et al., 1988; Edeline et al., 1994; Chen and Yan, 2007; Froemke et al., 2007). The enhancement in AC responses can be explained by the observation that pairing Nucleus Basalis stimulation with a tone increases the EPSPs and decreases the IPSPs generated in response to the tone (Froemke et al., 2007). The long lasting mAChR-mediated depolarizing potentials observed in corticocollicular neurons after exogenous and endogenous release of ACh release are consistent with the enhancement of tone-evoked EPSPs after pairing of the tone with Nucleus Basalis stimulation (Froemke et al., 2007). Behavioral studies show that pairing a stimulus with Nucleus Basalis stimulation induces stimulus-specific associative memory in the AC (Weinberger et al., 2006). The underlying mechanism for such a phenomenon could also involve ACh-mediated increase in excitability of cortical neurons, as seen in corticocollicular neurons via mAChRs.

It has also been proposed that the combined effect of ACh on nAChRs and mAChRs shapes the receptive field breadth of the AC, which involves suppression of AC responses to non-characteristic frequencies (characteristic frequency-CF) but facilitation of AC responses to CFs and near CFs (Metherate, 2011). nAChRs are thought to play a role in the facilitation of responses to CF and near CFs as they can increase the excitability of thalamocortical projections to the AC by increasing the excitability

of thalamocortical axons (Kawai et al., 2007). Indeed, blockade of nAChRs in thalamic white matter (containing thalamocortical axons) decreases the amplitude of CF tone-evoked responses in the AC (Kawai et al., 2007). Our results show that ACh release also increases excitability by generation of nAChR-mediated depolarizing potentials in both corticocallosal and corticocollicular neurons. This finding may represent another mechanism by which nAChRs contribute to the facilitation of responses in the AC to CFs and near CFs. On the other hand, the biphasic and inhibitory responses (where the hyperpolarizing potential is mediated by mAChRs) seen in corticocallosal neurons could represent a mechanism to limit the receptive field breadth by suppression of responses to non CFs.

4.2.7 General role of neuromodulators in shaping the activity of IT and PT neurons

PT and IT neurons in various cortical areas differ in their anatomy (Dembrow et al., 2010; Sun et al., 2013), intrinsic properties (Chen et al., 1996; Dembrow et al., 2010; Suter et al., 2013; Joshi et al., 2015) and synaptic (Morishima and Kawaguchi, 2006; Kiritani et al., 2012; Lee et al., 2014; Joshi et al., 2015). Additionally, studies show that neuromodulatory systems also affect the excitability of PT and IT neurons differentially. In the prefrontal cortex, noradrenergic modulation selectively alters the subthreshold activity of PT neurons by closure of HCN channels leading to a reduction in I_h, whereas no such modulation is seen in IT neurons (Wang et al., 2007; Dembrow et al., 2010); this reduction in I_h increases temporal summation of EPSPs and drives the generation of APs in PT neurons (Dembrow et al., 2010). Dopaminergic modulation augments spiking in PT neurons and not IT neurons in the prefrontal cortex due to the selective expression of D2 receptors on PT neurons; the opening of D2 receptors causes increased afterdepolarization which enhances firing in PT neurons (Gee et al., 2012). Serotonin also affects PTs and ITs differentially in the medial prefrontal cortex as it causes excitation in IT but inhibition in PT neurons (Avesar and Gulledge, 2012). PT and IT neurons in prefrontal cortex are also distinctly modulated by ACh. Similar to noradrenergic modulation, cholinergic activation alters subthreshold activity in PT neurons by reducing I_h while leaving IT neurons unaffected; additionally, cholinergic

activation in the prefrontal cortex causes persistent firing in PT neurons and but not in IT neurons (Dembrow et al., 2010).

Our results also show that cholinergic modulation affects AC L5B corticocallosal (IT-type) and corticocollicular (PT-type) neurons distinctly. The presence of mAChR-mediated slow depolarizing potentials promotes persistent firing in corticocollicular neurons, while corticocallosal neurons which lack mAChR-mediated slow depolarizing potentials do not fire persistently. Thus, our results add to the growing list of literature which shows that numerous factors, including neuromodulators, control the excitability of PT and IT neurons in the neocortex.

4.3 PART 3

4.3.1 Potential relevance of our findings toward understanding auditory disorders

Tinnitus, the perception of a phantom sound in the absence of acoustic stimuli, is a debilitating auditory disorder that affects nearly 5-15% of the population (Li et al., 2013). The primary auditory cortex (A1) has been implicated in the perception of tinnitus (Eggermont and Roberts, 2004; Llinas et al., 2005; Leaver et al., 2011). Existing literature reports spontaneous hyperactivity of A1 in human patients of tinnitus (Arnold et al., 1996; Schecklmann et al., 2013). Increases in spontaneous firing rates of A1 neurons in animal models of noise induced hearing loss (which often accompanies tinnitus) have also been reported (Eggermont and Komiya, 2000; Eggermont, 2006). Hence, literature thus far has revealed important neural correlates of tinnitus in A1 but the mechanistic understanding of tinnitus remains poor due to the lack of understanding of the direct neuronal and synaptic/circuit changes in A1 that cause tinnitus.

Emerging evidence suggests that disorders of the central nervous system may involve the improper functioning of IT and PT neurons. For example autism spectrum disorders are accompanied

with the thinning of the corpus callosum, which implicates the involvement of IT neurons (Just et al., 2007; Keary et al., 2009; Frazier et al., 2012), and reduced firing rates in PT neurons (but not IT neurons) in the motor cortex of primates after induction of parkinsonism implicates PT neurons in Parkinson's disease (Pasquereau and Turner, 2011). In general, schizophrenia, autism spectrum disorders, and obsessive compulsive disorders appear to involve IT neurons and PT neurons seem to be involved in conditions such as amyotrophic lateral sclerosis and Parkinson's disease (reviewed in Shepherd, 2013). A recent study showed that people suffering from Asperger's syndrome, a part of autism spectrum disorder (though to involve IT neuron dysfunction) also experience hyperacusis (abnormal sensitivity to sound) and tinnitus (Danesh et al., 2015). This suggests that dysfunction of projection-specific neurons could contribute to auditory disorders such as tinnitus.

Our results show that projection specific intrinsic and synaptic properties (including neuromodulation) shape the activity of AC neurons. Changes in intrinsic and synaptic properties that favor excitability of pyramidal neurons have been seen in models of hearing loss (which often accompanies tinnitus) (Kotak et al., 2005; Takesian et al., 2013). Given the dysfunction of IT and PT neurons in various neurological and neurodegenerative disorders, a cell-specific inquiry into the intrinsic and synaptic/circuit properties of AC IT and PT neurons in animal models of tinnitus may provide a novel understanding of the changes in neuronal and/or synaptic/circuit properties that underlie tinnitus.

4.3.2 Conclusions

Pyramidal neurons in the cortex are broadly classified into distinct categories based on their axonal projection targets. In the AC, L5B corticocallosal neurons fall into the category of intratelencephalic (IT) neurons, which project to the contralateral cortex, and corticocollicular neurons fall into the category of pyramidal tract (PT) neurons, which project to the subcortical structures (Shepherd, 2013). Studies in other cortical areas show that IT and PT neurons differ not only in their axonal projection targets, but also display differences in their intrinsic (Dembrow et al., 2010; Sheets et al., 2011; Slater et al., 2013; Suter et

al., 2013) and synaptic properties (Morishima and Kawaguchi, 2006; Anderson et al., 2010; Dembrow et al., 2010; Kiritani et al., 2012; Lee et al., 2014). These differences in intrinsic and synaptic properties favor tonic or sustained activity in PT neurons and transient or phasic activity in IT neurons. Furthermore, studies also show that neuromodulatory systems affect the excitability of IT and PT neurons differently, and promote sustained activity in PT neurons and transient activity in IT neurons (Dembrow et al., 2010). Our results show that in comparison to corticocallosal neurons, corticocollicular neurons have narrower APs and a lack of spike frequency adaptation, which favor sustained activity in corticocollicular neurons and transient activity in corticocallosal neurons. Distinct short term plasticity of L2/3 inputs also favors sustained activity in corticocollicular neurons and transient activity in corticocallosal neurons, as L2/3 inputs to corticocollicular neurons are non-depressing whereas L2/3 inputs to corticocallosal neurons are depressing. Additionally, cholinergic neuromodulation preferentially enhances the excitability of corticocollicular neurons in comparison to corticocallosal neurons. In corticocallosal neurons, ACh generates nAChR-mediated monophasic depolarizing potentials, biphasic responses where nAChRs mediate the depolarizing potential and mAChRs mediate the hyperpolarizing potential, and mAChR-mediated monophasic hyperpolarizing potentials; these ACh-mediated responses lead to transient firing in corticocallosal neurons. On the other hand, ACh generates nAChR-mediated depolarizing potentials, as well as mAChR-mediated long lasting depolarizing potentials in corticocollicular neurons; the long-lasting mAChR-mediated depolarizing potentials generate persistent firing in corticocollicular neurons. Collectively, our results also show that in L5B of the AC, intrinsic and synaptic properties as well as neuromodulatory mechanisms support transient or phasic activity in IT neurons and sustained or tonic activity in PT neurons.

BIBLIOGRAPHY

Abbott LF, Regehr WG (2004) Synaptic computation. Nature 431:796-803.

Adesnik H, Scanziani M (2010) Lateral competition for cortical space by layer-specific horizontal circuits. Nature 464:1155-1160.

Akintunde A, Buxton DF (1992) Origins and collateralization of corticospinal, cortiopontine, corticorubral, and corticostriatal tracts - a multiple retrograde fluorescent tracing study. Brain research 586:208-218.

Albuquerque EX, Pereira EF, Alkondon M, Rogers SW (2009) Mammalian nicotinic acetylcholine receptors: from structure to function. Physiological reviews 89:73-120.

Anderson CT, Sheets PL, Kiritani T, Shepherd GMG (2010) Sublayer-specific microcircuits of corticospinal and corticostriatal neurons in motor cortex. Nature neuroscience 13:739-U116.

Andrade R (1991) Cell excitation enhances muscarinic cholinergic responses in rat association cortex. Brain research 548:81-93.

Apicella AJ, Wickersham IR, Seung HS, Shepherd GMG (2012) Laminarly Orthogonal Excitation of Fast-Spiking and Low-Threshold-Spiking Interneurons in Mouse Motor Cortex. Journal of Neuroscience 32:7021-7033.

Arnold W, Bartenstein P, Oestreicher E, Romer W, Schwaiger M (1996) Focal metabolic activation in the predominant left auditory cortex in patients suffering from tinnitus: a PET study with [18F]deoxyglucose. ORL; journal for oto-rhino-laryngology and its related specialties 58:195-199.

Atencio CA, Schreiner CE (2010a) Columnar Connectivity and Laminar Processing in Cat Primary Auditory Cortex. Plos One 5.

Atencio CA, Schreiner CE (2010b) Laminar Diversity of Dynamic Sound Processing in Cat Primary Auditory Cortex. Journal of Neurophysiology 103:192-205.

Atzori M, Lei S, Evans DIP, Kanold PO, Phillips-Tansey E, McIntyre O, McBain CJ (2001) Differential synaptic processing separates stationary from transient inputs to the auditory cortex. Nature neuroscience 4:1230-1237.

Avesar D, Gulledge AT (2012) Selective serotonergic excitation of callosal projection neurons. Front Neural Circuits 6:12.

Bajo VM, Nodal FR, Moore DR, King AJ (2010) The descending corticocollicular pathway mediates learning-induced auditory plasticity. Nature neuroscience 13:253-U146.

Barak O, Tsodyks M (2014) Working models of working memory. Curr Opin Neurobiol 25:20-24.

Barbour DL, Wang XQ (2003) Auditory cortical responses elicited in awake primates by random spectrum stimuli. Journal of neuroscience 23:7194-7206.

Bear MF, Singer W (1986) Modulation of visual cortical plasticity by acetylcholine and noradrenaline. Nature 320:172-176.

Bejanin S, Cervini R, Mallet J, Berrard S (1994) A unique gene organization for two cholinergic markers, choline acetyltransferase and a putative vesicular transporter of acetylcholine. The Journal of biological chemistry 269:21944-21947.

Bell LA, Bell KA, McQuiston AR (2015) Activation of muscarinic receptors by ACh release in hippocampal CA1 depolarizes VIP but has varying effects on parvalbumin-expressing basket cells. The Journal of physiology 593:197-215.

Brown DA (2010) Muscarinic acetylcholine receptors (mAChRs) in the nervous system: some functions and mechanisms. Journal of molecular neuroscience : MN 41:340-346.

Brown SP, Hestrin S (2009a) Intracortical circuits of pyramidal neurons reflect their long-range axonal targets. Nature 457:1133-U1189.

Brown SP, Hestrin S (2009b) Cell-type identity: a key to unlocking the function of neocortical circuits. Current Opinion in Neurobiology 19:415-421.

Calford MB, Semple MN (1995) Monaural inhibition in cat auditory cortex. Journal of neurophysiology 73:1876-1891.

Cervini R, Houhou L, Pradat PF, Bejanin S, Mallet J, Berrard S (1995) Specific vesicular acetylcholine transporter promoters lie within the first intron of the rat choline acetyltransferase gene. The Journal of biological chemistry 270:24654-24657.

Chen G, Yan J (2007) Cholinergic modulation incorporated with a tone presentation induces frequency-specific threshold decreases in the auditory cortex of the mouse. The European journal of neuroscience 25:1793-1803.

Chen W, Zhang JJ, Hu GY, Wu CP (1996) Electrophysiological and morphological properties of pyramidal and nonpyramidal neurons in the cat motor cortex in vitro. Neuroscience 73:39-55.

Covic EN, Sherman SM (2011) Synaptic Properties of Connections between the Primary and Secondary Auditory Cortices in Mice. Cerebral Cortex 21:2425-2441.

Danesh AA, Lang D, Kaf W, Andreassen WD, Scott J, Eshraghi AA (2015) Tinnitus and hyperacusis in autism spectrum disorders with emphasis on high functioning individuals diagnosed with Asperger's Syndrome. International journal of pediatric otorhinolaryngology 79:1683-1688.

Dani JA, Bertrand D (2007) Nicotinic acetylcholine receptors and nicotinic cholinergic mechanisms of the central nervous system. Annual review of pharmacology and toxicology 47:699-729.

de la Mothe LA, Blumell S, Kajikawa Y, Hackett TA (2006) Cortical connections of the auditory cortex in marmoset monkeys: core and medial belt regions. The Journal of comparative neurology 496:27-71.

de la Rocha J, Marchetti C, Schiff M, Reyes AD (2008) Linking the response properties of cells in auditory cortex with network architecture: cotuning versus lateral inhibition. Journal of Neuroscience 28:9151-9163.

De Pasquale R, Sherman SM (2011) Synaptic properties of corticocortical connections between the primary and secondary visual cortical areas in the mouse. Journal of Neuroscience 31:16494-16506.

De Pasquale R, Sherman SM (2012) Modulatory effects of metabotropic glutamate receptors on local cortical circuits. Journal of Neuroscience 32:7364-7372.

Dembrow NC, Chitwood RA, Johnston D (2010) Projection-specific neuromodulation of medial prefrontal cortex neurons. Journal of Neuroscience 30:16922-16937.

Doucet JR, Ryugo DK (2003) Axonal pathways to the lateral superior olive labeled with biotinylated dextran amine injections in the dorsal cochlear nucleus of rats. Journal of Comparative Neurology 461:452-465.

Doucet JR, Molavi DL, Ryugo DK (2003) The source of corticocollicular and corticobulbar projections in area Te1 of the rat. Experimental Brain Research 153:461-466.

Edeline JM, Hars B, Maho C, Hennevin E (1994) Transient and prolonged facilitation of tone-evoked responses induced by basal forebrain stimulations in the rat auditory cortex. Exp Brain Res 97:373-386.

Eggermont JJ (2006) Cortical tonotopic map reorganization and its implications for treatment of tinnitus. Acta oto-laryngologica Supplementum:9-12.

Eggermont JJ, Komiya H (2000) Moderate noise trauma in juvenile cats results in profound cortical topographic map changes in adulthood. Hear Res 142:89-101.

Eggermont JJ, Roberts LE (2004) The neuroscience of tinnitus. Trends in neurosciences 27:676-682.

Egorov AV, Unsicker K, von Bohlen und Halbach O (2006) Muscarinic control of graded persistent activity in lateral amygdala neurons. The European journal of neuroscience 24:3183-3194.

Egorov AV, Hamam BN, Fransen E, Hasselmo ME, Alonso AA (2002) Graded persistent activity in entorhinal cortex neurons. Nature 420:173-178.

Erickson JD, Varoqui H, Schafer MK, Modi W, Diebler MF, Weihe E, Rand J, Eiden LE, Bonner TI, Usdin TB (1994) Functional identification of a vesicular acetylcholine transporter and its expression from a "cholinergic" gene locus. The Journal of biological chemistry 269:21929-21932.

Fransen E, Tahvildari B, Egorov AV, Hasselmo ME, Alonso AA (2006) Mechanism of graded persistent cellular activity of entorhinal cortex layer v neurons. Neuron 49:735-746.

Frazier TW, Keshavan MS, Minshew NJ, Hardan AY (2012) A two-year longitudinal MRI study of the corpus callosum in autism. Journal of autism and developmental disorders 42:2312-2322.

Froemke RC, Merzenich MM, Schreiner CE (2007) A synaptic memory trace for cortical receptive field plasticity. Nature 450:425-429.

Games KD, Winer JA (1988) Layer-V in rat auditory-cortex - projections to the inferior colliculus and contralateral cortex. Hearing Research 34:1-26.

Gao WJ, Zheng ZH (2004) Target-specific differences in somatodendritic morphology of layer V pyramidal neurons in rat motor cortex. Journal of Comparative Neurology 476:174-185.

Gee S, Ellwood I, Patel T, Luongo F, Deisseroth K, Sohal VS (2012) Synaptic Activity Unmasks Dopamine D2 Receptor Modulation of a Specific Class of Layer V Pyramidal Neurons in Prefrontal Cortex. Journal of Neuroscience 32:4959-4971.

Gotti C, Clementi F (2004) Neuronal nicotinic receptors: from structure to pathology. Progress in neurobiology 74:363-396.

Gulledge AT, Stuart GJ (2005) Cholinergic inhibition of neocortical pyramidal neurons. Journal of neuroscience 25:10308-10320.

Gulledge AT, Park SB, Kawaguchi Y, Stuart GJ (2007) Heterogeneity of phasic cholinergic signaling in neocortical neurons. Journal of Neurophysiology 97:2215-2229.

Gulledge AT, Bucci DJ, Zhang SS, Matsui M, Yeh HH (2009) M1 receptors mediate cholinergic modulation of excitability in neocortical pyramidal neurons. Journal of neuroscience 29:9888-9902.

Guo W, Chambers AR, Darrow KN, Hancock KE, Shinn-Cunningham BG, Polley DB (2012) Robustness of Cortical Topography across Fields, Laminae, Anesthetic States, and Neurophysiological Signal Types. Journal of neuroscience 32:9159-9172.

Hackett TA (2015) Anatomic organization of the auditory cortex. Handbook of clinical neurology 129:27-53.

Hackett TA, Phillips D (2011) The commissural auditory system. In: The Auditory Cortex J.A. Winer and C.E. Schreiner, Editors. 2011, Springer: New York. p. 117-132).

Haj-Dahmane S, Andrade R (1996) Muscarinic activation of a voltage-dependent cation nonselective current in rat association cortex. Journal of neuroscience 16:3848-3861.

Haj-Dahmane S, Andrade R (1998) Ionic mechanism of the slow afterdepolarization induced by muscarinic receptor activation in rat prefrontal cortex. Journal of neurophysiology 80:1197-1210.

Haj-Dahmane S, Andrade R (1999) Muscarinic receptors regulate two different calcium-dependent non-selective cation currents in rat prefrontal cortex. The European journal of neuroscience 11:1973-1980.

Harris KD, Shepherd GM (2015) The neocortical circuit: themes and variations. Nature neuroscience 18:170-181.

Hasselmo ME, Stern CE (2006) Mechanisms underlying working memory for novel information. Trends in cognitive sciences 10:487-493.

Hasselmo ME, Sarter M (2011) Modes and models of forebrain cholinergic neuromodulation of cognition. Neuropsychopharmacology : official publication of the American College of Neuropsychopharmacology 36:52-73.

Hattox AM, Nelson SB (2007) Layer V neurons in mouse cortex projecting to different targets have distinct physiological properties. Journal of neurophysiology 98:3330-3340.

Hedrick T, Waters J (2015) Acetylcholine excites neocortical pyramidal neurons via nicotinic receptors. Journal of neurophysiology 113:2195-2209.

Hefti BJ, Smith PH (2000) Anatomy, physiology, and synaptic responses of rat layer V auditory cortical cells and effects of intracellular GABA(A) blockade. Journal of neurophysiology 83:2626-2638.

Herrero JL, Roberts MJ, Delicato LS, Gieselmann MA, Dayan P, Thiele A (2008) Acetylcholine contributes through muscarinic receptors to attentional modulation in V1. Nature 454:1110-1114.

Himmelheber AM, Sarter M, Bruno JP (2000) Increases in cortical acetylcholine release during sustained attention performance in rats. Brain research Cognitive brain research 9:313-325.

Honma Y, Tsukano H, Horie M, Ohshima S, Tohmi M, Kubota Y, Takahashi K, Hishida R, Takahashi S, Shibuki K (2013) Auditory Cortical Areas Activated by Slow Frequency-Modulated Sounds in Mice. Plos One 8.

Ishii M, Kurachi Y (2006) Muscarinic acetylcholine receptors. Current pharmaceutical design 12:3573-3581.

Issa JB, Haeffele BD, Agarwal A, Bergles DE, Young ED, Yue DT (2014) Multiscale Optical Ca2+ Imaging of Tonal Organization in Mouse Auditory Cortex. Neuron 83:944-959.

Ji XY, Zingg B, Mesik L, Xiao Z, Zhang LI, Tao HW (2015) Thalamocortical Innervation Pattern in Mouse Auditory and Visual Cortex: Laminar and Cell-Type Specificity. Cerebral cortex (New York, NY : 1991).

Joshi A, Middleton JW, Anderson CT, Borges K, Suter BA, Shepherd GM, Tzounopoulos T (2015) Cell-specific activity-dependent fractionation of layer 2/3-->5B excitatory signaling in mouse auditory cortex. Journal of neuroscience 35:3112-3123.

Just MA, Cherkassky VL, Keller TA, Kana RK, Minshew NJ (2007) Functional and anatomical cortical underconnectivity in autism: evidence from an FMRI study of an executive function task and corpus callosum morphometry. Cerebral cortex (New York, NY : 1991) 17:951-961.

Kaas J (2011) The evolution of auditory cortex: the core areas. In: The Auditory Cortex J.A. Winer and C.E. Schreiner, Editors. 2011, Springer: New York. p. 407-428)

Kampa BM, Letzkus JJ, Stuart GJ (2006) Cortical feed-forward networks for binding different streams of sensory information. Nature neuroscience 9:1472-1473.

Kassam SM, Herman PM, Goodfellow NM, Alves NC, Lambe EK (2008) Developmental excitation of corticothalamic neurons by nicotinic acetylcholine receptors. Journal of neuroscience 28:8756-8764.

Kawai H, Lazar R, Metherate R (2007) Nicotinic control of axon excitability regulates thalamocortical transmission. Nature neuroscience 10:1168-1175.

Keary CJ, Minshew NJ, Bansal R, Goradia D, Fedorov S, Keshavan MS, Hardan AY (2009) Corpus callosum volume and neurocognition in autism. Journal of autism and developmental disorders 39:834-841.

Kilgard M (2003) Cholinergic modulation of skill learning and plasticity. Neuron 38:678-680.

Kilgard MP, Merzenich MM (1998a) Plasticity of temporal information processing in the primary auditory cortex. Nature neuroscience 1:727-731.

Kilgard MP, Merzenich MM (1998b) Cortical map reorganization enabled by nucleus basalis activity. Science (New York, NY) 279:1714-1718.

Kiritani T, Wickersham IR, Seung HS, Shepherd GMG (2012) Hierarchical Connectivity and Connection-Specific Dynamics in the Corticospinal-Corticostriatal Microcircuit in Mouse Motor Cortex. Journal of neuroscience 32:4992-5001.

Kolisnyk B, Guzman MS, Raulic S, Fan J, Magalhaes AC, Feng G, Gros R, Prado VF, Prado MA (2013) ChAT-ChR2-EYFP mice have enhanced motor endurance but show deficits in attention and several additional cognitive domains. The Journal of neuroscience 33:10427-10438.

Kotak VC, Fujisawa S, Lee FA, Karthikeyan O, Aoki C, Sanes DH (2005) Hearing loss raises excitability in the auditory cortex. Journal of neuroscience 25:3908-3918.

Leach ND, Nodal FR, Cordery PM, King AJ, Bajo VM (2013) Cortical cholinergic input is required for normal auditory perception and experience-dependent plasticity in adult ferrets. Journal of neuroscience 33:6659-6671.

Leaver AM, Renier L, Chevillet MA, Morgan S, Kim HJ, Rauschecker JP (2011) Dysregulation of limbic and auditory networks in tinnitus. Neuron 69:33-43.

Lee AT, Gee SM, Vogt D, Patel T, Rubenstein JL, Sohal VS (2014) Pyramidal Neurons in Prefrontal Cortex Receive Subtype-Specific Forms of Excitation and Inhibition. Neuron 81:61-68.

Lee CC, Sherman SM (2008) Synaptic properties of thalamic and intracortical inputs to layer 4 of the first- and higher-order cortical areas in the auditory and somatosensory systems. Journal of neurophysiology 100:317-326.

Lee CC, Sherman SM (2010) Topography and physiology of ascending streams in the auditory tectothalamic pathway. Proc Natl Acad Sci U S A 107:372-377.

Lefort S, Tomm C, Sarria JCF, Petersen CCH (2009) The Excitatory Neuronal Network of the C2 Barrel Column in Mouse Primary Somatosensory Cortex. Neuron 61:301-316.

Lehmann J, Nagy JI, Atmadia S, Fibiger HC (1980) The nucleus basalis magnocellularis: the origin of a cholinergic projection to the neocortex of the rat. Neuroscience 5:1161-1174.

Levey AI, Kitt CA, Simonds WF, Price DL, Brann MR (1991) Identification and localization of muscarinic acetylcholine receptor proteins in brain with subtype-specific antibodies. Journal of neuroscience 11:3218-3226.

Li N, Chen TW, Guo ZV, Gerfen CR, Svoboda K (2015) A motor cortex circuit for motor planning and movement. Nature 519:51-56.

Li S, Choi V, Tzounopoulos T (2013) Pathogenic plasticity of Kv7.2/3 channel activity is essential for the induction of tinnitus. Proceedings of the National Academy of Sciences of the United States of America 110:9980-9985.

Little JP, Carter AG (2013) Synaptic Mechanisms Underlying Strong Reciprocal Connectivity between the Medial Prefrontal Cortex and Basolateral Amygdala. Journal of neuroscience 33:15333-15342.

Llinas R, Urbano FJ, Leznik E, Ramirez RR, van Marle HJ (2005) Rhythmic and dysrhythmic thalamocortical dynamics: GABA systems and the edge effect. Trends in neurosciences 28:325-333.

Major G, Tank D (2004) Persistent neural activity: prevalence and mechanisms. Curr Opin Neurobiol 14:675-684.

McCormick DA, Prince DA (1986) Mechanisms of action of acetylcholine in the guinea-pig cerebral cortex invitro. Journal of Physiology-London 375:169-194.

McKenna TM, Ashe JH, Hui GK, Weinberger NM (1988) Muscarinic agonists modulate spontaneous and evoked unit discharge in auditory cortex of cat. Synapse (New York, NY) 2:54-68.

Metherate R (2004) Nicotinic acetylcholine receptors in sensory cortex. Learning & Memory 11:50-59.

Metherate R (2011) Functional connectivity and cholinergic modulation in auditory cortex. Neurosci Biobehav Rev 35:2058-2063.

Metherate R, Ashe JH (1993) Nucleus basalis stimulation facilitates thalamocortical synaptic transmission in the rat auditory cortex. Synapse (New York, NY) 14:132-143.

Metherate R, Cox CL, Ashe JH (1992) Cellular bases of neocortical activation: modulation of neural oscillations by the nucleus basalis and endogenous acetylcholine. Journal of neuroscience 12:4701-4711.

Middleton JW, Kiritani T, Pedersen C, Turner JG, Shepherd GMG, Tzounopoulos T (2011) Mice with behavioral evidence of tinnitus exhibit dorsal cochlear nucleus hyperactivity because of decreased GABAergic inhibition. Proceedings of the National Academy of Sciences of the United States of America 108:7601-7606.

Miller MN, Okaty BW, Nelson SB (2008) Region-Specific Spike-Frequency Acceleration in Layer 5 Pyramidal Neurons Mediated by Kv1 Subunits. Journal of neuroscience 28:13716-13726.

Malmierca SM, Ryugo DK (2011) Descending connections of auditory cortex to the midbrain and brainstem. In: The Auditory Cortex J.A. Winer and C.E. Schreiner, Editors. 2011, Springer: New York. p. 189-208)

Morishima M, Kawaguchi Y (2006) Recurrent connection patterns of corticostriatal pyramidal cells in frontal cortex. Journal of neuroscience 26:4394-4405.

Oswald A-MM, Reyes AD (2008) Maturation of intrinsic and synaptic properties of layer 2/3 pyramidal neurons in mouse auditory cortex. Journal of neurophysiology 99:2998-3008.

Parikh V, Sarter M (2008) Cholinergic mediation of attention - Contributions of phasic and tonic increases in prefrontal cholinergic activity. Molecular and Biophysical Mechanisms of Arousal, Alertness, and Attention 1129:225-235.

Pasquereau B, Turner RS (2011) Primary motor cortex of the parkinsonian monkey: differential effects on the spontaneous activity of pyramidal tract-type neurons. Cerebral cortex (New York, NY : 1991) 21:1362-1378.

Penetar DM, McDonough JH, Jr. (1983) Effects of cholinergic drugs on delayed match-to-sample performance of rhesus monkeys. Pharmacology, biochemistry, and behavior 19:963-967.

Poorthuis RB, Bloem B, Schak B, Wester J, de Kock CPJ, Mansvelder HD (2013) Layer-Specific Modulation of the Prefrontal Cortex by Nicotinic Acetylcholine Receptors. Cerebral Cortex 23:148-161.

Purves D, Augustine GJ, Fitzpatrick D, et al., editors. Neuroscience. 2nd edition. Sunderland (MA): Sinauer Associates; 2001. The Auditory Cortex. Available from: http://www.ncbi.nlm.nih.gov/books/NBK10900/.

Rahman J, Berger T (2011) Persistent activity in layer 5 pyramidal neurons following cholinergic activation of mouse primary cortices. European Journal of Neuroscience 34:22-30.

Ramanathan D, Tuszynski MH, Conner JM (2009) The Basal Forebrain Cholinergic System Is Required Specifically for Behaviorally Mediated Cortical Map Plasticity. Journal of neuroscience 29:5992-6000.

Reed A, Riley J, Carraway R, Carrasco A, Perez C, Jakkamsetti V, Kilgard MP (2011) Cortical map plasticity improves learning but is not necessary for improved performance. Neuron 70:121-131.

Reichova I, Sherman SM (2004) Somatosensory corticothalamic projections: distinguishing drivers from modulators. Journal of neurophysiology 92:2185-2197.

Reyes AD (2011) Synaptic short-term plasticity in auditory cortical circuits. Hearing Research 279:60-66.

Robinson RB, Siegelbaum SA (2003) Hyperpolarization-activated cation currents: from molecules to physiological function. Annual review of physiology 65:453-480.

Roghani A, Feldman J, Kohan SA, Shirzadi A, Gundersen CB, Brecha N, Edwards RH (1994) Molecular cloning of a putative vesicular transporter for acetylcholine. Proceedings of the National Academy of Sciences of the United States of America 91:10620-10624.

Schecklmann M, Landgrebe M, Poeppl TB, Kreuzer P, Manner P, Marienhagen J, Wack DS, Kleinjung T, Hajak G, Langguth B (2013) Neural correlates of tinnitus duration and distress: a positron emission tomography study. Human brain mapping 34:233-240.

Schon K, Atri A, Hasselmo ME, Tricarico MD, LoPresti ML, Stern CE (2005) Scopolamine reduces persistent activity related to long-term encoding in the parahippocampal gyrus during delayed matching in humans. The Journal of neuroscience 25:9112-9123.

Schreiner CE, Mendelson JR, Sutter ML (1992) Functional topography of car primary auditory cortex - Representation of tone intensity. Experimental Brain Research 92:105-122.

Sheets PL, Suter BA, Kiritani T, Chan CS, Surmeier DJ, Shepherd GM (2011) Corticospinal-specific HCN expression in mouse motor cortex: I(h)-dependent synaptic integration as a candidate microcircuit mechanism involved in motor control. Journal of neurophysiology 106:2216-2231.

Shepherd GM (2013) Corticostriatal connectivity and its role in disease. Nature reviews Neuroscience 14:278-291.

Shepherd GM, Stepanyants A, Bureau I, Chklovskii D, Svoboda K (2005) Geometric and functional organization of cortical circuits. Nat Neurosci 8:782-790.

Shibuki K, Hishida R, Murakami H, Kudoh M, Kawaguchi T, Watanabe M, Watanabe S, Kouuchi T, Tanaka R (2003) Dynamic imaging of somatosensory cortical activity in the rat visualized by flavoprotein autofluorescence. Journal of Physiology-London 549:919-927.

Slater BJ, Willis AM, Llano DA (2013) Evidence for layer-specific differences in auditory corticocollicular neurons. Neuroscience 229:144-154.

Song H, Ming G, Fon E, Bellocchio E, Edwards RH, Poo M (1997) Expression of a putative vesicular acetylcholine transporter facilitates quantal transmitter packaging. Neuron 18:815-826.

Stebbings KA, Lesicko AM, Llano DA (2014) The auditory corticocollicular system: molecular and circuit-level considerations. Hear Res 314:51-59.

Stiebler I, Neulist R, Fichtel I, Ehret G (1997) The auditory cortex of the house mouse: left-right differences, tonotopic organization and quantitative analysis of frequency representation. Journal of Comparative Physiology a-Sensory Neural and Behavioral Physiology 181:559-571.

Suga N (2012) Tuning shifts of the auditory system by corticocortical and corticofugal projections and conditioning. Neuroscience and Biobehavioral Reviews 36:969-988.

Suga N, Ma XF (2003) Multiparametric corticofugal modulation and plasticity in the auditory system. Nature Reviews Neuroscience 4:783-794.

Suga N, Xiao ZJ, Ma XF, Ji WQ (2002) Plasticity and corticofugal modulation for hearing in adult animals. Neuron 36:9-18.

Sun YJ, Kim Y-J, Ibrahim LA, Tao HW, Zhang LI (2013) Synaptic Mechanisms Underlying Functional Dichotomy between Intrinsic-Bursting and Regular-Spiking Neurons in Auditory Cortical Layer 5. Journal of neuroscience 33:5326-5339.

Suter BA, Migliore M, Shepherd GMG (2013) Intrinsic Electrophysiology of Mouse Corticospinal Neurons: a Class-Specific Triad of Spike-Related Properties. Cerebral Cortex 23:1965-1977.

Suter BA, O'Connor T, Iyer V, Petreanu LT, Hooks BM, Kiritani T, Svoboda K, Shepherd GM (2010) Ephus: multipurpose data acquisition software for neuroscience experiments. Front Neural Circuits 4:100.

Suzuki WA, Miller EK, Desimone R (1997) Object and place memory in the macaque entorhinal cortex. Journal of neurophysiology 78:1062-1081.

Takahashi K, Hishida R, Kubota Y, Kudoh M, Takahashi S, Shibuki K (2006) Transcranial fluorescence imaging of auditory cortical plasticity regulated by acoustic environments in mice. European Journal of Neuroscience 23:1365-1376.

Takesian AE, Kotak VC, Sharma N, Sanes DH (2013) Hearing loss differentially affects thalamic drive to two cortical interneuron subtypes. Journal of neurophysiology 110:999-1008.

Thiele A (2013) Muscarinic signaling in the brain. Annual review of neuroscience 36:271-294.

Thomson AM, Lamy C (2007) Functional maps of neocortical local circuitry. Frontiers in neuroscience 1:19-42.

Turner JG, Hughes LF, Caspary DM (2005) Divergent response properties of layer-V neurons in rat primary auditory cortex. Hearing Research 202:129-140.

Vanderzee EA, Streefland C, Strosberg AD, Schroder H, Luiten PGM (1992) Visualization of cholinoceptive neurons in the rat neocortex - colocalization of muscarinic and nicotinic acetylcholine-receptorsV. Molecular Brain Research 14:326-336.

Viaene AN, Petrof I, Sherman SM (2011a) Synaptic properties of thalamic input to the subgranular layers of primary somatosensory and auditory cortices in the mouse. Journal of neuroscience 31:12738-12747.

Viaene AN, Petrof I, Sherman SM (2011b) Synaptic properties of thalamic input to layers 2/3 and 4 of primary somatosensory and auditory cortices. Journal of neurophysiology 105:279-292.

Viaene AN, Petrof I, Sherman SM (2011c) Properties of the thalamic projection from the posterior medial nucleus to primary and secondary somatosensory cortices in the mouse. Proceedings of the National Academy of Sciences of the United States of America 108:18156-18161.

Volkov IO, Galazjuk AV (1991) Formation of spike response to sound tones in cat auditory cortex neurons - interaction of excitatory and inhibitory effects. Neuroscience 43:307-321.

Wallace MN, Jufang H (2011) Intrinsic connections of the auditory cortex. In: The Auditory Cortex J.A. Winer and C.E. Schreiner, Editors. 2011, Springer: New York. p. 133-146).

Wang M, Ramos BP, Paspalas CD, Shu Y, Simen A, Duque A, Vijayraghavan S, Brennan A, Dudley A, Nou E, Mazer JA, McCormick DA, Arnsten AF (2007) Alpha2A-adrenoceptors strengthen working memory networks by inhibiting cAMP-HCN channel signaling in prefrontal cortex. Cell 129:397-410.

Wang XJ (2001) Synaptic reverberation underlying mnemonic persistent activity. Trends in neurosciences 24:455-463.

Wang XQ, Lu T, Snider RK, Liang L (2005) Sustained firing in auditory cortex evoked by preferred stimuli. Nature 435:341-346.

Wang Y, Markram H, Goodman PH, Berger TK, Ma JY, Goldman-Rakic PS (2006) Heterogeneity in the pyramidal network of the medial prefrontal cortex. Nature neuroscience 9:534-542.

Weedman DL, Ryugo DK (1996a) Pyramidal cells in primary auditory cortex project to cochlear nucleus in rat. Brain research 706:97-102.

Weedman DL, Ryugo DK (1996b) Projections from auditory cortex to the cochlear nucleus in rats: synapses on granule cell dendrites. The Journal of comparative neurology 371:311-324.

Weinberger NM (2003) The nucleus basalis and memory codes: auditory cortical plasticity and the induction of specific, associative behavioral memory. Neurobiology of learning and memory 80:268-284.

Weinberger NM, Miasnikov AA, Chen JC (2006) The level of cholinergic nucleus basalis activation controls the specificity of auditory associative memory. Neurobiology of learning and memory 86:270-285.

Williams SR, Atkinson SE (2007) Pathway-specific use-dependent dynamics of excitatory synaptic transmission in rat intracortical circuits. Journal of Physiology-London 585:759-777.

Winer JA (2006) Decoding the auditory corticofugal systems (vol 207, pg 1, 2005). Hearing Research 212:1-8.

Winer JA, Prieto JJ (2001) Layer V in cat primary auditory cortex (AI): cellular architecture and identification of projection neurons. J Comp Neurol 434:379-412.

Winkler J, Suhr ST, Gage FH, Thal LJ, Fisher LJ (1995) Essential role of neocortical avetylcholine in spatial memory. Nature 375:484-487.

Yamashita T, Isa T (2003a) Ca2+-dependent inward current induced by nicotinic receptor activation depends on Ca2+/calmodulin-CaMKII pathway in dopamine neurons. Neuroscience Research 47:225-232.

Yamashita T, Isa T (2003b) Fulfenamic acid sensitive, Ca2+-dependent inward current induced by nicotinic acetylcholine receptors in dopamine neurons. Neuroscience Research 46:463-473.

Yamawaki N, Shepherd GM (2015) Synaptic circuit organization of motor corticothalamic neurons. The Journal of neuroscience 35:2293-2307.

Yamawaki N, Borges K, Suter BA, Harris KD, Shepherd GM (2014) A genuine layer 4 in motor cortex with prototypical synaptic circuit connectivity. eLife 3:e05422.

Yan J, Ehret G (2002) Corticofugal modulation of midbrain sound processing in the house mouse. European Journal of Neuroscience 16:119-128.

Yan J, Zhang YF, Ehret G (2005) Corticofugal shaping of frequency tuning curves in the central nucleus of the inferior colliculus of mice. Journal of neurophysiology 93:71-83.

Young BJ, Otto T, Fox GD, Eichenbaum H (1997) Memory representation within the parahippocampal region. The Journal of neuroscience 17:5183-5195.

Zhang Z, Seguela P (2010) Metabotropic Induction of Persistent Activity in Layers II/III of Anterior Cingulate Cortex. Cerebral Cortex 20:2948-2957.

Zhao S, Ting JT, Atallah HE, Qiu L, Tan J, Gloss B, Augustine GJ, Deisseroth K, Luo M, Graybiel AM, Feng G (2011) Cell type-specific channelrhodopsin-2 transgenic mice for optogenetic dissection of neural circuitry function. Nat Methods 8:745-752.

Zolles G, Wagner E, Lampert A, Sutor B (2009) Functional Expression of Nicotinic Acetylcholine Receptors in Rat Neocortical Layer 5 Pyramidal Cells. Cerebral Cortex 19:1079-1091.